

TRANSLATIONAL CONTROL BY THE RIBOSOME-ASSOCIATED COMPLEX
IN THE UNFOLDED PROTEIN RESPONSE

APPROVED BY SUPERVISORY COMMITTEE

Philip J. Thomas, Ph.D.

Jerry Shay, Ph.D.

Joshua Mendell, M.D., Ph.D.

Benjamin Tu, Ph.D.

To my family, Steve, Catherine, Andrew, and Maui & Moony,
for all your love and support

TRANSLATIONAL CONTROL BY THE RIBOSOME-ASSOCIATED COMPLEX
IN THE UNFOLDED PROTEIN RESPONSE

by

I-HUI WU

DISSERTATION

Presented to the Faculty of the Graduate School of Biomedical Sciences

The University of Texas Southwestern Medical Center at Dallas

In Partial Fulfillment of the Requirements

For the Degree of

DOCTOR OF PHILOSOPHY

The University of Texas Southwestern Medical Center at Dallas

Dallas, Texas

December, 2020

Copyright

by

I-Hui Wu, 2020

All Rights Reserved

Acknowledgements

“Circumstances don't make the man, they only reveal him to himself.” — Epictetus

My PhD journey has been a voyage of self-discovery. It is like running a 7-year long marathon: learning how to pace myself, stay focused, and stay resilient. I could not have done it without the support of my mentor, Philip Thomas. You pointed out my blind spot that I had never noticed myself. You taught me how to deliver a professional talk-
“Less is more.” I have kept this in mind. I really appreciated that you gave me the freedom to explore research projects independently, supported me to conferences, and acted as a cheerleader when my experiment didn't work. Your guidance makes me a better scientist and a better person.

I would like to thank my committee, Joshua Mendell, Benjamin Tu, and Jerry Shay, for their supports and valuable insights. I must also thank my bench mate, Emile Pinarbasi. It was really nice to have you around to joke around and bounce ideas. Thanks our lab manager, Linda Millen, for your patience and assistance. Our lab will be out of control without you. Additionally, thanks for prior and current Thomas's lab members for the supports, Andrey Karamyshev, Michael Torres, Ali Vetter, Henry Hudson, Carlos Huerta, Cayce Harness-Brumley, Zemfira Karamysheva, Yair Peres, Melissa Coquelin, Linde De Keyzer, Zena Ghazala, and Amy Dettori.

I would like to thank my collaborators for assisting me in completing this study. The *in vitro* mammalian cell-free lysates were harvested with the aid of Qian Yang in Yi

Liu's lab. Although the experiment was thought implausible, it turns out that the results were very fruitful. I really appreciate your assistance in working long hours in the cold room with me, and your valuable feedbacks. Next, the ribosome profiling experiments were performed with the aid of Jae Seok Yoon at the Cystic Fibrosis Foundation Therapeutics (CFFT) in Lexington, Massachusetts. Thanks to Phil, William Skach, Martin Mense, and Jae, I've learned a lot regarding translational regulation at the CFFT.

I would also like to thank my collaborators whom kindly provided me with reagents and technical supports: Elizabeth Craig's lab in the University of Wisconsin-Madison for the knockout RAC yeast strains, Peter Walter's lab in the UCSF for the T-REx293 IRE1-GFP cell line, Sabine Rospert's lab in the University of Freiburg, Germany, for anti-Mpp11 antibody, Ineke Braakman's Lab in the University Utrecht, Netherlands, for one of the knockout Hsp70L1 cell line, Christopher Nicchitta in Duke University for technical advice of the differential detergent cell fractionation experiments, Benjamin Tu's lab for yeast technical supports, Jen Liou's lab for microscope technical supports, and the microscope imaging core at the Physiology department at UTSW. Special thanks to the Cancer Biology program, the Mechanisms of Disease and Translational Science (MoDTS) graduate track, the Physiology department at UTSW, as well as funding from the Howard Hughes Medical Institute (HHMI) sponsored Med into Grad scholarship.

It has been a great pleasure to work with you all!

TRANSLATIONAL CONTROL BY THE RIBOSOME-ASSOCIATED COMPLEX
IN THE UNFOLDED PROTEIN RESPONSE

I-Hui Wu, Ph.D.

The University of Texas Southwestern Medical Center at Dallas, 2020

Mentor: Philip J. Thomas, Ph. D.

Ribosome-associated chaperones are ubiquitous and highly conserved. There are two classes of ribosome-associated chaperones in eukaryotes, the nascent polypeptide-associated complex (NAC) and the ribosome-associated complex (RAC). Mammalian RAC consists of Hsp70L1, an Hsp70 chaperone homologue, and Mpp11, a DnaJ cofactor. RAC interacts with the nascent chain near the polypeptide exit tunnel and the decoding center on the 60S and 40S ribosomal subunits, respectively. Its unique position on the ribosome implies the coordinating role of *de novo* protein folding with translation. Deletion of RAC causes growth defects and sensitizes to osmotic, cold, and

aminoglycoside stresses in yeast. Furthermore, studies have shown that Mpp11 is over-expressed in head and neck squamous cell cancer and leukemia. However, the function of RAC in stress responses and its role in oncogenesis remain obscure.

The current hypothesis predicts that RAC supports co-translational folding of nascent cytosolic polypeptides. To directly test this hypothesis, I altered levels of RAC components and monitored the cytosolic heat shock response (HSR) and the unfolded protein response (UPR) in the ER, two stress pathways known to be activated by accumulation of misfolded proteins. Contrary to its presumptive role in cytosolic protein folding, the reduction of RAC expression did not activate the cytosolic HSR. Unexpectedly, reduction of RAC sensitizes cells to ER stress by selectively attenuating activation of the IRE1 branch of UPR. When RAC is reduced, Xbp1 mRNA splicing is inhibited upon ER stress. Consistent with this activity, ER stress induces changes in the subcellular distribution of RAC, which coincides with the localization of Xbp1 mRNA. Mechanistically, reduction of RAC affects the pathway at a very early step, as IRE1 self-association is inhibited. Additionally, this study shows that the reduction of RAC enhances cellular mRNA translation, including Xbp1 mRNA translation. Interestingly, reduction of Pelo, a protein involved in recognizing stalled ribosomes, counters the inhibition of Xbp1 mRNA splicing, and IRE1 foci formation due to RAC knockdown. Collectively, these results suggest that RAC plays a central role in the IRE1 branch of the UPR tuning IRE1 clustering and mRNA translation.

Table of Contents

Dedication	ii
Acknowledgements	v
Abstract	vii
Table of Contents	ix
Publications from Graduate Work at UTSW	xii
List of Figures	xiii
List of Tables	xvi
List of Appendices	xvii
List of Abbreviations	xviii
Chapter I. Introduction	1
Chapter II. Review of the Literature	5
<i>II-1. Ribosome-associated Chaperones</i>	5
Trigger factor (TF)	6
Nascent polypeptide associated complex (NAC)	8
Ribosome-associated complex (RAC)	11
Structure and cellular function of RAC	11
Zuo1/Mpp11	11
Ssz/Hsp70L1	15
RAC spans both the ribosomal subunits	15
RAC in <i>de novo</i> protein folding	16
RAC in translation	17
Ribosome-associated factors: Signal recognition particle (SRP)	18
SRP bridges both ribosomal subunits	22
The interplay between ribosome-associated factors	23
<i>II-2. Quality Control</i>	25
mRNA quality control	26
No-go decay (NGD)	26
Non-stop decay (NSD)	28

Regulates aberrant protein production (RAPP)	29
The unfolded protein response (UPR)	30
IRE1 branch	31
IRE1 stress-sensing models: the competition and direct binding models	34
IRE1 oligomerization	35
Hac1/Xbp1 mRNA splicing	36
Hac1 mRNA in yeast	36
Xbp1 mRNA in mammal	38
Regulated IRE1-dependent decay of mRNA (RIDD)	40
Mechanisms of IRE1 regulation	40
IRE1 stability and attenuation	41
IRE1 interactome	41
Chapter III. A Central Role for the Ribosome-Associated Complex in Modulating	
Activation of the IRE1 Branch of UPR	43
<i>Abstract</i>	43
<i>Introduction</i>	44
<i>Results</i>	48
Acute reduction of RAC selectively sensitizes cells to ER stress by attenuation of the IRE1 α arm of the UPR	48
RAC is not required for uXbp1 mRNA targeting to the ER membrane	55
Reduction of RAC inhibits IRE1 α kinase, endoribonuclease activity and high-order oligomerization	59
Reduction of RAC increases uXbp1 ribosome stalling	63
Reduction of Pelo counters the inhibition of uXbp1 ribosome stalling, Xbp1 mRNA splicing and IRE1 α clustering in RAC knockdown during ER stress	66
RAC modulates IRE1 α clustering <i>via</i> translation	70
<i>Discussions</i>	75
<i>Supplements</i>	79

<i>Material and Methods</i>	87
Cell culture, transfection and RNA interference experiments	87
Cell Viability (MTS assay)	87
RNA isolation, cDNA synthesis and quantitative real time-PCR	88
Xbp1 mRNA splicing assay	89
Protein analysis by immunoblotting	89
Phos-tag mobility shift assay	90
Subcellular Fractionation	90
RNA immunoprecipitation	91
IRE1 α foci imaging	92
Plasmids	93
<i>In vitro</i> transcription	94
<i>In vitro</i> translation by mammalian cell-free lysate	94
Native protein electrophoresis	95
Pulse labeling global nascent proteins with bioorthogonal non-canonical amino- acid tagging	96
Ribosome profiling	97
Statistical Analysis	98
Chapter IV. Conclusion and Future Directions	102
Mechanism of action of RAC	103
The unknown in the IRE1 branch	106
Physiological function and disease relevance of RAC	108
The role of RAC in cancer	108
The emerging role of IRE1 in cancer	110
The potential role of RAC in cancer therapeutics	112
Appendix	114
Bibliography	122

Publications from Graduate Work at UTSW

I-Hui Wu, Jae Seok Yoon, Qian Yang, William Skach, Philip J. Thomas. A central role for the ribosome-associated complex in modulating activation of the IRE1 branch of the UPR. *(In submission)*

Emile S. Pinarbasi, Andrey L. Karamyshev, Elena B. Tikhonova, **I-Hui Wu**, Henry Hudson, Philip J. Thomas. Pathogenic signal sequence mutations in progranulin disrupt SRP interactions required for mRNA stability. *Cell Reports*, 23, 2844–2851 (2018).

List of Figures

Figure 1. Structure of <i>Escherichia coli</i> trigger factor (TF)	7
Figure 2. Structure of nascent polypeptide associated complex (NAC)	9
Figure 3-1. Structure of ribosome-associated complex (RAC)	13
Figure 3-2. Structure of ribosome-associated complex (RAC) (continued)	14
Figure 4-1. SRP-dependent co-translational protein translocation machinery in eukaryotes	20
Figure 4-2. SRP-dependent co-translational protein translocation machinery in eukaryotes (continued)	21
Figure 5. The mechanism of no-go decay (NGD) and nonstop decay (NSD)	27
Figure 6. The three arms of the unfolded protein response in eukaryotes	32
Figure 7. The overall architecture of IRE1 α and the current model of IRE1 activation	33
Figure 8. Schematic of yeast Hac1 and human Xbp1 mRNA	37
Figure 9-1. Cells sensitivity to the UPR after RAC knockdown	49
Figure 9-2. Cells sensitivity to the UPR after RAC knockdown (continued)	50
Figure 9-3. Cells sensitivity to the UPR after RAC knockdown (continued)	51
Figure 10-1. Membrane targeting effect of RAC-associated uXbp1 mRNA in RAC knockdown	54
Figure 10-2. Membrane targeting effect of RAC-associated uXbp1 mRNA in RAC knockdown (continued)	56
Figure 10-3. Membrane targeting effect of RAC-associated uXbp1 mRNA in RAC knockdown (continued)	57
Figure 11-1. Selective inhibition effect on IRE1 α activity in RAC knockdown cells	60
Figure 11-2. Selective inhibition effect on IRE1 α activity in RAC knockdown cells (continued)	61
Figure 11-3. Selective inhibition effect on IRE1 α activity in RAC knockdown cells (continued).	62

Figure 12-1. Enhancement of Xbp1 ribosome stalling and translation rate of RAC knockdown by <i>in vitro</i> cell-free translation	64
Figure 12-2. Enhancement of Xbp1 ribosome stalling and translation rate of RAC knockdown by <i>in vitro</i> cell-free translation (continued)	65
Figure 13-1. Enhancement of Xbp1 ribosome stalling in RAC knockdown and counteract effect by Pelo knockdown in RAC knockdown under ER stress by ribosome profiling	68
Figure 13-2. Enhancement of Xbp1 ribosome stalling in RAC knockdown and counteract effect by Pelo knockdown in RAC knockdown under ER stress by ribosome profiling (continued)	69
Figure 14-1. Counteract effect of IRE1a activity by Pelo knockdown in RAC knockdown under ER stress	72
Figure 14-2. Counteract effect of IRE1a activity by Pelo knockdown in RAC knockdown under ER stress (continued)	73
Figure 15. RAC is an ER stress-responsive regulator	74
Figure S1. (Related to Figure 9) RAC does not affect the PERK and ATF6 branch of the UPR	79
Figure S2-1. (Related to Figure 11) Selective inhibition effect on IRE1 α activity in RAC knockdown	80
Figure S2-2. (Related to Figure 11) Selective inhibition effect on IRE1 α activity in RAC knockdown (continued)	81
Figure S3-1. (Related to Figure 12) Enhancement of Xbp1 ribosome stalling and cellular translation rate in RAC knockdown by <i>in vitro</i> cell-free translation	82
Figure S3-2. (Related to Figure 12) Enhancement of Xbp1 ribosome stalling and cellular translation rate in RAC knockdown by <i>in vitro</i> cell-free translation (continued)	83
Figure S4-1. (Related to Figure 13) Enhancement of Xbp1 ribosome stalling in RAC knockdown and counteract effect by Pelo knockdown in RAC knockdown under ER stress by ribosome profiling	84

Figure S4-2. (Related to Figure 13) Enhancement of Xbp1 ribosome stalling in RAC knockdown and counteract effect by Pelo knockdown in RAC knockdown under ER stress by ribosome profiling (continued)	85
Figure S5. (Related to Figure 14) Counteract effect of IRE1 α activity by Pelo knockdown in RAC knockdown cells	86

List of Tables

Table 1. Antibodies	99
Table 2. Key reagents	99
Table 3. siRNA sequences	100
Table 4. Primer sequences	101

List of Appendices

Appendix-1. RAC knockout in mammalian cells	114
Appendix 2. Knockdown RAC does not lead to protein aggregation	115
Appendix-3. Hsp70L1 associated to the ribosome via Mpp11 in mammalian cells	116
Appendix-4. Colocalization of RAC to the ER	117
Appendix-5. RAC may be in close proximity to IRE1 α	118
Appendix-Materials and methods	
Generation of knockout cell lines by CRISPR/Cas9	119
Subcellular localization of RAC by immunofluorescence	120
Analysis of protein aggregates	121

List of Abbreviations

Ago2	Argonaute 2
AML	Acute myeloid leukemia
AP	Arrest peptide
ASK1	Apoptosis signal-regulating kinase
ATF6	Activating transcription factor 6
BI-1	Bax inhibitor-1
<i>C. elegans</i>	<i>Caenorhabditis elegans</i>
CML	Chronic myeloid leukemia
Cryo-EM	Cryogenic electron microscopy
CTD	C-terminus domain
DC	Dendritic cells
DC	Decoding center
ECM	Extracellular matrix
eIF2 α	Eukaryotic translation initiation factor 2 α
EMT	Epithelial-to-mesenchymal transition
ER	Endothelial reticulum
eRF1	Eukaryotic release factor 1
ESC	Embryonic stem cells
FTLD	Frontotemporal lobar degeneration
GRN	Progranulin
HLH	helix-loop-helix
HNSCC	Head and neck squamous cell carcinoma
HPD motif	His, Pro and Asp tripeptide signature motif
HR2	Hydrophobic region 2
Hsf1	Heat-shock factor 1
HSR	Heat shock response
IDB	Insertion-box domain

IRE1 α	Inositol-requiring protein 1 α
JNK	c-Jun N-terminal kinase
LD	Luminal domain
MAP	Methionine aminopeptidase
MAPK	Mitogen activated protein kinase
MD	Middle domain
MHC I	Major histocompatibility complex I
MIDA1	Mouse Id associate 1
Mpp11	M-phase phosphoprotein 11
NAC	Nascent polypeptide associated complex
NAT	N-terminal acetyltransferases
NBD	Nucleotide-binding domain
NF-kB	Nuclear transcription factor-kB
NGD	No-go decay
NMD	Nonsense-mediated decay
NSD	Non-stop decay
ORF	Open reading frame
PDF	Peptide deformylase
Pdr1	Pleiotropic drug resistance 1
PERK	Double-stranded RNA-activated protein kinase (PKR)-like ER kinase
PPIase	Peptidyl prolyl cis/trans isomerase
PTC	Peptidyl transferase center
PTC	Premature termination codon
PTE	Peptide tunnel exit
PTP-1B	Protein-tyrosine phosphatase 1B
RA	Retinoic acid
RAC	Ribosome-associated complex
RAPP	Regulates aberrant protein production
RAR α	RA receptor α

RIDD	Regulated IRE1-dependent decay of mRNA
RNase	Endonuclease
RNC	Ribosome-nascent chain complex
RNP	Ribonucleoprotein
RPAP2	RNA polymerase II-associated protein 2
RQC	Ribosome-associated protein quality control
Rqc2	Ribosome quality control 2
<i>S. cerevisiae</i>	<i>Saccharomyces cerevisiae</i>
SBD	Substrate-binding domain
SR	SRP receptor
SRP	Signal recognition particle
SR α	SRP-receptor α -subunit
SURF	SMG1–UPF1–eRFs complex
TF	Trigger factor
Th1	T helper cell
TLR4	Toll like receptor 4
TNF- α	Tumor necrosis factor- α
TRAF2	TNF receptor-associated factor 2
UPF1	Up-frameshift proteins 1
UPR	The unfolded protein response
Xbp1s	Xbp1 spliced
Xbp1u	Xbp1 unspliced
ZHD	Zuotin homology doma

Chapter I

Introduction

Accurate protein synthesis is essential to all cellular functions. Without chaperone safeguarding protein homeostasis (proteostasis) by promoting accurate protein folding and detecting irreparably defective proteins for degradation, nascent proteins are at great risk of misfolding and accumulation as aggregated species (Balchin et al., 2016; Chen et al., 2011; Frydman, 2001; Hartl et al., 2011). Such defects are often linked to misfolding diseases, ranging from neurodegenerative diseases to cancer (Balchin et al., 2016; Dubnikov et al., 2017; Hipp et al., 2014). Accumulation of misfolded proteins and aggregates are the hallmark of aging, which is a primary cause of neurodegenerative diseases, including Parkinson's disease and Alzheimer's disease (Chiti and Dobson, 2006). Furthermore, cancer cells can hijack the chaperone networks to accommodate the increase in folding demand for uncontrolled cell division and proliferation (Valastyan and Lindquist, 2014b). Additionally, accumulating studies have indicated that ribosome-associated chaperones not only co-translationally promote *de novo* protein folding and degrade detrimental proteins, but also targets nascent polypeptides to destined organelles as well as modulate translation and mRNA stability (Deuerling et al., 2019; Kramer et al., 2009; Pechmann et al., 2013; Preissler and Deuerling, 2012; Zhang et al., 2017). Taken together, the central role of ribosome-associated chaperones in the proteostasis network makes them an attractive pharmacological target for treating misfolding diseases.

To ensure high fidelity of protein synthesis, protein and mRNA quality control machinery repair or eliminate the irreparably aberrant protein or its mRNA template. For secretory or membrane proteins, aberrant proteins are eliminated by endoplasmic-reticulum (ER)-associated degradation (ERAD) (Brodsky, 2012; Travers et al., 2000). When the defective proteins are overloaded, heat shock responses (HSR) (Anckar and Sistonen, 2011; Gomez-Pastor et al., 2018) in the cytosol or the unfolded protein response (UPR) in the endoplasmic reticulum (ER) (Buchberger et al., 2010; Schroder and Kaufman, 2005; Walter and Ron, 2011) or mitochondria (Pellegrino et al., 2013) will be activated to decrease cellular damage by reducing global protein translation and increase molecular chaperones expression. In mammals, cells activate UPR in the ER via three signal transducers, including inositol-requiring protein 1 α (IRE1 α), double-stranded RNA-activated protein kinase (PKR)-like endoplasmic reticulum kinase (PEKR), and activating transcription factor 6 (ATF6) (Adams et al., 2019; Hetz, 2012; Karagoz et al., 2017). While the downstream events of UPR are relatively well characterized, the activation and recovery of the signal transducers remain obscure.

Emerging studies indicate that the ribosome is a hub for co-translational quality control mechanisms (Kramer et al., 2009; Pechmann et al., 2013; Wilson and Beckmann, 2011), which can rapidly determine the fate of defective nascent proteins and mRNAs. Co-translational ubiquitination of defective nascent polypeptides (Duttler et al., 2013; Wang et al., 2013) on the 80S ribosome and ribosome-associated protein quality control (RQC) (Brandman and Hegde, 2016; Joazeiro, 2017, 2019) on the 60S-tRNA complex can ensure speedy elimination and minimization of aberrant protein production when still

associated to the ribosomes resulting in initiation of ribosome recycling. Aberrant proteins may result from misfolded polypeptides, aberrant mRNA, or defects in translation (Buskirk and Green, 2017; Inada, 2017). Co-translational mRNA surveillance can recognize aberrant mRNAs and preemptively eradicate damaged mRNAs (Karamyshev and Karamysheva, 2018; Shoemaker and Green, 2012). RNA quality control mechanisms include nonsense mediated decay (NMD), nonstop decay (NSD), no-go decay (NGD), and regulation of aberrant protein production (RAPP) (Karamyshev et al., 2014; Pinarbasi et al., 2018). RAPP is a novel mRNA surveillance mechanism detecting mutations in the signal sequence of secretory proteins discovered in our lab. When a signal recognition particle (SRP) fails to recognize the aberrant peptide in the signal sequence, selective degradation of defective mRNA is initiated.

To test the hypothesis that RAPP controls expression of a wider group of substrates, the original goal of this study was to investigate the role of the ribosome-associated complex (RAC), a presumed cytosolic ribosome-associated chaperone (Otto et al., 2005) parallel to SRP for secretory proteins, in regulation of mRNA turnover. To validate the presumed cytosolic chaperone function of RAC, insoluble protein aggregates and the HSR were analyzed, and the UPR was used as a negative control in knockdown mammalian RAC system. Unexpectedly, knockdown RAC neither induced the HSR or UPR nor lead to protein aggregation. Surprisingly, knockdown of RAC selectively inhibited nonconventional Xbp1 mRNA splicing. This unexpected surprise lead to the main story of this study.

This dissertation describes the novel function of RAC in the IRE1 α branch of the

UPR coordinating IRE1 α oligomerization and translation. Chapter II-1 addresses the current literature review on the networks of ribosome-associated chaperones, and Chapter II-2 describes the quality control mechanisms directly relevant to this study. Chapter III addresses the central role of RAC in the UPR. Finally, Chapter IV proposes prospective works that rise from this study and future potential therapeutic application.

Chapter II

Review of the Literature

II-1. Ribosome-associated Chaperones

As nascent polypeptides emerge from the ribosome, ribosome-associated chaperones co-translationally interact with nascent chains assisting *de novo* protein folding (Deuerling et al., 2019; Frydman et al., 1994; Zhang et al., 2017). The networks of ribosome-associated chaperones have evolved structurally distinct from prokaryotes to eukaryotes (Kramer et al., 2009; Pechmann et al., 2013; Preissler and Deuerling, 2012). Trigger factor (TF) is the only ribosome-associated chaperone in prokaryotes, whereas the chaperone network evolved into a more multifaceted system in eukaryotes, including a nascent polypeptide associated complex (NAC) and a ribosome-associated complex (RAC). Other ribosome-associated factors also engage with the nascent polypeptides as it emerge from the ribosome peptide tunnel exit (PTE), such as signal recognition particle (SRP) recognizing secretory and membrane polypeptides, methionine aminopeptidase (MAP) removing N-terminal methionine, or N-acetyltransferases (NAT) which carry out N-terminal acetylation. The substrate pools of ribosome-associated chaperones and interplay between ribosome-associated factors remain incompletely defined.

Trigger factor (TF)

Bacterial TF is the most well-studied ribosome-associated chaperone. Cells lack of both TF and Hsp70 chaperone DnaJ result in global protein aggregation and lower cell viability (Deuerling et al., 1999; Teter et al., 1999). TF has unique characteristics as a “holdase” and “unfoldase”, preventing incorrect folding and degradation of nascent polypeptides (Hoffmann et al., 2012; Hoffmann et al., 2006; Tomic et al., 2006). TF has a distinctive dragon-like structure (Figure 1), consisting of a N-terminus ribosome-binding domain, which is the tail motif, a peptidyl prolyl cis/trans isomerase (PPIase) domain in the middle, which resembles the head motif, and followed by a C-terminus domain, which acts as two arms (Ferbitz et al., 2004; Kramer et al., 2002). All three domains engage in nascent polypeptides binding during *de novo* protein folding (Lakshmipathy et al., 2007). TF tethers to the ribosome in a 1:1 stoichiometry by the ribosomal protein uL23 near the ribosome exit tunnel via its N-terminus domain (Ferbitz et al., 2004; Kramer et al., 2002). The duration of TF anchors to translating ribosomes is correlated to the extent of the hydrophobic motif in the unfolded nascent polypeptide chains and their aggregation tendency (Kaiser et al., 2006).

Biochemical experiments and selective ribosome profiling of TF-associated ribosomes reveals that TF interacts with the larger nascent polypeptide chains at an average length of around 100 amino acids, after 60-70 amino acids exposed outside the ribosome (Deuerling et al., 2003; Oh et al., 2011). The initial exclusion period of TF provides a window for processing factors, including methionine aminopeptidase (MAP), N-terminal acetyltransferases (NAT), or peptide deformylase (PDF), to engage in nascent

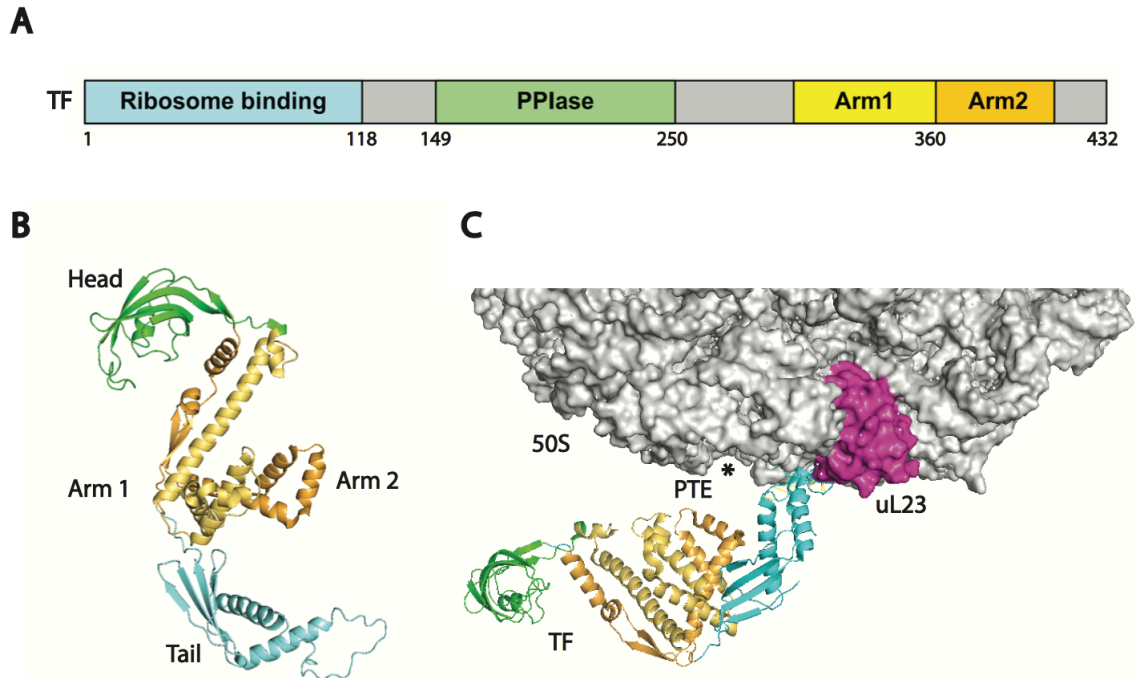


Figure 1. Structure of *Escherichia coli* trigger factor (TF)

(A) The overall architecture of TF. (B) Ribbon representation of the crystal structure of TF (PDB-1W26). The structure of TF resembles a dragon-shape, composing of the N-terminus ribosome-binding domain (cyan, tail motif), the peptidyl prolyl cis-trans isomerase (PPIase) domain (green, head motif), and followed by the C-terminus domain (yellow, orange, two arms). (C) Structure model of TF with the 50S ribosome. Full-length TF (PDB-1W26) was superimposed onto the ribosome-associated TF fragment 1-144 (PDB-1W2B). TF interacts with the ribosomal protein uL23 (magenta) on the large ribosome *via* its N-terminal ribosome binding domain (cyan). *, ribosomal peptide exit tunnel, PTE.

polypeptide chains (Giglione et al., 2009; Jha and Komar, 2011). Additionally, TF has a high preference toward outer membrane β -barrel and cytoplasmic proteins, excluding the ribosome nascent chain complex bearing signal sequences which are recognized by signal recognition particle (SRP) (Bornemann et al., 2014).

Nascent polypeptide associated complex (NAC)

NAC is a highly conserved dimeric complex, consisting of α -NAC and β -NAC subunits (Figure 2A, 2B) (Beatrix et al., 2000; Spreter et al., 2005). α -NAC contains a β -barrel-like NAC domain, which is involved in NAC dimerization, and an ubiquitin-associated (UBA) domain at the C-terminus, whose specific function remains unknown (Spreter et al., 2005; Wang et al., 2010). β -NAC consists of a NAC domain as well as an N-terminus conserved RRK(X)nKK ribosome binding motif. Cross-linking data suggest that NAC tethers to the ribosome at uL23 and eL31 *via* the N-terminus ribosome-binding motif of β -NAC (Pech et al., 2010; Wegrzyn et al., 2006) and uL29 *via* α -NAC (Figure 2C) (Nyathi and Pool, 2015). Biochemical data suggest that NAC is conformationally flexible (Martin et al., 2018). This is in agreement with earlier observations that NAC can interact with ribosomal proteins, uL23 and eL31, on the opposite side of the tunnel exit. However, the precise structural details of NAC's N- and C- terminus domain and its position near the ribosome tunnel exit are yet to be resolved.

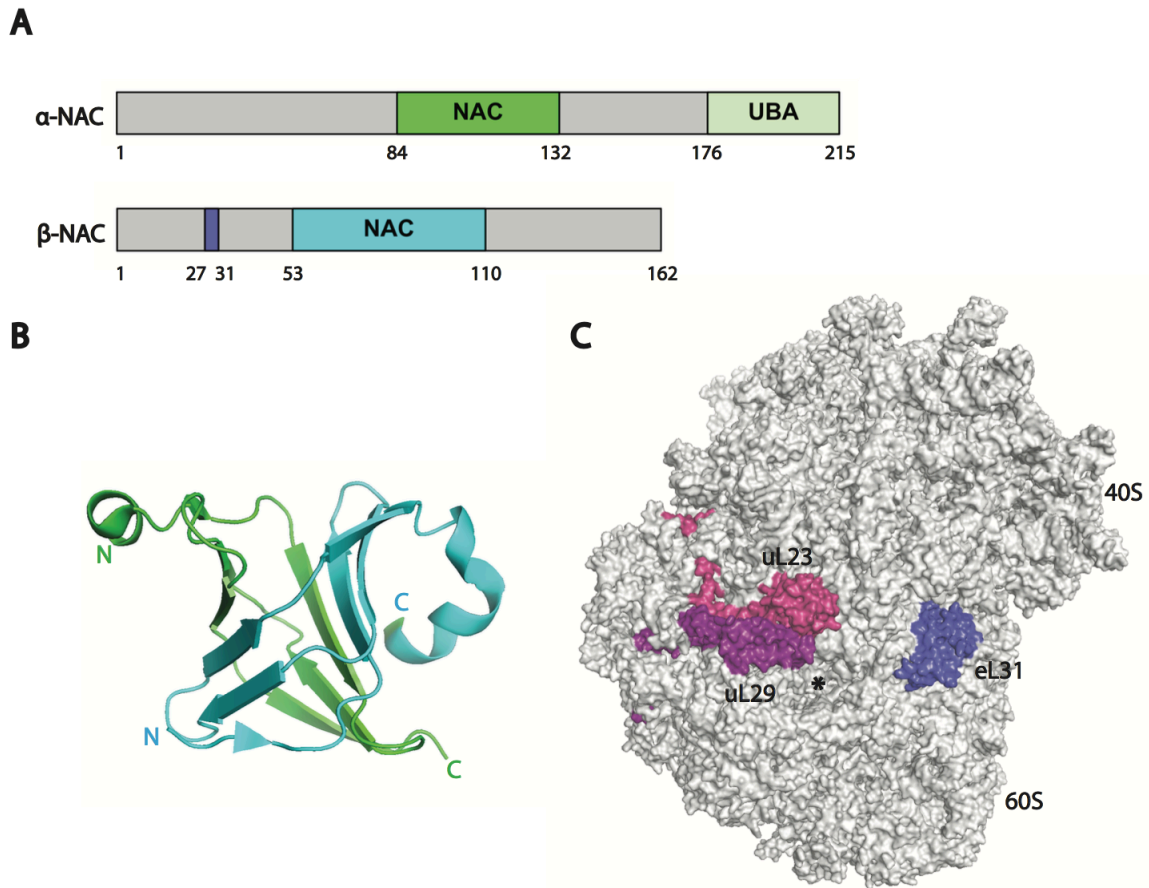


Figure 2. Structure of nascent polypeptide associated complex (NAC)

(A) The overall architecture of human NAC. NAC is a heterodimer. α -NAC composes of a NAC domain (green) involving in NAC dimerization, and an ubiquitin-associated (UBA) domain (palegreen) with unknown function. β -NAC consists of an N-terminus conversed RRK(X)nKK ribosome binding motif (purple) as well as a NAC domain (cyan). (B) Ribbon diagram showing the crystal structure of the interaction core of human NAC heterodimer, forming a β -barrel-like structure (PDB-3MCB), consisting of an α -NAC (green, residues 79–132) and a β -NAC (cyan, residues 53–110). (C) Potential ribosome-contact sites of NAC suggested by cross-linking data (Nyathi and Pool, 2015; Pech et al., 2010; Wegrzyn et al., 2006) on the 80S ribosome (PDB: 3J78). Violet, uL29. Magenta, uL23. Blue, eL31. *, ribosomal peptide exit tunnel, PTE.

Complete loss of NAC results in embryonic lethality and growth defects in *C. elegans*, *Drosophila*, mice, and human cells but not for *S. cerevisiae* (Deng and Behringer, 1995; Markesich et al., 2000; Reimann et al., 1999), suggesting that NAC may have evolved additional essential functions in higher eukaryotes. Moreover, knockdown of NAC, which shortens life span of *C. elegans* (Bloss et al., 2003), not only activates the unfolded protein response (UPR) in the endoplasmic reticulum (ER) but also UPR in mitochondria, and leads to cell death *via* apoptosis in *C. elegans* and human cells (Gamerding et al., 2015; Hotokezaka et al., 2009). A myriad of accumulated data suggested that NAC regulates co-translational protein transport to mitochondria in *S. cerevisiae* (del Alamo et al., 2011; Funfschilling and Rospert, 1999; George et al., 1998; George et al., 2002). Recent work has begun to illuminate that NAC not only is an essential player in preventing mitochondrial proteins from mistargeting to the ER but also modulates SRP specificity by blocking SRP-independent ribosome targeting to translocon in *C. elegans* (Gamerding et al., 2015). Interestingly, the different isoforms of NAC have diverse substrate specificities in *S. cerevisiae*. The most prevalent dimer of α -NAC (Egd2) and β -NAC (Egd1) subunits have a high affinity toward secretory and membrane proteins, while dimer bears β' -NAC (Btt1) show preference to mitochondrial or ribosomal proteins (del Alamo et al., 2011). However, how this general chaperone selectively regulates and recognizes the substrate pools remains obscure.

Ribosome-associated complex (RAC)

The ribosome-associated Hsp70-Hsp40 chaperone system is comprised of a stable heterodimeric ribosome-associated complex (RAC). An atypical Hsp70 (Ssz1) and an Hsp40 J domain protein (Zuo1), together with a ribosome-associated Hsp70 (Ssb) forming a chaperone triad in *S. cerevisiae* (Figure 3A); mammalian RAC, which is comprised of the unconventional Hsp70 chaperone homolog (Hsp70L1) and the Hsp40 (Figure 3A) (Mpp11, M-phase phosphoprotein 11), recruits and works together with a cytosolic Hsp70 chaperone (Gautschi et al., 2001; Gautschi et al., 2002; Hundley et al., 2005; Jaiswal et al., 2011; Otto et al., 2005). Knockout of either RAC or Ssb or both display similar phenotypes, which have growth defects and sensitivity to osmotic, cold and translational stress, suggesting that the chaperone triad work together as a stress-protective unit in the protein production pathway (Gautschi et al., 2002; Hundley et al., 2005; Nelson et al., 1992; Yan et al., 1998). RAC, which is tethered to the ribosome *via* its J domain partner, spans both the 40S and 60S ribosomal subunits. The bipartite interaction with the ribosome highlights RAC's cooperative role in *de novo* protein folding and translation (Deuerling et al., 2019; Pechmann et al., 2013; Preissler and Deuerling, 2012).

Structure and cellular function of RAC

Zuo1/Mpp11

Zuo1 was first identified as a left-handed Z-DNA binding protein in the nucleus (Zuo is pronounced as left in Mandarin) (Zhang et al., 1992). Subsequently, Zuo1 was

characterized as a tRNA (Wilhelm et al., 1994) and RNA binding protein that interacts with the 60S large ribosomal subunit (Yan et al., 1998). Zuo1 consists of an N-terminus (N), a J domain (J), a Zuotin homology domain (ZHD), a middle domain (MD), and followed by a four-helix bundle (4HB) domain (Figure 3A). The Zuo1 N domain interacts with the linker domain of Ssz1 (Figure 3B). The stable RAC heterodimer (Gautschi et al., 2001) is a unique Hsp70-Hsp40 pair, as canonical Hsp70-Hsp40 systems are characterized by transient interactions (Kampinga and Craig, 2010; Mayer and Bukau, 2005). The Zuo1 J domain contains a highly conserved His, Pro, and Asp tripeptide (HPD) signature motif. Zuo1 interacts with the 60S large ribosomal subunit *via* the ZHD domain and the 40S small ribosomal subunit *via* the 4HB domain, which the Helix I is essential for stable ribosome association (Lee et al., 2016; Leidig et al., 2013; Peisker et al., 2008; Yan et al., 1998; Zhang et al., 2014).

Yeast Zuo1 and human Mpp11 are highly conserved in domain structure, while two distinctions should be noted (Figure 3A): First, Zuo1 contains an additional C-terminal 13-residues of the 4HB domain (Shrestha et al., 2019), a hydrophobic fragment thought to act like a plug. This plug domain is essential for the activation of the Pdr1 transcription factor (Ducett et al., 2013), which is a unique function of Zuo1 in yeast due to its exclusive structure. Next, Mpp11 bears two SANT domains after the 4HB domain. The SANT domain has strong structural similarity to the DNA-binding domain of Myb-related proteins, involving in chromatin remodeling and transcriptional regulation by

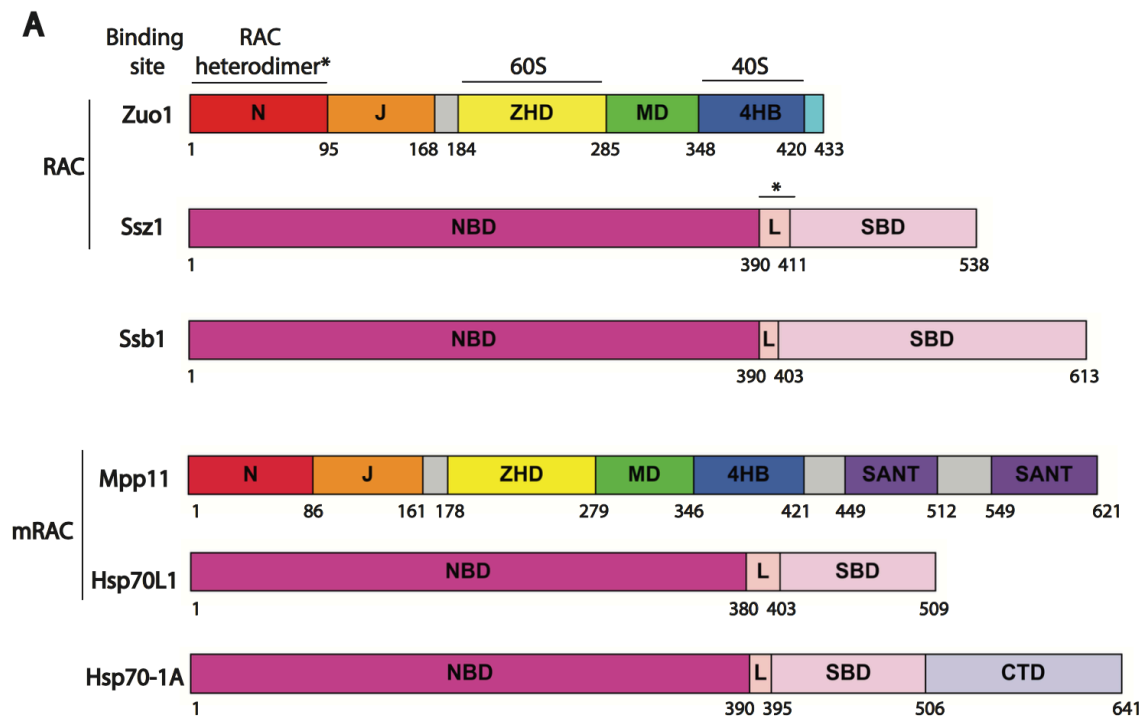


Figure 3-1. Structure of ribosome-associated complex (RAC)

(A) The overall architecture of yeast (top) and mammalian RAC (mRAC, bottom) and its supporting Hsp70 chaperone. Zuo1/Mpp11 consists of an N-terminus (red) that interacts with the Ssz1 linker domain (L, wheat), a J domain (orange), a Zuotin homology domain (ZHD, yellow) that interacts with the 60S large ribosomal subunit, a middle domain (MD, green), and followed by a four-helix bundle (4HB) domain (blue) that interacts with the 40S small ribosomal subunit. Zuo1 contains an additional C-terminal 13-residues (cyan), which is essential for Pdr1 activation. Mpp11 bears two SANT domains (purple) at the C-terminus, involving in chromatin remodeling and transcriptional regulation. Ssz1/Hsp70L1 composed of a nucleotide-binding domain (NBD, magenta) that binds and hydrolyze ATP, a flexible linker (L, wheat), and followed by a substrate-binding domain (SBD, pink) that binds neutral and hydrophobic amino acids. The canonical Hsp70-1A contains an additional C-terminus domain (CTD, lavender).

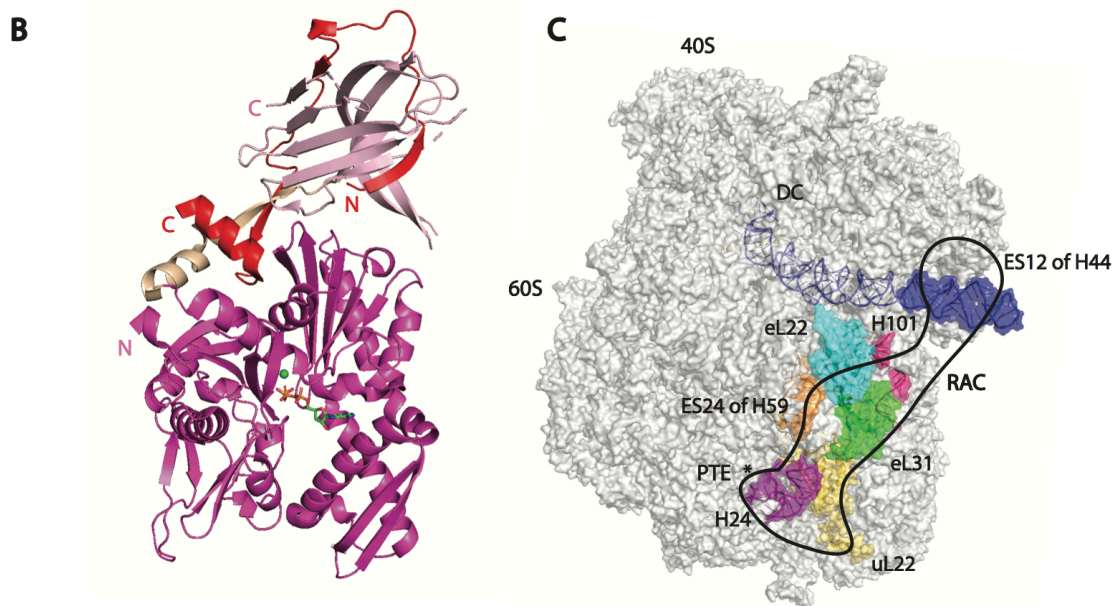


Figure 3-2. Structure of ribosome-associated complex (RAC) (continued)

(B) Ribbon diagram showing RAC heterodimer (full-length Ssz1 and Zuo1 residue 1-60 in *Chaetomium thermophilum*, PDB-6SR6) interacts *via* the Ssz1 linker domain (wheat) and the Zuo1 N-terminus (red). Magenta, NBD. Pink, SDB. **(C)** Structure model of interaction sites of RAC with the 80S ribosome (PDB: 3J78). On the 60S subunits, RAC binds near the PTE (*) *via* ribosomal protein eL22 (cyan), uL22 (yellow), and H24 (violet), H59 of 28S rRNA (orange) as well as eL31 (green) and H101 (magenta). On the 40S subunits, RAC contacts the ES12 of H44 of 18S rRNA (blue), which stems from the decoding center (DC).

recruiting histone acetylases and deacetylases (Boyer et al., 2002; Boyer et al., 2004; Zhang et al., 2017). These differences of Zuo1/Mpp11 between yeast and human indicate that mammalian RAC likely evolved additional functions.

Ssz/Hsp70L1

The canonical Hsp70 consists of a nucleotide-binding domain (NBD) that binds and hydrolyzes ATP, a substrate-binding domain (SBD) that binds neutral and hydrophobic amino acids and followed by a C-terminus domain (CTD) that acts as a lid (Figure 3A). Although Ssz1/Hsp70L1 lost the C-terminus domain of the canonical Hsp70, the nucleotide-binding domain (NBD) that binds and hydrolyzes ATP as well as the substrate-binding domain (SBD) that binds neutral and hydrophobic amino acids retains. Structural analysis indicates that the stable RAC heterodimer is connected *via* the linker domain of Ssz1 and the N-terminus of Zuo1 (Fiaux et al., 2010; Weyer et al., 2017). Although Ssz1 and Hsp70L1 share high structural similarities, they have evolved diverse strategies to assist protein folding of Hsp70 chaperones (Jaiswal et al., 2011). In yeast, RAC (Zuo1 and Ssz1) stimulates the ATP hydrolysis of Ssb (Huang et al., 2005). In mammalian cells, Mpp11 alone is efficient to stimulate the ATP hydrolysis of Hsp70, but requires ATP binding of Hsp70L1 for full function of RAC (Jaiswal et al., 2011).

RAC spans both the ribosomal subunits

RAC is a distinctive ribosome-associate factor that spans both the 40S and 60S ribosomal subunits (Figure 3C) besides the signal recognition particle (SRP) (Figure 4B).

RAC is tethered to the ribosome near the polypeptide exit site of the 60S subunit as well as to interact with the decoding center of the 40S subunit (Lee et al., 2016; Leidig et al., 2013; Peisker et al., 2008; Zhang et al., 2014). In *S. cerevisiae*, Zuo1 has three major contact sites on the ribosome. Genetic, cross-linking (Lee et al., 2016) and cryogenic electron microscopy (cryoEM) (Leidig et al., 2013; Yan et al., 1998; Zhang et al., 2014) data have been interpreted to indicate that on the 60S subunit Thr266, Val273 of Zuo1 interacts with Arg79, Glu81, and Val7 of eL31, and Arg247 and Arg251 of Zuo1 interacts with H24, H59 of 28S rRNA, and eL22. On the 40S subunit, the middle domain (MD) and first helix I domain of Zuo1 interacts with ES12 of H44 of 18S, which originated from the decoding center. The position of RAC on both ribosomal subunits put it in a perfect position to maintain protein homeostasis by coordinating co-translational protein folding and translation (Deuerling et al., 2019; Pechmann et al., 2013; Preissler and Deuerling, 2012; Zhang et al., 2017).

RAC in de novo protein folding

RAC is crucial for stimulating Ssb's ATP hydrolysis required for tight substrate binding and release (Huang et al., 2005; Jaiswal et al., 2011) as well as its substrate selectivity (Doring et al., 2017; Koplin et al., 2010; Willmund et al., 2013). Cross-linking data and genetics analysis revealed that Ssb directly interacts with nascent polypeptides, suggesting its role in *de novo* protein folding (Gautschi et al., 2002; Hundley et al., 2002; Nelson et al., 1992; Pfund et al., 1998). Although RAC has been suggested to have no direct contact with nascent chains (Conz et al., 2007; Gautschi et al., 2002), recent cross-

linking data indicates that Ssz1 can directly interact with the nascent polypeptides prior to Ssb contacts, which suggests that Ssz1 is an active chaperone for co-translational folding (Zhang et al., 2020). Knockout of RAC-Ssb shows a slower growth rate, hypersensitive to protein synthesis inhibitors, resulting in protein aggregation of ribosomal proteins (Koplin et al., 2010; Willmund et al., 2013) as well as ameliorating nuclear rRNA procession (Albanese et al., 2010).

Cells lacking both Ssb and NAC accentuate these phenotypes, suggesting that NAC works in concert with RAC-Ssb to assist *de novo* protein folding of ribosomal biogenesis factors (Albanese et al., 2010; Koplin et al., 2010). Interestingly, Ssb slows down the translation rate for efficient co-translation folding (Willmund et al., 2013). Structural analysis further supports the model that RAC may modulate translation speed by constraining the ribosomal subunits during translation elongation (Zhang et al., 2014). The role of RAC-Ssb in *de novo* folding has been extensively studied in yeast, yet the translation regulatory has just begun to emerge.

RAC in translation

Cells lacking Ssb or RAC display a similar hypersensitive phenotype to protein translation inhibitors, such as paromomycin (Gautschi et al., 2001; Nelson et al., 1992; Yan et al., 1998), which interacts with the helix 44 at the decoding center on the ribosome (Ogle et al., 2003; Zaher and Green, 2009) in yeast. Similarly, loss of mammalian RAC sensitizes to aminoglycoside, including paromomycin (Otto et al., 2005) and G418 (Jaiswal et al., 2011), suggesting a conserved role of RAC in eukaryote

translation. Reporter assays and genetic analyses indicate that loss of Ssb or RAC increases translational stop codon read-through (Lee et al., 2016; Rakwalska and Rospert, 2004) as well as enhanced ribosome pausing on C-terminus poly-AAG/A sequences. Poly-AAG/A is an internal stalling-prone sequence, leading to premature translation termination (Gribling-Burrer et al., 2019). Moreover, cells lacking RAC decreases by -1 programmed ribosomal frameshifting (Muldoon-Jacobs and Dinman, 2006), a strategy to translate protein isoforms or multiple proteins from an mRNA transcript (Caliskan et al., 2015). Structural and toeprinting analysis indicated that RAC interact with helix 44 of 18S RNA, which is at the A-site base of the decoding center, and 25S rRNA at the peptidyl transferase center (PTC) (Gribling-Burrer et al., 2019; Lee et al., 2016; Leidig et al., 2013; Peisker et al., 2008; Zhang et al., 2014). Collectively, functional and structural studies indicate that the RAC-Ssb system plays a crucial role in maintaining translational fidelity in *S. cerevisiae*. Yet, a translation regulatory role, conserved in higher eukaryotes currently lacks experimental support.

Ribosome-associated factors: Signal recognition particle (SRP)

The SRP-dependent protein targeting pathway is highly conserved across all kingdoms. In eukaryotes, the SRP and its membrane-bound SRP (SR) receptor orchestrate co-translational protein translocation machinery of nascent secretory and membrane polypeptides (Gilmore et al., 1982; Walter and Blobel, 1980) by three steps (Figure 4A) (Doudna and Batey, 2004; Halic et al., 2004; Keenan et al., 2001; Koch et al., 2003): first, SRP binds to the hydrophobic signal sequence of the newly polypeptides

as it emerges from the ribosome tunnel exit, and mediates the stalling of the peptide elongation (Pool et al., 2002); second, SRP facilitates the targeting of the mRNA-ribosome-nascent chain complex to the endoplasmic reticulum (ER) membrane in eukaryotes by docking to the membrane-bound SRP receptor (SR) in a GTP-dependent manner; third, the SRP-RNC complex transfers the RNC to the protein-conducting channel, translocon (Johnson and van Waes, 1999; Matlack et al., 1998; Pohlschroder et al., 1997). The eukaryotic SRP, a highly conserved ribonucleoprotein (RNP), is composed of six proteins (named by their molecular weight: SRP9, 14, 19, 54, 68, 72) and the 7S RNA (Figure 4B) (Walter and Blobel, 1981, 1982). SRP has two main structure domains (Figure 4B): the Alu domain, including the SRP9/14 heterodimer and the 5'- and 3'-terminus of 7S RNA, mediates the pausing of the peptide elongation (Siegel and Walter, 1986); the S domain, including the SRP 19, 54, 68/72 heterodimer and the middle domain of the 7S RNA, facilitates protein translocation (Siegel and Walter, 1988). SRP54, which is the key player for protein translocation, comprises of an N-terminus domain (N), a central GTPase domain (G), and a C-terminus methionine-rich domain (M) (Bernstein et al., 1989). The N and G domains are structurally and functionally coupled. The mammalian SRP-receptor (SR) is a heterodimer comprised of an α -subunit (SR α), which also contains an NG domain that is structurally similar to the NG domain of SRP54, and a β -subunit (SR β). SRP54 M domain mediates the recognition of the signal sequence (Bernstein et al., 1989; Zopf et al., 1990) as well as the interaction of the SRP RNA (Batey et al., 2000; Kurita et al., 1996; Romisch et al., 1990). Both SRP54 and SRP receptor, which are both GTPase, comprise a unique insertion-box

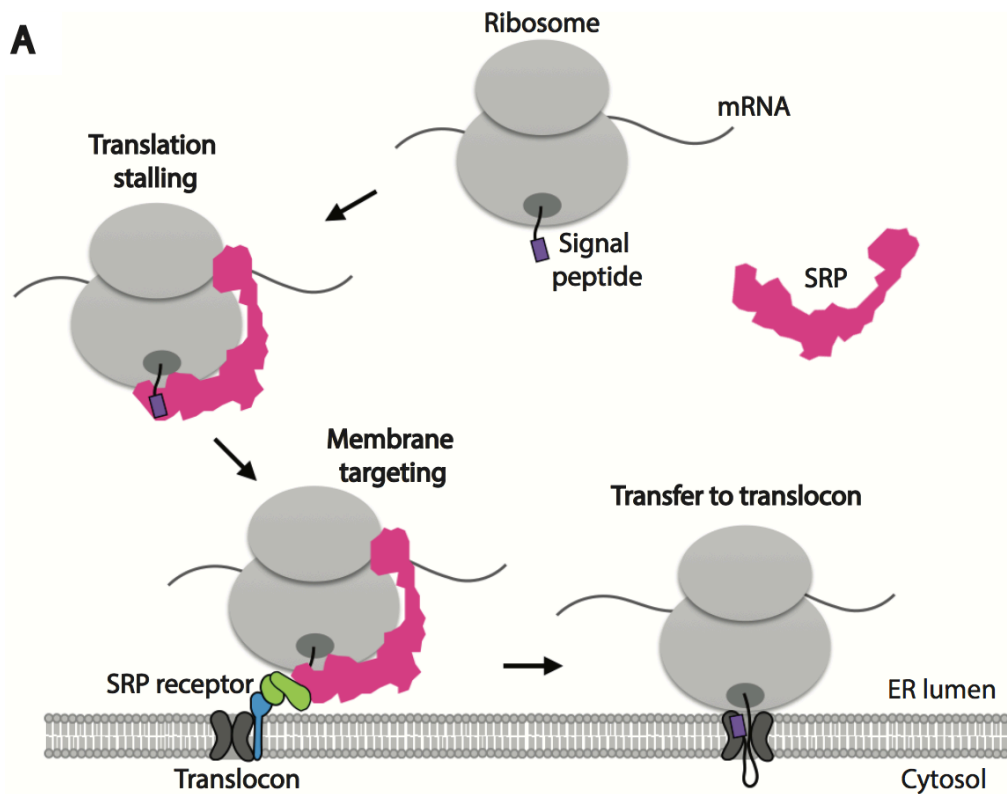


Figure 4-1. SRP-dependent co-translational protein translocation machinery in eukaryotes

(A) The current model of the co-translational targeting of nascent secretory and membrane polypeptides. First, SRP (magenta) binds to the hydrophobic signal sequence (purple) of the newly polypeptides as it emerges from the ribosome tunnel exit, forming a SRP-mRNA-ribosome-nascent chain (R-RNC) triggers a translational arrest; second, SRP facilitates the R-RNC membrane targeting in eukaryotes (plasma membrane in prokaryotes) by docking to the membrane-bound SRP receptor (SR) in a GTP-dependent manner; third, the SRP-R-RNC transfers the RNC to the translocon protein-conducting channel (Charcoal). Green, SR α . Cyan, SR β .

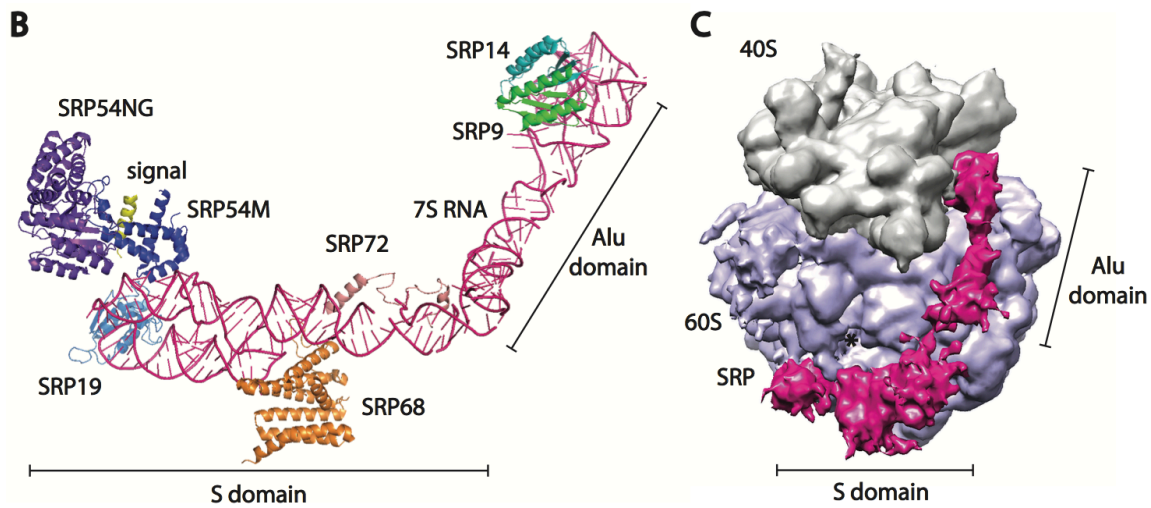


Figure 4-2. SRP-dependent co-translational protein translocation machinery in eukaryotes (continued)

(B) Ribbon representation of mammalian SRP. SRP68 and 72 (PDB-5M73) were modeled onto SRP (PDB-1RY1). SRP consists of six proteins (SRP9, 14, 19, 54, 68, 72) and the 7S RNA (magenta). SRP has two main structure domains: the Alu domain, including the SRP9 (green)/14 (cyan) heterodimer and the 5'- and 3'-terminus of 7S RNA, mediates the pausing of the peptide elongation; the S domain, including the SRP 19 (light blue), 54 (M, blue; NG, purple), 68 (orange) /72 (wheat) heterodimer and the middle domain of the 7S RNA, facilitates protein translocation. (C) Cryo-EM structure of mammalian SRP with the 80S ribosome (EMD-1063). SRP (magenta) spans both the 40S (grey) and 60S (lavender) ribosomal subunits.

domain (IBD) within the G domain carrying out not only nucleotide exchange but also SRP-SR interactions through their respective NG domains (Connolly and Gilmore, 1989; Freymann et al., 1997; Moser et al., 1997; Zopf et al., 1993).

SRP bridges both ribosomal subunits

Cross-linking and structure data suggest that SRP contacts ribosomal proteins uL23 and uL29 on the 60S subunit *via* NG domain of SRP54 (Figure 4C) (Beckmann et al., 2001; Gu et al., 2003; Halic et al., 2004; Pool et al., 2002). SRP54 also contacts ES24 of H59, H24 of 25S rRNA, and signal sequence *via* its M domain (Halic et al., 2004; Halic et al., 2006). These three SRP54-ribosome contact sites are shared with the ribosome contact sites used by translocon-ribosome, supporting the notion that SRP dissociates from the RNC as the RNC binds to the translocon. In addition, the Alu domain of SRP contacts the H5 and H15 of 18S RNA on the 40S subunit (Halic et al., 2006). Intriguingly, the Alu domain-ribosome contact sites are similarly occupied by eukaryotic translation elongation factor 2 (eEF2) (Gomez-Lorenzo et al., 2000; Halic et al., 2004; Spahn et al., 2004; Wilson et al., 2002), suggesting that the Alu domain-ribosome interaction disrupts peptide elongation by blocking eEF2 binding. Cryo-EM structure further indicated an empty ribosome A-site as SRP Alu domain binds to the RNC, indicating the arrest of peptide elongation (Halic et al., 2004). The SRP position on both ribosomal subunits supports its co-translational role not only in protein translocation but also in translation.

The interplay between ribosome-associated factors

As the nascent chain emerges from the ribosome tunnel exit, the ribosome-associated protein biogenesis factors directly interact with the nascent polypeptide chains to engage in enzymatic processing, folding, and/or targeting to designated organelles. In prokaryotes, the peptide deformylase (PDF) first contacts the nascent polypeptides followed by the methionine aminopeptidase (MAP) to remove N-terminal methionine (Gigliione et al., 2009; Jha and Komar, 2011). For secretory or membrane proteins bearing a strong hydrophobic signal sequence, SRP binds to the RNC complex and target to the membrane, while TF has a high preference to outer membrane β -barrel and cytoplasmic proteins (Bornemann et al., 2014). There has been controversy over whether SRP and TF work collaboratively or competitively with each other on the ribosome. Recent structural studies have supported the model that SRP and TF can simultaneously bind to the same translating ribosomes (Bornemann et al., 2014; Buskiewicz et al., 2004; Raine et al., 2004). TF ensures the fidelity of SRP substrate selectivity by modulating the initial SRP binding to the RNC, targeting of the SRP-RNC to the membrane, and ejection of SRP from the RNC as the nascent polypeptides chain reach longer length (Ariosa et al., 2015). Additionally, a study suggests that PDF and MAP can act not only sequentially but also simultaneously with SRP and TF on translating ribosomes (Bornemann et al., 2014). The interplay between ribosome-associated biogenesis factors is better understood in prokaryotes than in eukaryotes.

In eukaryotes, after MAP excises the N-terminal methionine of the nascent polypeptides, N-acetyltransferases (NAT) carries out N-terminal acetylation, which

occurs in 80% of the cytosolic mammalian proteins but is rarely found in prokaryotes. N-terminal acetylation can regulate protein stability by serving as a degradation signal (degron) that targeted by the ubiquitin ligase (Hwang et al., 2010; Varshavsky, 2011) or enhance accurate protein targeting machinery by acting as a cytosolic retention signal (Forte et al., 2011). Recent work has begun to illuminate that N-terminal acetylation modulates cellular apoptotic and metabolic state by regulating acetyl-CoA (Yi et al., 2011). Additionally, NAC, which partially resembles the substrate selective function of TF in bacteria, also modulates SRP specificity by blocking initial SRP binding and SRP-independent ribosome targeting to translocon in *C. elegans*, preventing mitochondrial proteins mistargeting to the ER (del Alamo et al., 2011; Gamerdinger et al., 2015; Zhang et al., 2012).

Interestingly, numerous ribosome-associated biogenesis factors, including MAP, NAT, SRP, translocon, TF, and NAC, share a universal docking site, uL23 (Ferbitz et al., 2004; Kramer et al., 2002; Polevoda et al., 2008; Pool, 2005; Pool et al., 2002; Ullers et al., 2003; Wegrzyn et al., 2006). This universal docking site could serve as a substrate selectivity checkpoint to modulate factor binding timing. Biochemical data suggest that NAC and MAP could bind simultaneously to translating ribosomes and have no impact on each other's binding affinity to the ribosomes (Nyathi and Pool, 2015). Notably, structural data suggest that SRP and RAC sterically clash when concomitantly modeled onto the ribosome (Zhang et al., 2014). This is consistent with the concept that SRP and Ssb have diverse substrate pools: SRP preferentially binds to secretory and membrane nascent polypeptides, while Ssb bind to predominately cytosolic and nuclear nascent

polypeptides (Willmund et al., 2013). On the other hand, it has been indicated that NAC and Ssb shared overlapping substrate pools (del Alamo et al., 2011; Koplín et al., 2010; Pechmann et al., 2013). A recent study indicates that NAC could modulate the binding quantity of Ssb substrates, while it has no effect on substrate selection of Ssb in yeast (Doring et al., 2017). Indeed, the dynamics of how SRP, RAC-Ssb, and NAC collaborate or compete with each other on the ribosome to engage in the nascent polypeptides remain obscure in the mammalian system.

II-2. Quality Control

To minimize aberrant protein production, co-translational surveillance pathways selectively degrade mRNAs that code for aberrant proteins, degrade the aberrant proteins themselves, and recycle the stalled ribosomal subunits for use in future translations. Aberrant mRNAs are recognized by nonsense-mediated decay (NMD), nonstop decay (NSD), no-go decay (NGD), and regulates aberrant protein production (RAPP) systems. Defective nascent polypeptides are recognized by ribosome-associated protein quality control (RQC) and trigger ribosome recycling. In parallel, misfolded proteins activate stress response mechanisms that alter proteostasis by reducing global protein translation and/or enhancing molecular chaperone production to adapt to stress. Two major stress response pathways are the heat shock response (HSR) in the cytosol and the unfolded protein response (UPR) in the ER. Quality control pathways relevant to this study will be reviewed in this chapter.

mRNA quality control

No-go decay (NGD)

NGD detects mRNAs that contain an obstacle to elongation caused by stable mRNA secondary structure (Doma and Parker, 2006; Tsuboi et al., 2012), such as stem-loops, pseudoknots, depurination of mRNA (Gandhi et al., 2008), or rare codons (Chen et al., 2010; Kuroha et al., 2010; Schuller and Green, 2018) (Figure 5). The endonucleolytic cleavage at the mRNA upstream of the stalled ribosome, which is the hallmark of NGD, was first demonstrated by northern blot (Doma and Parker, 2006) and further supported by sequencing analyses and high-resolution ribosome profiling recently (Arribere and Fire, 2018; Guydosh et al., 2017; Simms et al., 2017). A recent study suggested that ribosome collision on a polysome is a prerequisite to initiating NGD (Simms et al., 2017). Biochemical and sequencing analyses indicated that multiple stacked ribosomes trigger robust NGD, and the endonucleolytic cleavage occurs between colliding ribosomes by an unknown endonuclease.

A recent study has identified that Cue2 as the endonuclease triggering NGD in yeast (D'Orazio et al., 2019). Biochemical analysis and ribosome profiling suggested that Cue2 cleaves mRNA in the A-site of the colliding ribosome, and Dom34 (Pelo in mammal) rescues the collided ribosome. Dom34 and Hbs1, which structurally and functionally resembled the termination factors eRF1 and eRF3 (Atkinson et al., 2008; Chen et al., 2010; Graille et al., 2008), respectively, recruit to the A-site of the stalled ribosome (Becker et al., 2011). The ATPase Rli1 (ABCE1 in human) works together

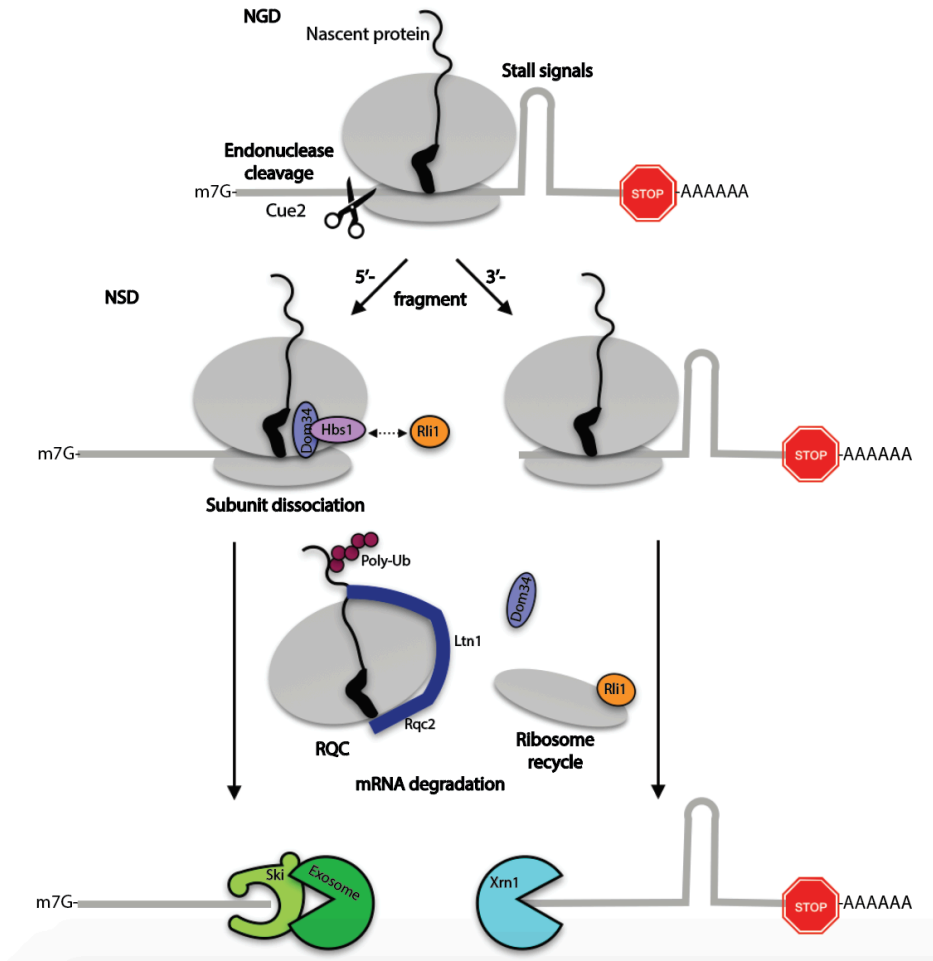


Figure 5. The mechanism of no-go decay (NGD) and nonstop decay (NSD)

NGD detects translation stalling when elongation is blocked by stable mRNA secondary structure. The mRNA endonucleolytic cleavage by Cue2 occurs upstream of the stalled ribosome. Nonstop transcripts may result from endonucleolytic cleavage that leads to truncated mRNA at the 3' end of the mRNA. The classification between NGD and NSD has become blurring, and both share similar mRNA decay machinery following endonucleolytic cleavage. The stalled targets of NGD and NSD are recognized by Dom34 (Pelo in mammal) and Hbs1, together with Rli1 (ABCE1 in mammalian cells), triggering ribosome-associated protein quality control (RQC) for degradation of defective nascent polypeptides, ribosome recycling, and mRNA degradation. The Ski complex and exosome degrade mRNA from 3'-to-5', while the exonuclease Xrn1 degrades mRNA from 5'-to-3'.

with Dom34, triggering ribosome subunit dissociation and mRNA release for ribosome recycling (Pisareva et al., 2011; Shoemaker et al., 2010; Tsuboi et al., 2012). Subsequently, the Ski complex and exosome degrade mRNA from 3'-to-5', while the exonuclease Xrn1 degrades mRNA from 5'-to-3'. NGD not only functions as an mRNA quality control mechanism but also regulates the stability of normal mRNA. For example, the CGS1 mRNA encoding the cystathionine gamma-synthase, which is a crucial enzyme in methionine biosynthesis, is regulated through NGD in *Arabidopsis thaliana* (Chiba et al., 1999; Chiba et al., 2003). Recent studies have begun to shed light on the mechanism of NGD in yeast (Harigaya and Parker, 2010; Ikeuchi et al., 2018), fly (Passos et al., 2009), and plant (Szadeczky-Kardoss et al., 2018); however, the mechanisms in mammals remain incompletely defined.

Non-stop decay (NSD)

NSD detects mRNAs that lack a termination codon triggering rapid mRNA degradation from the 3'-end independent of deadenylation (Frischmeyer et al., 2002; van Hoof et al., 2002). Nonstop transcripts may result from endonucleolytic cleavage that leads to truncated mRNA without poly(A) tail at the 3' end of the mRNA or erroneous poly(A) within the open reading frame (ORF) (Figure 5). Emerging studies have suggested that the ribosome may not be stalled at the 3' end of the mRNA in poly(A) read-through, early ribosome stalling may occur instead *via* the interaction between the positively charged polylysine peptide and the negatively charged ribosome tunnel exit (Ito-Harashima et al., 2007; Lu and Deutsch, 2008). The classification between NSD and

NGD has become blurring and both share similar mRNA decay machinery following endonucleolytic cleavage.

Biochemical and structural analysis suggested that Dom34 and Hbs1 work in concert with Rli1 (ABCE1 in mammal) promote ribosome subunits dissociation, mRNA release, peptidyl-tRNA drop off, and recruit the exosome-Ski complex in yeast (Pisarev et al., 2010; Pisareva et al., 2011; Shoemaker et al., 2010; Shoemaker and Green, 2011; Tsuboi et al., 2012). Cryo-EM data further supported that Pelo occupies the empty A-site on the stalled ribosome (Kobayashi et al., 2010), and ABCE1 induces ribosome splitting (Becker et al., 2012). In yeast, Ski7, which may have a redundant role with Dom34 (Tsuboi et al., 2012), is structurally related to Hbs1 and is capable of recognizing stalled ribosomes and initiating recruitment of the exosome which degrades mRNA from 3'-to-5' (Frischmeyer et al., 2002; van Hoof et al., 2002). Accumulating studies have indicated that nonstop mutations in certain genes may cause diseases (Klauer and van Hoof, 2012). For example, nonstop mutation in DEFB126 gene produces nonfunctional β -defensin 126 protein, which is essential for sperm function (Yudin et al., 2005), and is associated with lower fertility in man (Tollner et al., 2011).

Regulates aberrant protein production (RAPP)

Recently, our lab uncovered a novel mRNA surveillance mechanism detecting mutations in the signal sequence of secretory proteins that interfered with SRP54 binding, termed regulates aberrant protein production (RAPP). As the nascent polypeptides emerge from the ribosomal tunnel exit, the mutant peptide fails to interact with its

original targeting factor SRP, and the defective mRNA is selectively degraded (Karamyshev et al., 2014; Popp and Maquat, 2014). A study has indicated that RAPP plays a role in neurodegenerative disease frontotemporal lobar degeneration (FTLD) through modulating the mRNA stability of the secretory protein progranulin (GRN) (Pinarbasi et al., 2018). The mRNA of A9D and W7R GRN disease-causing mutations are endogenous substrates for RAPP. A9D and W7R GRN, which the mutation in the N-terminal signal sequence disrupts the hydrophobic region, disturbs co-translational interaction with SRP. Next, the aberrant mRNA degraded preemptively preventing defective protein production. Moreover, the nuclease responsible for RAPP remains obscure. Whether RAPP has a broader substrate pool, besides the current identified secretory proteins, remains undefined.

The unfolded protein response (UPR)

In eukaryotes, the ER is the key organelle for producing secretory and membrane proteins. To ensure protein homeostasis in the ER, the UPR senses misfolded proteins and responds to cellular stresses *via* translational and transcriptional regulation (Walter and Ron, 2011). If the ER stress is not resolved, ER stress drives cell fate decision and lead to human diseases, including cancer, neurodegeneration, and metabolic syndromes (Walter and Ron, 2011; Wang and Kaufman, 2016). In mammalian cells, three branches are involved in the UPR pathway, each directed by its unique signal transducer in the ER membrane: inositol-requiring protein 1 α (IRE1 α), double-stranded RNA-activated protein kinase (PKR)-like endoplasmic reticulum kinase (PERK), and activating

transcription factor 6 (ATF6). Upon ER stress, IRE1 α oligomerizes, autophosphorylates, and *via* endonucleolytic cleavage, splices Xbp1 mRNA as well as degrades ER-bound mRNAs (RIDD) (Figure 6); PERK oligomerizes, autophosphorylates and phosphorylates the translation initiation factor eIF2 α , down-tuning global translation; ATF6 transports to Golgi, processed by protease, and the N-terminal cytosolic fragment releases to the nucleus, transcriptionally activating UPR target genes. The IRE1 α branch is the main focus of this study. The downstream regulation of the stress sensors is relatively well characterized, yet, the sensing mechanism remains controversial.

IRE1 branch

IRE1, a bifunctional transmembrane protein, is the best understood and conserved UPR branch in eukaryotes (Cox et al., 1993; Mori et al., 1993) and the only branch in yeast (Mori, 2009). In mammals, IRE1 has two isoforms: IRE1 α is ubiquitously expressed in all tissues, while IRE1 β selectively expressed in the digestive track (Bertolotti et al., 2001; Tsuru et al., 2013). IRE1 α is composed of an N-terminal ER luminal domain (LD), a transmembrane helix, a flexible cytosolic linker, and followed by a kinase and a C-terminal endonuclease (RNase) domain (Figure 7A) (Back et al., 2005). IRE1 detects ER stress through its LD domain (Credle et al., 2005; Zhou et al., 2006), and triggers face-to-face dimerization (Liu et al., 2000; Oikawa et al., 2009; Tirasophon et al., 1998) facilitating trans-autophosphorylation (Mori et al., 1993; Shamu and Walter, 1996; Zhou et al., 2006) (Figure 7B). Next, the binding of nucleotide

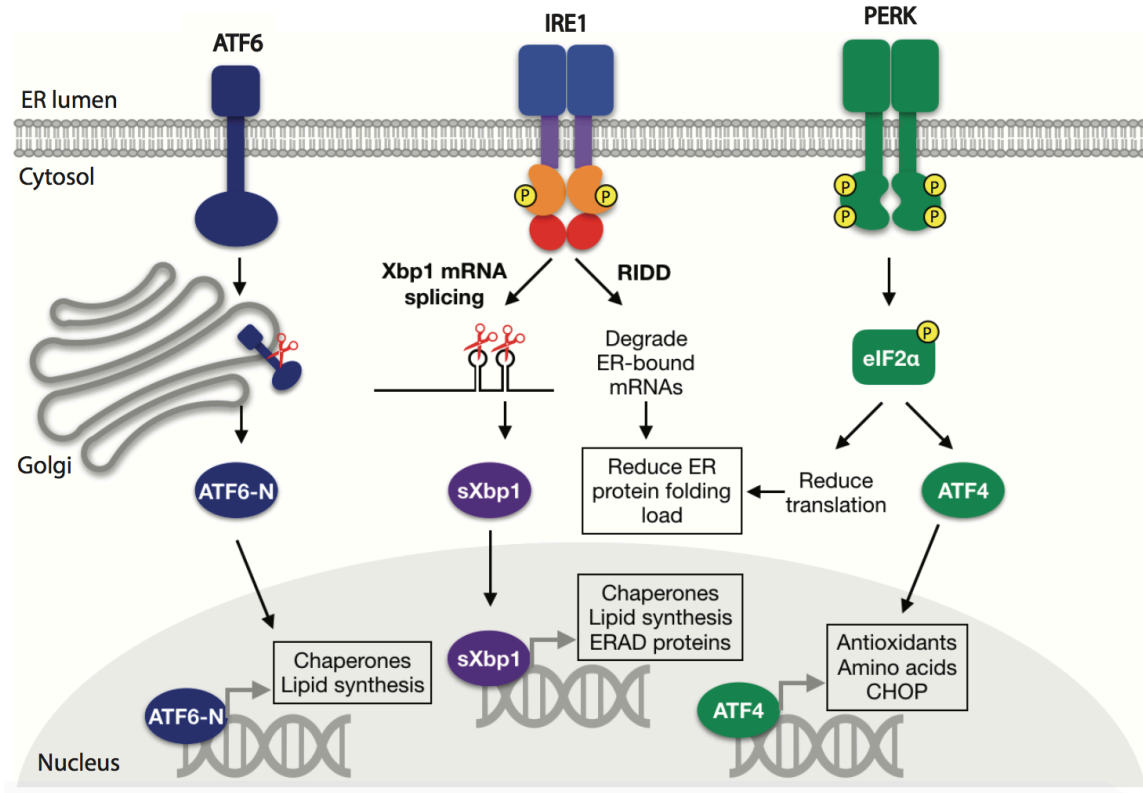


Figure 6. The three arms of the unfolded protein response in eukaryotes

In mammalian cells, three signal transduction pathways in the ER membrane direct the activation of three distinct unfolded protein responses. In the presence of ER stress, IRE1 oligomerizes, autophosphorylates, and noncanonically splices the Xbp1 mRNA as well as degrades ER-bound mRNAs (RIDD); PERK oligomerizes, autophosphorylates and phosphorylates the translation initiation factor eIF2 α , reducing global translation; ATF6 transports to Golgi, processed by protease, and the N-terminal cytosolic fragment releases to the nucleus. Transcriptional factors activate UPR target genes to increase protein folding capacity, while IRE1 and PERK reduce ER protein folding load by down-regulating translation.

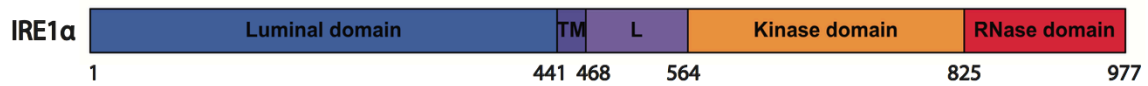
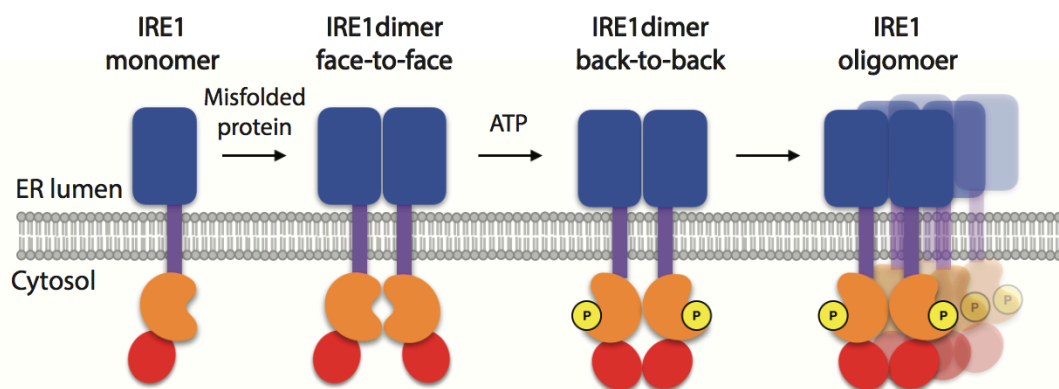
A**B**

Figure 7. The overall architecture of IRE1 α and the current model of IRE1 activation

(A) Protein domain of human IRE1 α . IRE1 α consists of an N-terminal ER luminal domain (LD, blue), a transmembrane helix (TM, purple), a flexible linker (L, purple), and followed by a kinase (orange) and a C-terminal endonuclease domain (RNase, red). (B) IRE1 detects ER stress through its luminal domain (LD), triggers face-to-face dimerization, facilitates trans-autophosphorylation, stabilizes back-to-back dimer configuration by the binding of nucleotide, and stacks into higher-order oligomers enabling active RNase activity.

(ATP/ADP) stabilizes a back-to-back dimer configuration (Lee et al., 2008) and stacks into high-order oligomers (Korennykh et al., 2009) enabling active ribonuclease activity. Then, IRE1 splices Hac1 mRNA in yeast (Cox and Walter, 1996; Sidrauski and Walter, 1997) (Xbp1 in mammals) (Calfon et al., 2002; Yoshida et al., 2001) in a non-canonical spliceosome-independent manner, producing a stress-responsive transcriptional factors Hac1/Xbp1 (Cox and Walter, 1996).

IRE1 stress-sensing models: the competition and direct ligand binding models

Two models have been proposed for sensing ER stress *via* IRE1 LD: the competition and the direct ligand binding model (Adams et al., 2019; Karagoz et al., 2017). The competition model proposed that BiP (also name GRP78, HSPA5), an ER Hsp70 chaperone, is the primary regulator of IRE1 activation *via* dissociation of BiP from the IRE1 LD upon ER stress. The model was supported by overexpression of BiP, the UPR activation reduced in mammalian cells (Dorner et al., 1992) and yeast (Kohno et al., 1993) as well as increased cell viability upon ER stress (Morris et al., 1997). Additionally, studies indicated that BiP binds to the ER stress sensors, IRE1, PERK, and ATF6, and dissociated upon ER stress (Bertolotti et al., 2000; Okamura et al., 2000; Shen et al., 2002). However, in yeast, depletion of the BiP-binding domain of IRE1 did not abrogate IRE1 activation upon tunicamycin treatment (Kimata et al., 2004), but prolongs the recovery time after IRE1 activation (Pincus et al., 2010). This suggests that BiP is not required for IRE1 activation, but rather facilitates the de-oligomerization and deactivation of IRE1, which is incompatible with the competition model. Due to the current lack of

structural analysis of the BiP and IRE1 interaction, the detailed role of BiP in modulating IRE1 remains incomplete.

The direct binding model proposed that IRE1 senses ER stress *via* direct binding of unfolded proteins to IRE1 LD, stabilizing its oligomeric state for activity. Structural data suggest that the dimerization interface of the yeast IRE1 core luminal domain contains anti-parallel β -sheets forming a deep groove, which architecturally resembles the major histocompatibility complex I (MHC I) (Credle et al., 2005). This suggests that unfolded protein is able to bind to yeast IRE1 LD as a direct ligand for MHCs. Biochemistry data further indicated that yeast IRE1 could directly bind to peptides with a high preference toward basic and hydrophobic residues and forms larger oligomers in the presence of peptides (Gardner and Walter, 2011). Additionally, although there are structural differences between yeast and human IRE1, structural and biochemical analysis indicates that the IRE1 ER stress sensing mechanism conserved across yeast to human, which unfolded protein act as a ligand directly binds to IRE1 LD and induces oligomerization favorable conformational changes (Karagoz et al., 2017).

IRE1 oligomerization

Oligomerization is the essential step for IRE1 activation both in yeast (Aragon et al., 2009; Kimata et al., 2007) and mammal (Li et al., 2010). Structural analysis indicated that the oligomer is composed of back-to-back IRE1 dimers stacking together in a clockwise manner that resembles the architecture of the DNA double helix (Korennykh et

al., 2009). Mutations in all three interfaces in the oligomer disrupt RNase activity, suggesting the extensive molecular surface of oligomer may be central to IRE1 activation. Additionally, IRE1 oligomers can be monitored by foci formation *in vivo* utilizing an IRE1-GFP cassette after challenge with either tunicamycin (Li et al., 2010) or thapsigargin (Tam et al., 2014). After ER stress is initiated, IRE1 α forms visible foci at 1 hr, condenses to large foci at 4 hr, and dissolves by 8 hr in mammals, the time course of Xbp1 splicing activity correlates with the formation and dissolution of the large foci (Li et al., 2010; Tam et al., 2014). Currently, the detailed mechanism of formation of IRE1 foci and how IRE1 recycles after activation remain obscure.

Hac1/Xbp1 mRNA splicing

Hac1 mRNA in yeast

In yeast, in the absence of ER stress, ribosome stalled on Hac1 unspliced mRNA. The translational attenuation of Hac1 results from the base-pairing interaction between the Hac1 5' UPR and the intron (Ruegsegger et al., 2001) and is a prerequisite for mRNA targeting to UPR-induced IRE1 foci (Aragon et al., 2009) (Figure 8A). The targeting of Hac1 mRNA to the IRE1 foci is mediated by the 3'UPR bipartite element (3'BE), a conserved region of an extended stem-loop in the 3'UTR (Aragon et al., 2009). Upon ER stress, IRE1 cleaves Hac1 mRNA at both splice junctions in a non-canonical spliceosome independent manner (Gonzalez et al., 1999; Sidrauski and Walter, 1997). The Rlg1 tRNA ligase rejoins the exons after the excision of the 252 nucleotides long intron (Sidrauski et al., 1996; Sidrauski and Walter, 1997). Mutation in the Hac1 mRNA translation stalling

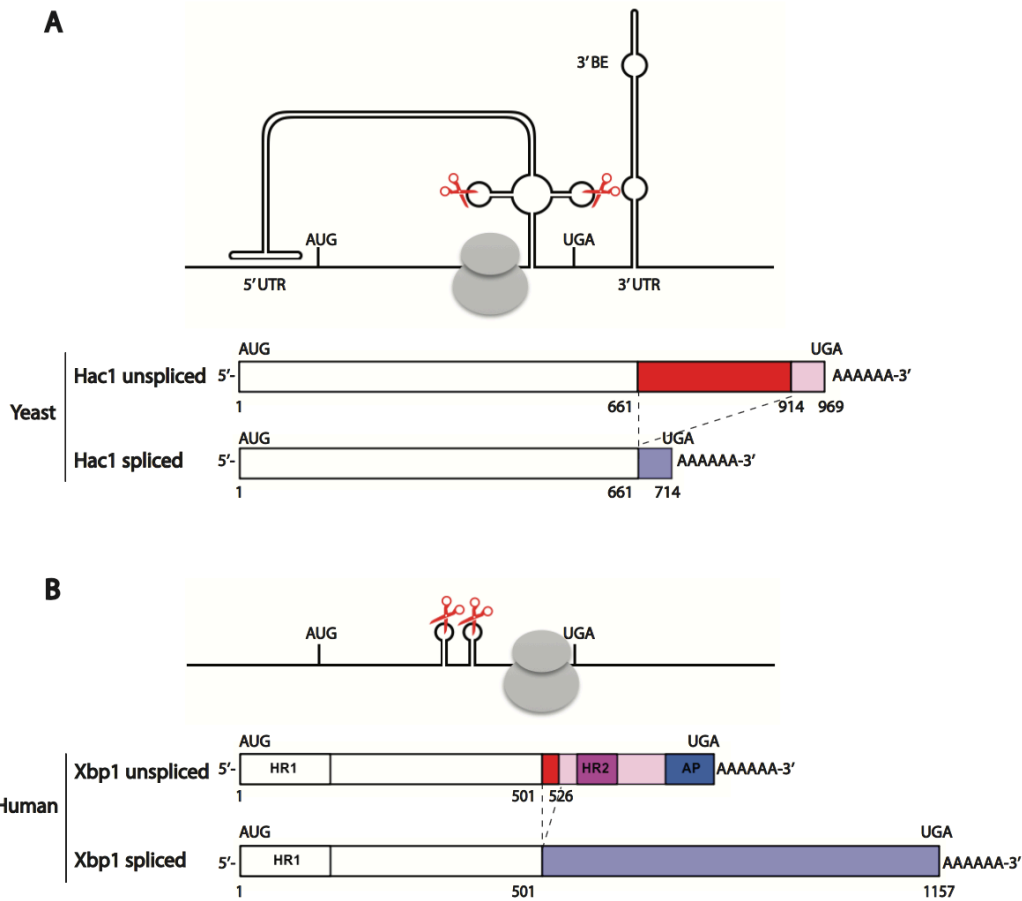


Figure 8. Schematic of yeast Hac1 and human Xbp1 mRNA

(A) In yeast, the translational stalling of Hac1 results from the base-pairing interaction between the Hac1 5'UPR and the intron. The targeting of Hac1 mRNA to IRE1 is mediated by the 3'UPR bipartite element (3'BE), an extended stem-loop in the 3'UTR. Upon ER stress, IRE1 cleaves Hac1 mRNA at both splice junctions (scissors), excising the 252 nucleotides long intron. White region, the shared domain of both uHac1 and sHac1. Red region, spliced intron. Pink and lavender region, the distinct segment of uHac1, sHac1, respectively. (B) In mammals, the C-terminal 26 residues act as an arrest peptide (AP, blue) in the ribosomal tunnel forming a unique turn distorts the PTC and induce the translational pausing of Xbp1 mRNA. The hydrophobic region 2 (HR2, magenta) of Xbp1 is essential for targeting Xbp1 mRNA to the ER membrane *via* SRP-dependent mechanism. Upon ER stress, IRE1 excises out the 26-bases intron (scissors).

(Aragon et al., 2009; Ruegsegger et al., 2001), mRNA targeting (Aragon et al., 2009), or exon ligation (Sidrauski et al., 1996; Sidrauski and Walter, 1997) machinery disturb Hac1 mRNA splicing, indicating its central role in UPR.

Xbp1 mRNA in mammal

Similar to Hac1 in yeast, translation of unspliced Xbp1 (Xbp1u) is initiated and then stalls as required for efficient targeting of the complex to the ER membrane in the absence of ER stress and relocalizes to the cytosol after endonucleolytic cleavage upon ER stress (Yanagitani et al., 2009) (Figure 8B). A tRNA ligase, RtcB, rejoins the exons after excision of the 26-bases intron (Jurkin et al., 2014; Kosmaczewski et al., 2014; Lu et al., 2014). In mammals, the Xbp1u protein is translated in the absence of ER stress (Calfon et al., 2002; Yoshida et al., 2001), unlike HAC1 in yeast. A study has indicated that Xbp1u protein is a negative regulator of Xbp1 spliced (Xbp1s) protein by forming an Xbp1u-Xbp1s complex triggering proteasome degradation and shuts off the UPR (Yoshida et al., 2001). Although translation stalling is required for both Hac1 and Xbp1 mRNA, the pausing and targeting mechanisms are different in yeast to mammals.

In mammals, studies have indicated that the hydrophobic region 2 (HR2) of Xbp1 is critical for targeting Xbp1 mRNA to the ER membrane (Yanagitani et al., 2009; Yanagitani et al., 2011). Furthermore, although Xbp1 mRNA does not contain a canonical signal sequence, studies have indicated that Xbp1 mRNA targets to Sec61 β in an SRP-dependent manner *via* SRP binding to the HR2 of Xbp1 (Kanda et al., 2016; Plumb et al., 2015). Additionally, the proximity of the IRE1 α kinase/RNase and its

substrate Xbp1 is vital for efficient Xbp1 splicing. Studies have suggested that IRE1 α interacts with translocon Sec61 β *via* its C-terminal end of the luminal domain, amino acid 434 to 443 (Kanda et al., 2016; Plumb et al., 2015). Knockdown of SRP54 diminishes Xbp1 mRNA targeting to Sec61 β and Xbp1 splicing activity, and knockdown of SR α or Sec61 β abolishes Xbp1 splicing activity (Kanda et al., 2016; Plumb et al., 2015).

Kohno's group had identified that the C-terminal 26 amino acid of Xbp1u is essential for translation pausing at an unknown mechanism (Yanagitani et al., 2011). Interestingly, recent structural data indicated that the C-terminal 26 residues act as an arrest peptide (AP) in the ribosomal tunnel forming a unique turn distorts the PTC and induces the translational stalling of Xbp1u mRNA (Shanmuganathan et al., 2019). With the advancement of ribosome profiling, the ribosome stalling of Xbp1 mRNA can be monitored *in vivo* in mouse embryonic stem cells (Ingolia et al., 2011). When translation stalled at the 3' end of mRNA, Dom34 and Hbs1 senses the aberrant mRNA and initiates no-go decay (NGD). Emerging studies have demonstrated that deletion of Dom34 or Hbs1 in *S. cerevisiae* (Guydosh and Green, 2014) and deletion of both Pelo and Ski complex in *C. elegans* (Arribere and Fire, 2018) enhance Xbp1 ribosome stalling, suggesting that the clearance of Xbp1u stalling transcripts is mediated *via* NGD by Dom34 and Hbs1. The translation pausing mechanism of Xbp1 mRNA has begun to uncover, however, how Xbp1u mRNA releases from the pausing complex in the absence of ER stress and how Xbp1s mRNA reinitiates translation and release in the presence of ER stress remain obscure.

Regulated IRE1-dependent decay of mRNA (RIDD)

Besides performing HAC1/Xbp1 mRNA splicing, IRE1 also engages in regulated IRE1-dependent decay of mRNA (RIDD) to alleviate ER stress (Maurel et al., 2014). Interestingly, a biochemical analysis indicated that Hac1/Xbp1 mRNA splicing is carried out by IRE1 oligomer, while RIDD is performed by IRE1 dimer (Tam et al., 2014). RIDD, which is first discovered in *Drosophila*, preferentially degrades ER-localized mRNAs that cleaved the Xbp1-like consensus site (Hollien and Weissman, 2006). Emerging studies indicated that RIDD also is observed in mammals (Han et al., 2009; Hollien and Weissman, 2006), *S. pombe* (Guydosh et al., 2017; Kimmig et al., 2012) (Nicholas R Guydosh 2017), and *Arabidopsis* (Mishiba et al., 2013). Studies further suggested that RIDD may be a sequence-specific event, recognizing substrates bearing 5'-CUGCAG-3' in mammal (Oikawa et al., 2010) or 5'-UGCU-3' in *S. pombe* (Kimmig et al., 2012). However, these putative substrates have yet to be validated *in vivo*. Studies indicated that RIDD induces cell death when ER stress is irremediable (Han et al., 2009; Tam et al., 2014). Yet, how RIDD distinguishes basal and pro-death signals remains undefined.

Mechanisms of IRE1 regulation

IRE1 is a master regulator in cell fate decisions upon ER stress. IRE1 activates Xbp1 splicing for pro-survival response and initiates RIDD for pro-apoptotic response. This section discusses other modulatory mechanisms of IRE1 activity, including IRE1 stability, attenuation, and adaptor proteins regulating downstream responses in cell fate

determination.

IRE1 stability and attenuation

A study indicated that the Hsp90 chaperone stabilizes IRE1 protein by interaction with the IRE1 cytosolic domain, and the Hsp90-IRE1 interaction is stable in the absence and presence of the ER stress (Marcu et al., 2002). IRE1 activity can also modulate through IRE1 attenuation by two mechanisms. From the ER luminal side, the BiP co-chaperone ERdj4 acts as an IRE1 repressor associated with IRE1 LD recruiting BiP and abolishes IRE1 dimers (Amin-Wetzel et al., 2017). Knockout of ERdj4 increases IRE1 phosphorylation. Expression of H54Q ERdj4 mutant, which abolishes its interaction with its Hsp70, did not counteract the IRE1 activity in ERdj4 knockout cells, and biochemical assay indicated that the ERdj4 mutant disturbs the complex formation between IRE1 and BiP. From the cytosolic side, PERK attenuates IRE1 *via* RNA polymerase II-associated protein 2 (RPAP2). Knockdown of phosphatase RPAP2 enhances IRE1 phosphorylation upon ER stress induced by brefeldin A, and overexpression of RPAP2 inhibits IRE1 phosphorylation in PERK knockdown cells, indicating that RPAP2 acts downstream of PERK (Chang et al., 2018). The detailed mechanisms of IRE1 attenuation begin to unfold.

IRE1 interactome

The kinase domain of IRE1 recruits adaptor proteins to modulate downstream responses. In the presence of ER stress, IRE1 recruits the TNF receptor-associated factor

2 (TRAF2) (Urano et al., 2000) mediating activation of the apoptosis signal-regulating kinase (ASK1) (Nishitoh et al., 2002) and the c-Jun N-terminal kinase (JNK) inducing programmed cell death as well as the nuclear transcription factor-kB (NF-kB) (Kaneko et al., 2003) inducing stress responsive prosurvival genes. Additionally, IRE1 also recruits the proapoptotic BCL-2 family members BAX and BAK upon ER stress (Hetz et al., 2006). The complex formation of IRE1 with BAX/BAK couples the core apoptotic pathway to UPR. A study also has indicated that the Hsp72 chaperone interacts with the IRE1 cytosolic domain, and Hsp72's ATPase domain is crucial for IRE1 interaction (Gupta et al., 2010). Overexpression of Hsp72 prevents ER Stress-induced apoptosis by increasing Xbp1 splicing. Studies also indicated that protein-tyrosine phosphatase 1B (PTP-1B) potentiates IRE1 activity (Delibegovic et al., 2009; Gu et al., 2004). However, the physical interaction between PTP-1B and IRE1 remains unknown. Notably, the majority of the regulatory proteins increase IRE1 activity, while Bax inhibitor-1 (BI-1) serves as a negative regular of IRE1 nuclease activity by forming a stable IRE1-BAX complex (Lisbona et al., 2009). The essential role of IRE1 in cell fate determination upon irremediable ER stress makes it an attractive therapeutic target.

Chapter III

A Central Role for the Ribosome-Associated Complex in Modulating Activation of the IRE1 Branch of UPR

Abstract

The ubiquitous and highly conserved ribosome-associated complex (RAC) spans the ribosome, contacting the ribosome near the polypeptide exit tunnel and the decoding center, putting it in position to coordinate co-translational protein folding and translation. Knockout of RAC results in growth defects and sensitization to aminoglycoside stress in both yeast and mammals and to cold and osmotic stresses in yeast. The relationship of RAC's position on the ribosome to its role in responding to certain stresses remains obscure. Data presented here uncover an essential function of mammalian RAC in the endoplasmic reticulum (ER) stress, coupling the inositol-requiring protein 1 α (IRE1 α) branch of the unfolded protein response (UPR) to translation. Knockdown of RAC sensitizes mammalian cells to ER stress by selectively interfering with IRE1 α clustering in a translation-dependent manner. Higher-order oligomerization of IRE1 α kinase/endoribonuclease, as required for IRE1 α mediated Xbp1 mRNA splicing activity, depends upon RAC, as does accurate ribosome stalling of Xbp1 mRNA. The loss of RAC is counteracted by reduction of Pel α , a factor that rescues stalled ribosomes. These results reveal a previously unappreciated surveillance function of RAC serving as a stress

responsive regulator on the ribosomes: modulating IRE1 α clustering and the fitness of Xbp1 mRNA splicing in coordination with translation.

Introduction

Within the protein-dense interior of the cell, molecular chaperones maintain protein homeostasis by facilitating post-translational folding and degradation under a wide range of environmental stresses (Balchin et al., 2016; Bukau et al., 2006; Hartl and Hayer-Hartl, 2009; Rosenzweig et al., 2019). Ribosome-associated chaperones, in addition to their probable roles in co-translational folding and degradation of nascent chains, occupy a position that enables them to preemptively influence the production of the protein (Deuerling et al., 2019; Kramer et al., 2009; Pechmann et al., 2013; Preissler and Deuerling, 2012; Zhang et al., 2017). As such, these complexes are at the forefront of quality control and homeostatic mechanisms. By contrast to post-translational chaperone mechanisms, chaperone actions on the ribosome remain less well understood. Elucidation of the details of ribosome-associated chaperone activity should offer insight into the known involvement of these systems in cancer, neurodegenerative disorders and other human diseases (Hipp et al., 2014; Pechmann et al., 2013; Valastyan and Lindquist, 2014a).

Eukaryotes express two classes of co-translational ribosome-associated chaperones; the nascent polypeptide-associated complex (NAC), and the ribosome-associated complex (RAC). Both NAC and RAC are ubiquitous, highly conserved, and directly bind to ribosomes near the polypeptide exit tunnel (PTE) with a 1:1

stoichiometry (Pech et al., 2010; Peisker et al., 2008; Wegrzyn et al., 2006; Yan et al., 1998). NAC, which consists of α -NAC and β -NAC subunits (Beatrix et al., 2000; Spreter et al., 2005), contacts the 60S ribosomal subunit at uL23 and eL31 near the PTE (Pech et al., 2010; Wegrzyn et al., 2006). Deletion of NAC results in embryonic lethality and growth defects in *C. elegans*, *Drosophila*, mice, and human cells (Bloss et al., 2003; Deng and Behringer, 1995; Markesich et al., 2000). Moreover, the transient reduction of NAC leads to activation of protein folding stress in the endoplasmic reticulum (ER) and mitochondria (del Alamo et al., 2011; Gamerdinger et al., 2015; Hotokezaka et al., 2009), suggesting NAC interacts broadly with nascent secretory and mitochondrial polypeptides to influence their folding. Biochemical and structural studies have suggested that NAC and the signal recognition particle (SRP), which recognizes the hydrophobic signal sequence of the newly polypeptides, share the uL23 universal docking site on the ribosome (Beckmann et al., 2001; Pool et al., 2002; Wegrzyn et al., 2006). Their overlapping position on the ribosome demands that NAC modulate the activity of SRP (Gamerdinger et al., 2015). NAC blocks initial SRP binding, impedes SRP-independent mRNA-ribosome-nascent chain (R-RNC) complex targeting to translocon, and prevents mitochondrial proteins mistargeting to the ER in *C. elegans* (Gamerdinger et al., 2015).

Mammalian RAC is a heterodimer composed of the non-canonical heat-shock protein 70 (Hsp70) homolog Hsp70L1 and its Hsp40 partner Mpp11 (Hundley et al., 2005; Jaiswal et al., 2011; Otto et al., 2005) (Ssz1 and Zuo1 in yeast) (Gautschi et al., 2001; Gautschi et al., 2002). Although Ssz1/Hsp70L1 lack the C-terminus domain of a canonical Hsp70, they retain the nucleotide-binding domain (NBD) that binds and

hydrolyzes ATP as well as the substrate-binding domain (SBD) that binds neutral and hydrophobic amino acids (Kampinga and Craig, 2010). Recent cross-linking data indicates Ssz1 can directly interact with nascent polypeptides prior to Hsp70 chaperone Ssb1 contacts, consistent with the idea that Ssz1 is an active chaperone for co-translational folding (Zhang et al., 2020)

RACs are highly conserved yet have evolved functional diversity from yeast to higher eukaryotes. In yeast, RAC (Ssz1 and Zuo1) and its supporting Hsp70 chaperone Ssb1 are both tethered to the ribosomes forming a functional chaperone triad (Gautschi et al., 2001; Gautschi et al., 2002), while mammalian RAC is directly anchored to the ribosomes and recruits the cytosolic Hsp70 near the exit tunnel in a non-ribosome associated manner. The stoichiometric difference between yeast and mammals implies additional regulation for mammalian RAC. In yeast, RAC stimulates the ATP hydrolysis of Ssb (Huang et al., 2005); in human, Mpp11 alone is efficient to stimulate moderate ATP hydrolysis of Hsp70, but requires the ATP binding of Hsp70L1 for fully ATPase activity of RAC (Jaiswal et al., 2011). These data indicated that RAC has evolved diverse strategies to assist protein folding mediated by cytosolic Hsp70 chaperones in higher eukaryotes.

RAC, which associates with the ribosome near the PTE *via* its J domain partner Zuo1/Mpp11, spans the 60S and 40S ribosomal subunits (Peisker et al., 2008; Yan et al., 1998). Cross-linking and cryo-EM data indicates that Zuo1 interacts with eL31, close to the PTE, as well as eL22 and H24/H59 of 28S rRNA on the 60S subunit. On the 40S subunit, Zuo1 interacts with ES12 of H44 of 18S rRNA, which originated from the

ribosome A-site base of the decoding center (Lee et al., 2016; Leidig et al., 2013; Zhang et al., 2014). Interestingly, a study suggests that Ssb slows down translation rate for efficient co-translation folding (Willmund et al., 2013). These structural characteristics fortify the emerging roles of RAC in coordinating not only direct *de novo* protein folding (Gautschi et al., 2001; Hundley et al., 2002; Pfund et al., 2001), but also translational activity of the ribosome (Nelson et al., 1992), including modulation of translation stop codon read-through (Lee et al., 2016; Rakwalska and Rospert, 2004), -1 programmed ribosomal frameshifting (Muldoon-Jacobs and Dinman, 2006) as well as ribosome stalling and premature translation termination at C-terminus poly-AAG/A sequences (Gribbling-Burrer et al., 2019), by currently unknown mechanisms.

Reduction of RAC is known to cause growth defects and sensitivity to aminoglycoside stress in both yeast and mammalian cells as well as to cold and osmotic stress in yeast (Gautschi et al., 2002; Hundley et al., 2005; Nelson et al., 1992; Yan et al., 1998). Yet, the mechanistic role of RAC in these stress responses remains obscure. Furthermore, there is a dearth of information regarding the physiological co-translational substrates of mammalian RAC. The homology of mammalian RAC to canonical Hsp70 chaperones and its presumed localization on cytosolic ribosomes led to the hypothesis that RAC supports co-translational folding of nascent cytosolic polypeptides (Otto et al., 2005). Here, we find that RAC is also on ER associated ribosomes and that reduction in its expression does not activate the cytosolic heat shock response (HSR), but rather plays a central role, *via* modulation of translation, in activation of the IRE1 α branch of the unfolded protein response (UPR).

Results

Acute reduction of RAC selectively sensitizes cells to ER stress by attenuation of the IRE1 α arm of the UPR

The hypothesis that RAC supports co-translational folding of nascent cytosolic polypeptides predicts that a reduction in RAC should lead to an accumulation of incompletely folded cytosolic proteins and, thus, activation of the cytosolic heat shock response (HSR). To test this prediction, we reduced levels of RAC by transient transfection of small interfering RNA (siRNA) pools against Hsp70L1, a RAC component, for 48 hr in HeLa cells and monitored the cytosolic HSR. As previously observed in yeast (Gautschi et al., 2001), reduction in Hsp70L1 led to a loss of its partner Mpp11 in HeLa cells (Figure 9A), which presumably requires the formation of the complex for stability. However, Hsp70L1 knockdown neither led to global protein aggregation (Appendix 2) nor sensitized cells to heat shock induced loss of viability by celastrol, which induces HSR by activating heat shock factor 1 (HSF1) (Westerheide et al., 2004) (Figure 9B). Moreover, no measurable activation of the cytosolic HSR was observed after reduction of RAC by monitoring either phosphorylation of HSF1 (Figure 9C, top) or Hsp70 mRNA levels (Figure 9C, bottom).

We also monitored the unfolded protein response (UPR) in the endoplasmic reticulum (ER), another stress pathway known to be activated by the accumulation of misfolded proteins in the ER. By contrast to the cytosolic HSR (Figure 9B), reduction in Hsp70L1 expression sensitized cells to treatment with an ER stress induced by thapsigargin (Figure 9D) or DTT (data not shown), which induce ER stress by

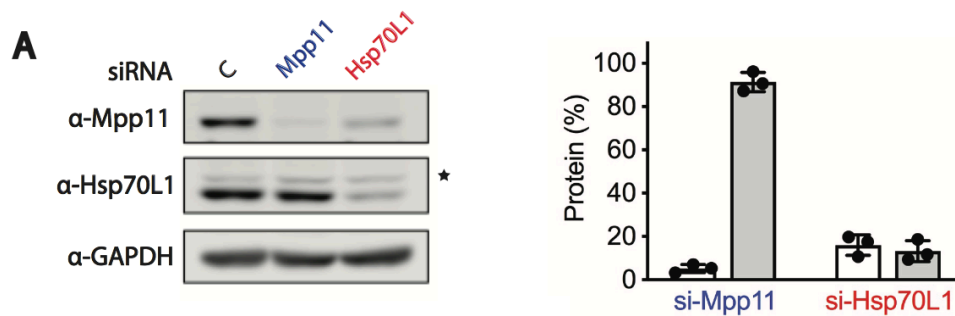


Figure 9-1. Cells sensitivity to the unfolded protein response (UPR) after RAC knockdown

Effects of Hsp70L1 knockdown on the molecular correlates of the cytosolic heat shock stress response and IRE1 α branch of the UPR in the ER. Cytosolic or ER stress was induced in HeLa cells by treatment with celastrol, which induces heat shock response (HSR) by activating heat shock transcription factor 1 (HSF1) or thapsigargin, which induces ER stress by inhibiting the sarco-endoplasmic reticulum Ca²⁺ ATPase (SERCA), respectively. (A) (left) Representative western blot and (right) quantification analysis by *LI-COR* of RAC components in HeLa whole cell lysates after transiently transfection of siRNA against either control, Mpp11 or Hsp70L1 for 48 hr. The protein expression levels were normalized to loading control, GAPDH, and si-control was set as 100%. ★, non-specific band.

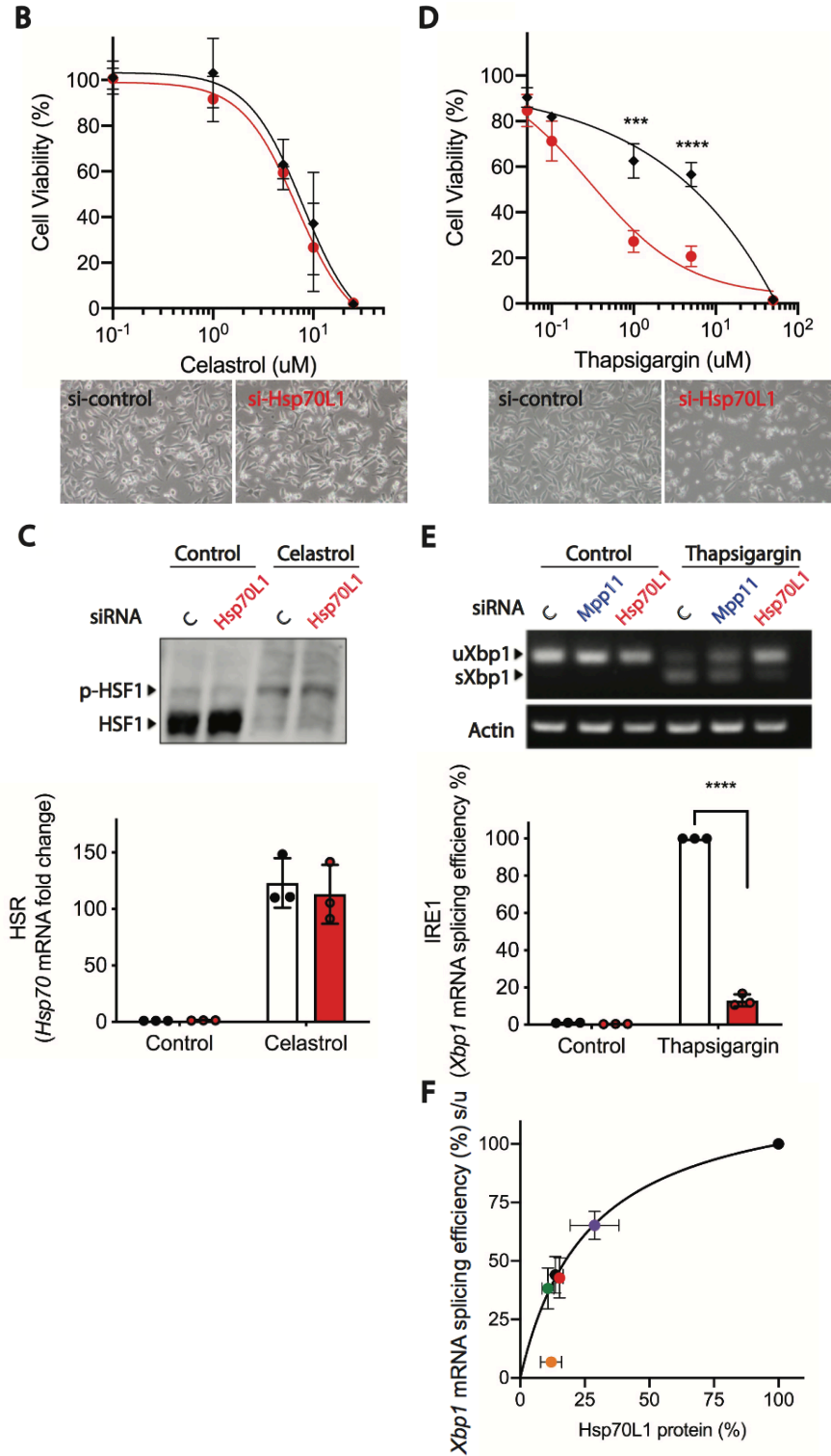


Figure 9-2. Cells sensitivity to the UPR after RAC knockdown (continued)

Figure 9-3. Cells sensitivity to the UPR after RAC knockdown (continued)

Cell viability analysis by MTS assay in HeLa cells pretreated with siRNA against either control (black diamond) or Hsp70L1 (red circle) for 48 hr followed by 24 hr treatment of DMSO negative control, celastrol (0.1, 1, 5, 10, 25 μ M) (**B**) or Thapsigargin (0.05, 0.1, 1, 5, 50 μ M) (**D**) (top) Cell viability (%) was normalized to DMSO control of si-control cells. (bottom) Representative microscopic images of cell viability (**C**) (top) Representative phos-tag gel analysis of HSF1 phosphorylation and (bottom) qRT-PCR of Hsp70 mRNA fold change in HeLa cells pretreated with either control (white bar) or Hsp70L1 (red bar) siRNA for 48 hr followed by 3 hr challenge with celastrol (2.5 μ M). mRNA expression level was normalized to internal control, HPRT, relative to si-control and shown as fold change ($2^{-\Delta\Delta CT}$). Three branches of the UPR activation were examined in HeLa cells pretreated with either vehicle control or Hsp70L1 siRNA for 48 hr followed by 4 hr challenge with thapsigargin (0.5 μ M). (**E**) IRE1 α branch activity was shown by representative Xbp1 mRNA splicing assay using (top) RT-PCR and (bottom) qRT-PCR. Relative Xbp1 splicing efficacy (%) was calculated as [(spliced Xbp1/unspliced Xbp1) normalized to thapsigargin 4 hr of vehicle si-control] X 100%. n=3, ***p<0.001, ****p<0.0001. For PERK and ATF6 branch activity, see Figure S1A, S1B. (**F**) Dose-response curve of Xbp1 mRNA splicing efficiency (%) for individual siRNA against different targeting sequences of Hsp70L1. Hsp70L1 protein levels were determined by *LI-COR* of SDS-PAGE. Black circle as si-c, purple, navy, green, orange, and red as si-Hsp70L1-1, 2, 3, 4, and pools, respectively. n=5. Error bars, mean \pm SD.

respectively inhibiting the sarco/endoplasmic reticulum Ca^{2+} ATPase (SERCA) or changing the luminal redox potential. Like the cytosolic HSR, the basal UPR pathway, as monitored by Xbp1 mRNA splicing, was not activated by a simple reduction in RAC (Figure 9E). However, contrary to the prediction of a role in promoting folding of nascent polypeptides, reduction in RAC inhibited activation of UPR after induction of a UPR response (Figure 9E).

To better understand the generality of sensitization of cells to thapsigargin (0.5 μM) induced ER stress after Hsp70L1 and Mpp11 reduction, we monitored the activation of each of the three known arms of the UPR: the inositol-requiring enzyme 1 α (IRE1 α) branch, the PRKR-like ER kinase (PERK) branch, and the activating transcription factor 6 α (ATF6) branch. Rather than sensitizing all three arms as predicted for a generic role in ER co-translational folding, Hsp70L1 reduction selectively attenuated the activation of the IRE1 α branch as reflected in a reduced ability to splice Xbp1 mRNA as required for activation of transcription of many UPR responsive genes (Figure 9E) upon ER stress. This effect exhibited a clear dose-dependence with the amount of Hsp70L1 protein remaining introduced by siRNAs against different Hsp70L1 target sequences (Figure 9F). Altered RAC levels had no significant effect on the PERK (Figure S1A) or the ATF6 (Figure S1B) branches of the UPR, either before or after activation of an ER stress response by thapsigargin for 4 hr.

Xbp1 mRNA splicing is a non-canonical spliceosome-independent splicing event (Cox and Walter, 1996; Mori et al., 1993), which takes place on the ER membrane (Yanagitani et al., 2009). There are three steps required for Xbp1 mRNA splicing: First,

translation of uXbp1 mRNA is initiated and paused (Yanagitani et al., 2009; Yanagitani et al., 2011). Next, the stalled uXbp1 mRNA-ribosome-nascent chain (R-RNC) complex is targeted to the ER membrane *via* its hydrophobic region 2 (HR2) (Yanagitani et al., 2009). Then, upon ER stress, IRE1 α is activated by sequential steps of dimerization (Liu et al., 2000; Tirasophon et al., 1998), trans-autophosphorylation (Mori et al., 1993; Shamu and Walter, 1996; Zhou et al., 2006) and further high-order oligomerization (Korennykh et al., 2009; Lee et al., 2008) to enable active IRE1 α endoribonuclease activity excising the cryptic Xbp1 intron (Calfon et al., 2002; Yoshida et al., 2001). Once the 26 nt intron is removed, the 5' and 3' fragments are rejoined by RtcB tRNA ligase (Jurkin et al., 2014; Kosmaczewski et al., 2014; Lu et al., 2014). The properly spliced Xbp1 mRNA is then translation terminated and released to the cytosol producing a stress responsive transcriptional factors sXbp1 (Cox and Walter, 1996). Understanding of the details of uXbp1 mRNA ribosome stalling effect remains incomplete. Since Xbp1 lacks a canonical signal sequence, novel mechanisms of targeting the stalled uXbp1 mRNA-ribosome-nascent chain (R-RNC) complex to the ER membrane are also thought to be employed (Kanda et al., 2016; Plumb et al., 2015; Yanagitani et al., 2011).

The position of RAC on the ribosome (Figure 10A), contacting both the 60S ribosomal subunit near the polypeptide exit tunnel and the 40S at the decoding center, puts it in position to potentially coordinate co-translational regulation of Xbp1 mRNA splicing. This arrangement provided a structural basis for formulating hypotheses to explain the unexpected selective inhibition of Xbp1 mRNA splicing in RAC knockdown cells. Three hypothetical mechanisms for RAC regulation of Xbp1 mRNA splicing were

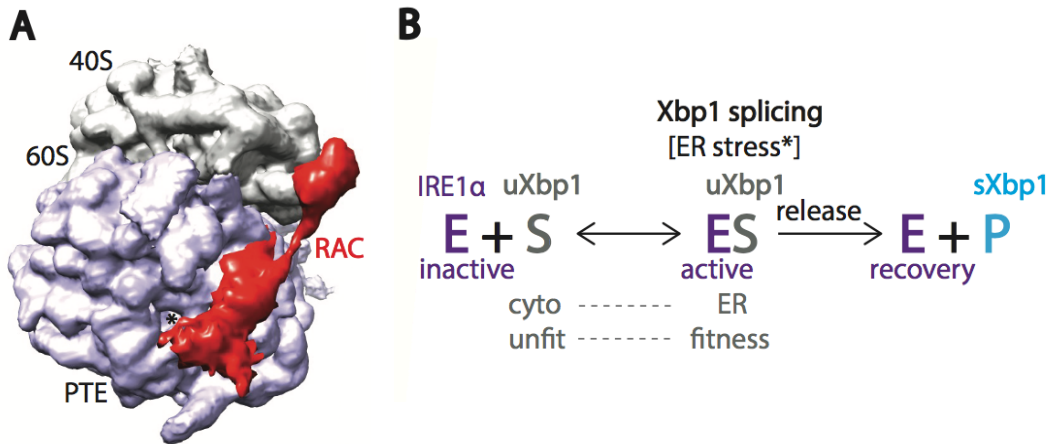


Figure 10-1. Membrane targeting effect of RAC-associated uXbp1 mRNA in RAC knockdown

Probable mechanisms of RAC regulation on Xbp1 mRNA splicing. **(A)** Cryo-EM density map of RAC with the 80S ribosome in *S. cerevisiae* by *Chimera* (EMD: 6103). RAC contacts both the 40S and 60S ribosomal subunits. RAC, red. 40S, grey. 60S, lavender.

*, PTE, polypeptide tunnel exit. **(B)** The mechanism of Xbp1 splicing. In basal condition, the IRE1 α kinase-endonuclease, E, maintaining at inactive state. IRE1's substrate uXbp1, S, which the ribosome stalled to ensure efficient membrane targeting (fitness), is translocated from cytosol to the translocon on the ER near IRE1 (ES). Upon ER stress, IRE1 α phosphorylated, oligomerized and spliced out the intron of uXbp1, releasing its product sXbp1, P. IRE1 α attenuated during stress recovery. RAC may modulate Xbp1 splicing through any process above.

posed: through modulating substrate (uXbp1 mRNA) localization to the nuclease (IRE1 α) on the ER prior to stress, through direct activation of the nuclease (IRE1 α phosphorylation, endoribonuclease activity and high-order oligomerization) upon ER stress, and/or through effects on substrate presentation or fitness (correct stalling) of the ribosome-associated mRNA substrate (Figure 10B).

RAC is not required for uXbp1 mRNA targeting to the ER membrane

Since Xbp1 mRNA splicing occurs on the ER membrane (Yanagitani et al., 2009), we predicted that RAC localizes to ER ribosomes in addition to its known localization in the cytosol (Otto et al., 2005). To further analyze the subcellular localization of RAC in response to ER stress, we performed cell fractionation experiments by differential detergent method (Jagannathan et al., 2011) after challenge with 4 hr of thapsigargin (0.5 μ M) or DMSO negative control (Figure 10C) in HeLa cells. Mpp11 and Hsp70L1 are both enriched in the ER fraction under basal conditions, in agreement with the immunostaining of Mpp11 (Appendix 4), and concurrent with ribosome distribution of 60% in the ER fractionation and 40% in the cytosol giving a membrane localization ratio (ER to cytosol) of nearly 1.6. These results suggest that RAC generally associates with most ribosomes. After ER stress, both Mpp11 and ribosomes are released from the ER to the cytosol with an attendant lower membrane localization ratio (ER to cytosol ratio) of less than 1. The altered cellular localization of Mpp11 and ribosomes in response to ER stress may be due to cells reducing global translation or regulated IRE1-dependent decay of mRNA (RIDD) as well as release of stalled Xbp1

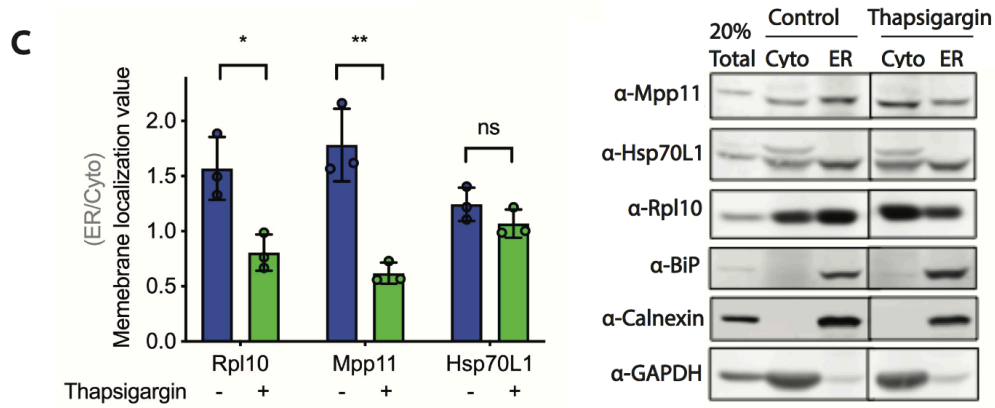


Figure 10-2. Membrane targeting effect of RAC-associated uXbp1 mRNA in RAC knockdown (continued)

(C) Subcellular fractionation of HeLa cells was harvested after 4 hr of DMSO control (blue bar) or thapsigargin (0.5 μ M) (green bar) treatment by sequential detergent extraction method. 20% of total lysate was loaded, cytosol (Cyto) and ER membrane-bound fraction were collected and loaded equal amount in each lane. Quantification of western blot analysis (left) by *LI-COR* was shown as membrane localization value (ER/Cyto). Representative western blot images of subcellular fractionation (right). Rpl10 was used as a ribosome marker, BiP as ER lumen marker, Calnexin as ER membrane marker, and GAPDH as cytosol marker. n=3, *p<0.05, **p<0.01. Error bars, mean \pm SD.

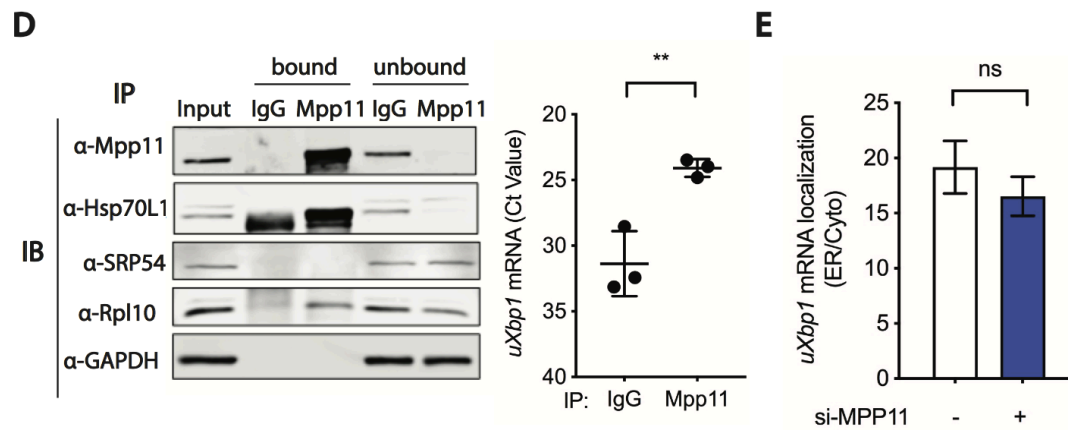


Figure 10-3. Membrane targeting effect of RAC-associated uXbp1 mRNA in RAC knockdown (continued)

(D) RNA immunoprecipitation was performed in HeLa cells immunoprecipitated with antibody against IgG control of Mpp11 and the coprecipitated RNA was analysis by qRT-PCR. (left) Representative western blot of bound and unbound fraction of IP. 1% total lysate as input. (right) uXbp1 mRNA was shown as Ct value. n=3, **, p<0.01. Error bars, mean ± SD. **(E)** Subcellular fractionation of RNA by the differential detergent method in HeLa cells pretreated with either vehicle control (white) or Mpp11 (blue) siRNA for 48 hr. RNA was analyzed by qRT-PCR, samples were compared to vehicle si-control and calculated as $2^{-\Delta CT}$ and uXbp1 mRNA localization was shown as ER/cytosol. n=2. Error bars, mean ± SEM.

R-RNC. Interestingly, by contrast to the relocalization of Mpp11 with ribosome to the cytosol, Hsp70L1 remains on the ER after ER stress, suggesting that Hsp70L1 could be playing an additional role in modulating the UPR on the ER membrane.

To dissect the mechanism of how RAC regulates Xbp1 mRNA splicing, we first monitored whether RAC is on the uXbp mRNA-ribosome-nascent chain complex by RNA co-immunoprecipitation in HeLa cells. Cells were immunoprecipitated with antibody against either Mpp11 or IgG, and the coprecipitated RNA was analyzed by qRT-PCR. Both Hsp70L1 and the ribosome were pulled down by Mpp11 (Figure 10D, left), consistent with intactness of the RAC-associated ribosome complex. Additionally, SRP54, a component of the signal-recognition-particle (SRP) targeting secretory proteins to the ER, was not detected in the Mpp11 pull-down. This finding is to be expected considering that structural analysis indicates that SRP54 and RAC sterically clash while concomitantly modeling onto the ribosome, suggesting SRP54 and RAC may not bind concurrently to the same ribosome (Zhang et al., 2014). The results indicate that RAC and uXbp1 mRNA are in the same macromolecular complex as reflected in uXbp1 mRNA enrichment in the Mpp11 pull-down fraction (Figure 10D, right) as compared to IgG control.

Further, to directly test whether RAC regulates membrane targeting of uXbp1 mRNA, subcellular fractionation of uXbp1 mRNA (Figure 10E) from HeLa cells pretreated with either vehicle control (white) or Mpp11 (blue) siRNA for 48 hr was performed. The localization of uXbp1 does not change in Mpp11 knockdown HeLa cells, suggesting that RAC does not regulate membrane targeting of uXbp1 mRNA. Consistent

with this finding, recent studies demonstrate that although Xbp1 does not contain a canonical signal sequence, SRP54 targets uXbp1 mRNA to SR receptor on the ER membrane by binding to its hydrophobic region 2 (HR2) (Kanda et al., 2016; Plumb et al., 2015).

Reduction of RAC inhibits IRE1 α kinase, endoribonuclease activity and high-order oligomerization

To determine whether RAC regulates Xbp1 mRNA splicing by modulating IRE1 α activity, we monitored the IRE1 α kinase activity by detecting IRE1 α phosphorylation using phos-tag gel (Figure 11A) and IRE1 α clustering (Figure 11B) utilizing an IRE1-GFP cassette driven by a tetracycline-inducible CMV promoter in a stable T-REx293 cell line (Li et al., 2010). Notably, acute reduction of RAC inhibited nearly 50% of IRE1 α hyperphosphorylation activity compared to vehicle control after challenge with thapsigargin (0.5 μ M) for 4 hr. In HEK293 cells, challenged with thapsigargin (0.5 μ M), IRE1 α formed multiple visible foci at 1 hr, which condensed to large foci at 4 hr (Figure 11B, 11C, 11D) and subsequently dissolved by 8 hr, consistent with prior reports (Tam et al., 2014). Reduction of RAC inhibited IRE1 α foci formation (Figure 11B, 11C, 11D, S2A, S2B) as early as 1h, concurrent with reduced Xbp1 splicing activity (Figure 11E, S2C). Recent biochemical data indicates that IRE1 oligomerization is required for Xbp1 mRNA splicing, while IRE1 dimer formation is required for RIDD activity due to different substrate-binding interfaces in each multimer (Tam et al., 2014). Interestingly, reduction of RAC only mildly affects RIDD activity, as shown by relative

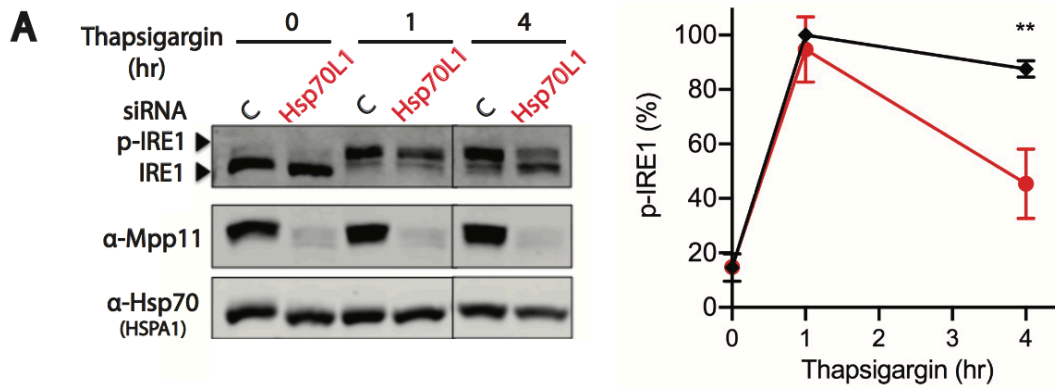


Figure 11-1. Selective inhibition effect on IRE1 α activity in RAC knockdown cells

(A) (left) Representative western blot images of IRE1 α kinase activity measured by phosphatase gel. HeLa cells were pretreated with either vehicle control (black diamond) or Hsp70L1 (red circle) siRNA for 48 hr and challenge with thapsigargin (0.5 μ M) for 0, 1 or 4 hr. Hsp70 was used as loading control. (right) p-IRE1 (%) was shown as phosphorylated IRE1/total IRE1. $n=3$, $**p<0.01$.

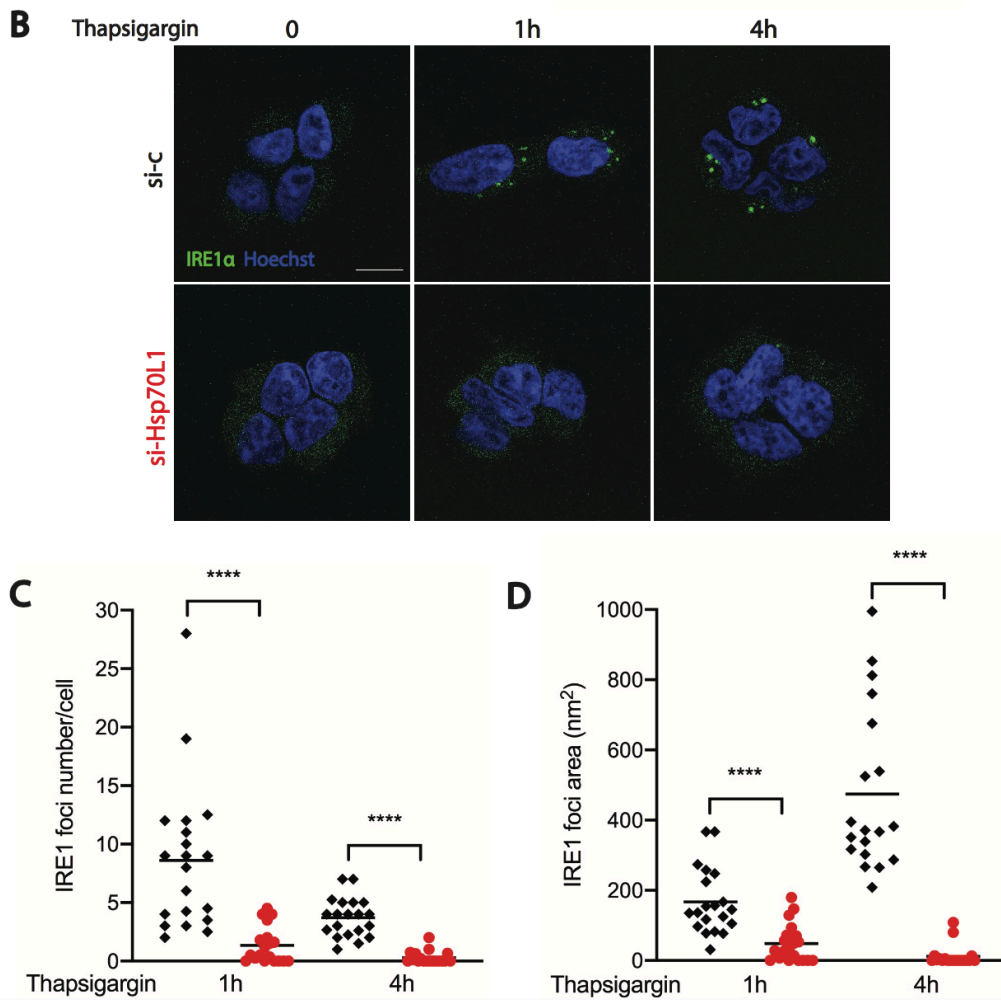


Figure 11-2. Selective inhibition effect on IRE1 α activity in RAC knockdown cells (continued)

(B) Representative fluorescent images of IRE1 α clustering using T-REx293 IRE1-GFP cell line pretreated with either vehicle control (black diamond) or Hsp70L1 (red circle) siRNA for 48 hr followed by doxycycline (50 ng/ μ l) induction of IRE1 α for 24 hr challenge with thapsigargin for 0, 1 or 4 hr. IRE1 α , green. Hoechst, blue. Scale bar, 10 μ m. Quantification of **(C)** IRE1 foci numbers and **(D)** foci area size by ImageJ. Results shown are representative of two independent replicates. See Figure S2 for biological replicates. Each dot represents one field, 20 fields were analyzed, an average of 60 cells was analyzed per condition. The mean was presented.

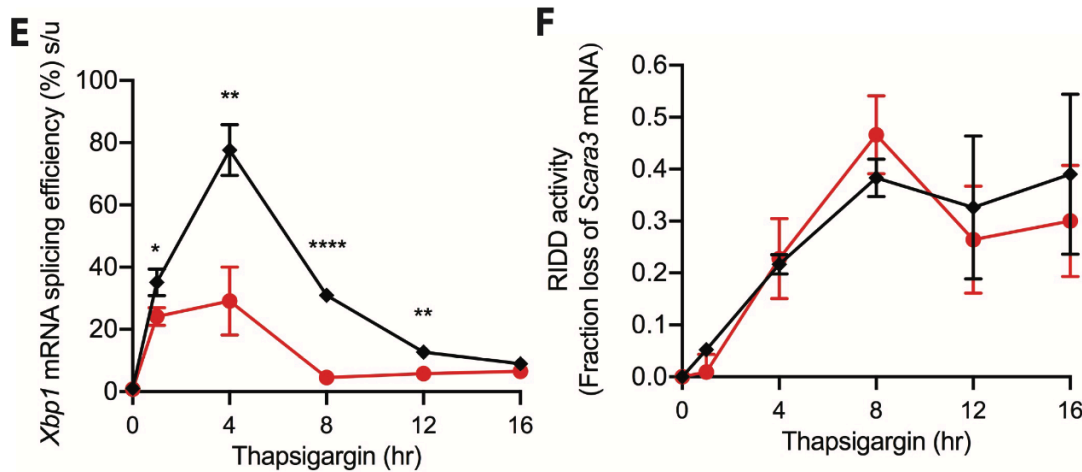


Figure 11-3. Selective inhibition effect on IRE1 α activity in RAC knockdown cells (continued)

(E) Xbp1 mRNA splicing efficiency (%) was monitored using qRT-PCR and (F) RIDD activity was monitored by mRNA fold change of Scavenger receptor class A member 3 (Scara3) over 16 hr thapsigargin time course in RAC knockdown HeLa cells. n=3, *p<0.05, **p<0.01, ****p<0.0001. Error bars, mean \pm SD.

mRNA levels of Scavenger receptor class A member 3 (Scara3) (Figure 11F, S2D) and Biogenesis of lysosome-related organelles complex-1 subunit 1 (Bloc1) (Figure S2E, S2F) as determined by qRT-PCR. These results demonstrate that reduction of RAC selectively inhibits IRE1 α high-order oligomerization leading to inhibition of Xbp1 mRNA splicing.

Reduction of RAC increases uXbp1 ribosome stalling

Recent studies have demonstrated that specific ribosome pausing of the Xbp1 mRNA is crucial for efficient Xbp1 mRNA splicing (Yanagitani et al., 2011). Although it is known that the C-terminal 26 residues region of uXbp1 are essential for translation pausing, the detailed mechanism remains unknown (Yanagitani et al., 2011). To test whether RAC contributes to translation stalling of Xbp1, we engineered N-terminal FLAG tagged uXbp1 and sXbp1 mRNA (Figure 12A) to monitor stalled translational intermediates and full-length product using NuPAGE Bis-Tris gel, under conditions that preserves the peptidyl-tRNA ester bond Xbp1, detected by α -FLAG antibody. *In vitro* translation was performed in a mammalian cell-free lysate (Figure 12B) pretreated with either vehicle control or Hsp70L1 siRNA for 48 hr. Stalling intermediates of uXbp1 migrate around 47 kDa, confirmed by RNase A digestion, while full-length product is around 27 kDa (Figure 12C), as previously observed in rabbit reticulocyte lysate cell-free system (Yanagitani et al., 2011). The hypothesis predicts that the reduction of Xbp1 splicing activity is due to abnormal ribosome stalling of uXbp1 upon loss of RAC. Interestingly, reduction of RAC enhanced both stalled and full-length products of uXbp1

Figure 12-2. Enhancement of Xbp1 ribosome stalling and translation rate of RAC knockdown by *in vitro* cell-free translation (continued)

(A) Scheme of uXbp1 and sXbp1 mRNA template. Both mRNAs were engineered to carry an N-terminal FLAG. White box, the shared domain of both uXbp1 and sXbp1. Blue box, the region of the spliced intron. Green and magenta box, the distinct segment of uXbp1, sXbp1, respectively. (B) Representative western blot images of *in vitro* translation lysate. HEK293T cells were harvested after either vehicle control (black) or Hsp70L1 (red) siRNA treatment for 48 hr. *In vitro* translation assay of (C) uXbp1 and (D) sXbp1 mRNA in HEK293T cell free lysate separated by (left) NuPAGE Bis-Tris gel and (right) quantified using *LI-COR*. RNase A was supplemented to confirm the stalling intermediate by breaking the peptidyl-tRNA ester bond. ◆, uXbp1 stalling intermediates. ★, non-specific band. ●, uXbp1 full-length product. ■, sXbp1 full-length product. n=2. See S3 for biological replicates. (E) Pulse labeling of nascent proteins with Click-IT AHA (L-Azidohomoalanine), a methionine analog, for 5 hr in knockdown Mpp11 HeLa cells and analyzed by *LI-COR* of SDS-PAGE.

and sXbp1 mRNA (Figure 12C, 12D, S3A, S3B), but not the non-mammalian proteins GFP (Figure S3C) or Luciferase (Figure S3D) in the *in vitro* cell-free system. Notably, a recent study indicated that cells lack of RAC results in ribosome stalling and premature translation termination at C-terminus poly-AAG/A sequences (Gribling-Burrer et al., 2019), together with our study, these results indicate that RAC may play a general role in modulating ribosome pausing. Additionally, significantly more *de novo* translated proteins were observed in knockdown Mpp11 cells monitored by pulse labeling with Click-it AHA, a non-radioactive methionine analog L-Azidohomoalanine. This result is consistent with the enhancement of Xbp1 translation rate in knockdown RAC mammalian cell-free assay.

Reduction of Pelo counters the inhibition of uXbp1 ribosome stalling, Xbp1 mRNA splicing and IRE1 α clustering in RAC knockdown during ER stress

Co-translational mRNA quality control systems recognize ribosome stalling to prevent aberrant product production and protect ribosomes for critical activates. In eukaryotes, when a ribosome stalls at the 3' end of mRNA or endonucleolytic cleavage occurs, Pelo and Hbs1 in mammals (Dom34 and Hbs1 in yeast) trigger ribosome subunit dissociation, mRNA degradation and ribosome recycling *via* the non-stop decay (NSD) or no-go decay (NGD) mRNA surveillances pathway (Pisareva et al., 2011; Shoemaker and Green, 2012; Tsuboi et al., 2012). Emerging studies have indicated that Dom34/Pelo recognizes ribosome stalled at the of Hac1/Xbp1 splice site in *S. cerevisiae* (Guydosh and Green, 2014; Guydosh et al., 2017) and *C. elegans* (Arribere and Fire, 2018).

To further understand the detailed mechanism by which RAC regulates Xbp1 translation stalling, ribosome profiling was performed. Additionally, disturbance of the mRNA surveillance pathway by manipulating Pelo expression was assessed for the ability to rescue the RAC dependent ribosome stalling event. Knockdown of Pelo was predicted to rescue the inhibition effect in knockdown RAC cells. Under basal conditions (Figure 13A), Xbp1 translating ribosomes stalled at codon Asn261, the position in accordance with the structural analysis (Shanmuganathan et al., 2019). Upon ER stress, the ribosome density at this stalling position was diminished in vehicle control (Figure S4), indicating the release of ribosome stalling coordinated with splicing. Since IRE1 α splices a 26-nucleotide intron from uXbp mRNA, this results in a frameshift that encodes sXbp1 protein with a unique C-terminus from uXbp1. To distinguish the signal of the uXbp1 transcripts from the sXbp1 transcripts, we utilized the different ribosome 3-nt periodicity signal between uXbp1 and sXbp1 (Figure 13B). As predicted, upon ER stress, ribosomes accumulated at the uXbp1 pausing site in knockdown RAC cells and the knockdown of Pelo counteracted this accumulation (Figure 13C). Notably, modest ribosomes accumulation at the uXbp1 stalling site also occurs in knockdown of Pelo cells, which may due to reduction of Pelo interference with Xbp1 release (Figure 13C).

To monitor whether the observed inhibition of IRE1 α activity resulted from the aberrant ribosome stalling in knockdown RAC cells, Xbp1 mRNA splicing and IRE1 α high-order oligomerization were monitored in Pelo and RAC double knockdown cells. In HEK293 cells, knockdown of Pelo increased Xbp1 mRNA splicing (Figure 14A), consistent with the concept that Dom34/Pelo evolves in the mRNA surveillance pathway

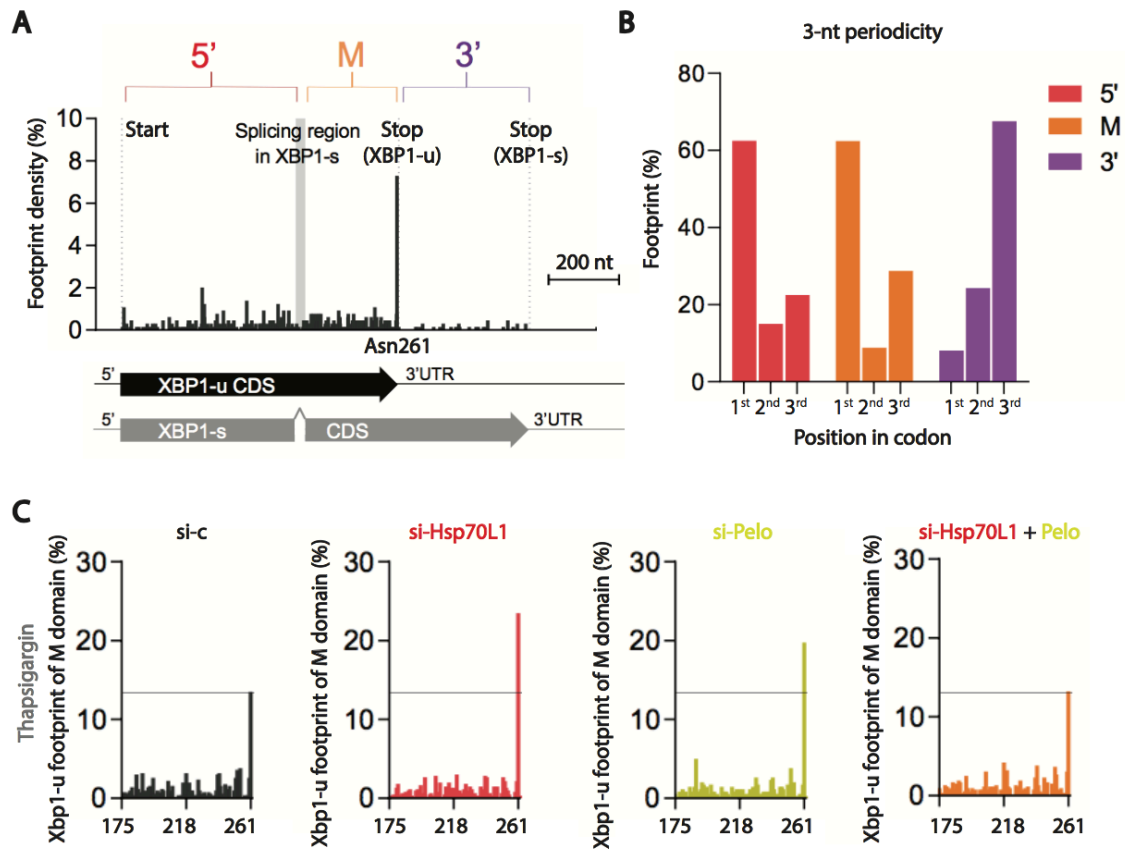


Figure 13-1. Enhancement of Xbp1 ribosome stalling in RAC knockdown and counteract effect by Pelo knockdown in RAC knockdown under ER stress by ribosome profiling

Figure 13-2. Enhancement of Xbp1 ribosome stalling in RAC knockdown and counteract effect by Pelo knockdown in RAC knockdown under ER stress by ribosome profiling (continued)

(A) Relative ribosome occupancy within the Xbp1 transcript from siRNA against vehicle control under basal condition, with footprint displayed the position of ribosome A-site. First dot line, start site of Xbp1. Second dot line, stop codon of Xbp1-u. Third dot line, stop codon of Xbp1-s. Grey box, the Xbp1 splicing region. Scale bar, 200 nt. (B) The 3-nt periodicity of Xbp1 transcript from the 5' region (from start codon to the splicing region, red), the middle region (from downstream splicing region to the stop codon of Xbp1-u, M, orange), and the 3' region (from the stop codon of Xbp1-u to Xbp1-s, purple). (C) Relative ribosome occupancy within the Xbp1-u transcript from footprints mapped on the 1st-base of codons in the M-region of the transcript. Cells were harvested after pretreated with designated siRNA (vehicle control, black; Hsp70L1, red; Pelo, chartreuse; both Hsp70L1 and Pelo, orange) for 48 hr and challenge with thapsigargin (0.5 μ M) for 4 hr.

of Hac1/Xbp1 in *S. cerevisiae* (Guydosh and Green, 2014; Guydosh et al., 2017) and *C. elegans* (Arribere and Fire, 2018). Knockdown of Pelo countered the inhibition effect of Xbp1 mRNA splicing in RAC knockdown HEK293 cells (Figure 14A), consistent with the ribosome profiling results. Finally, knockdown of Pelo partly rescued the inhibition effect of RAC knockdown on IRE1 α clustering in HEK293 cells (Figure 14B, 14C, S5A).

To examine whether the inhibition of IRE1 α clustering in RAC knockdown is directly due to lack of fitness of its Xbp1 substrate, we knocked down Xbp1 mRNA and monitored IRE1 α clustering. In the presence of ER stress, there were no significant differences in IRE1 α clustering ability between vehicle control and knockdown Xbp1 cells (Figure 14D, S5B), which is consistent with previous findings in yeast (Aragon et al., 2009), suggesting the presence of this substrate is not required for formation of the active IRE1 α endonuclease complexes. However, knockdown of Xbp1 did activate IRE1 α foci formation under basal conditions. Together, these data indicates that the activation of IRE1 α clustering does not require Xbp1 mRNA, suggesting that inhibition of IRE1 α foci formation in RAC knockdown is not due to a lack of fitness of the Xbp1 substrate.

RAC modulates IRE1 α clustering via translation

Since we also observed that RAC reduces translation rate, we hypothesized that the inhibition of IRE1 α clustering could result from the slowdown of the global translation rate. To test this hypothesis, we pretreated cells with the translation inhibitors,

harringtonine and cycloheximide, which inhibit translation initiation and elongation, respectively, and then challenged with thapsigargin (0.5 μ M). Strikingly, IRE1 α clustering was dramatically inhibited as early as 1 hr after ER stress in translation-inhibited cells (Figure 14E), indicating that translation of substrates other than Xbp1 are required for IRE1 α clustering. Together, these results suggest a model in which RAC plays an essential role as a stress-responsive regulator on the ribosome (Figure 15): RAC coordinates IRE1 α activation, including IRE1 α kinase activity, higher-order oligomerization and activation of the attendant endonuclease activity, as well as ribosomal translational activity, Xbp1-mediated ribosome stalling and substrate fitness.

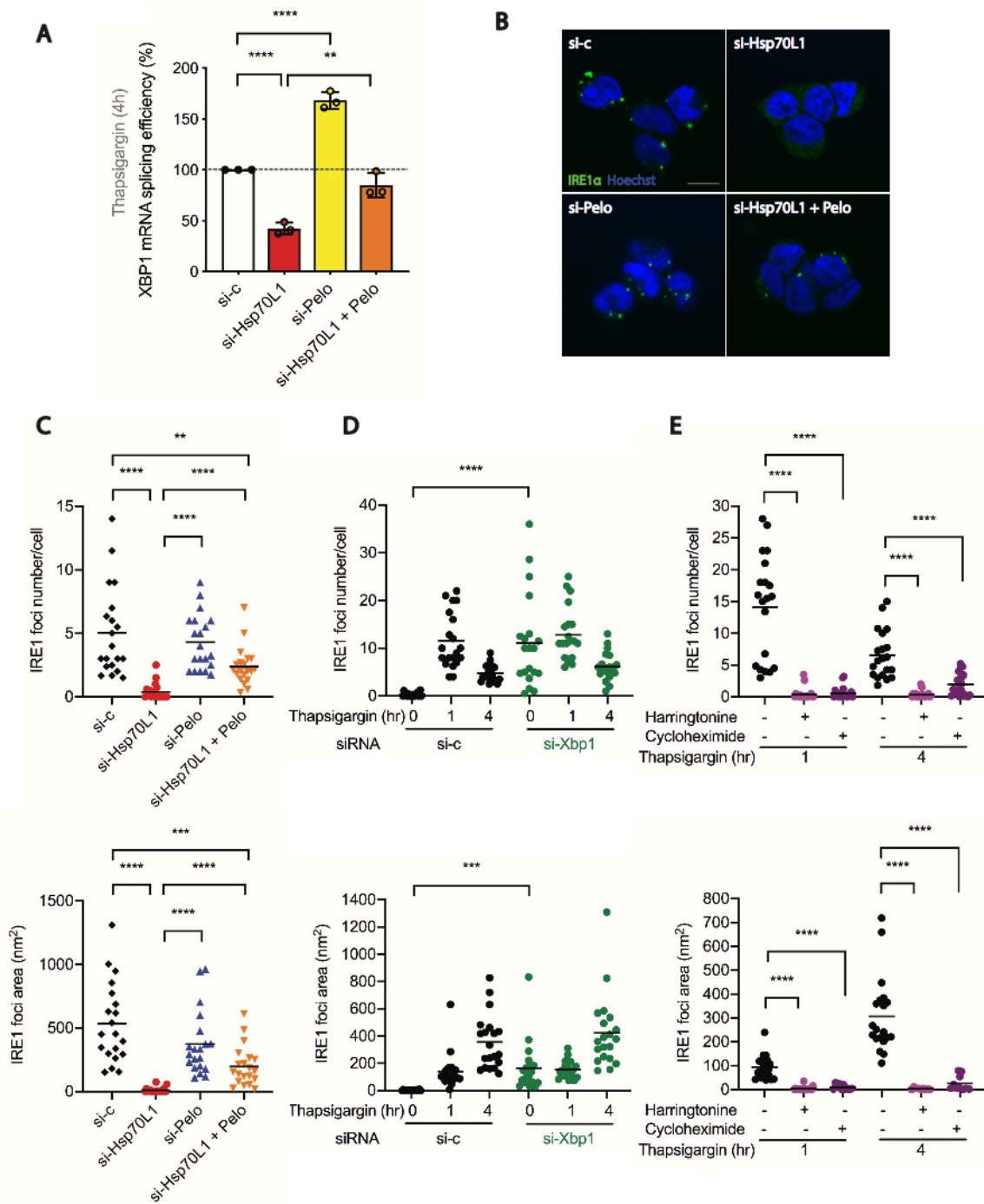


Figure 14-1. Counteract effect of IRE1 α activity by Pelo knockdown in RAC knockdown under ER stress

Figure 14-2. Counteract effect of IRE1 α activity by Pelo knockdown in RAC knockdown under ER stress (continued)

Cells were transiently transfected with siRNA against vehicle control, Hsp70L1, Pelo, or both Hsp70L1 and Pelo for 48 hr. **(A)** Quantification of Xbp1 mRNA splicing efficiency of designated siRNA knockdown by qRT-PCR upon 4 hr of thapsigargin (0.5 μ M) treatment in HeLa cells. n=3. Error bars, mean \pm SD. **(B)** Representative fluorescent images and **(C, D, E)** quantification of IRE1 α foci number (top) and foci area size (bottom) by ImageJ in T-REx293 IRE1-GFP cell line after designated treatments. IRE1 α , green. Hoechst, blue. **(C)** IRE1 α foci were monitored after challenge with thapsigargin for 4 hr in the designated knockdown cells. Each group was compared to either vehicle control or Hsp70L1 siRNA. **(D)** IRE1 α foci were examined through a time course of 0, 1, 4 hr of thapsigargin treatment after pretreated with either vehicle control or Xbp1 siRNA for 48 hr. Each condition was compared to the same time course treatments. **(E)** IRE1 α foci were examined after cells pretreated with either control, harringtonine (2 μ g/ml) or cycloheximide (100 μ g/ml) for 20 min followed by 1, 4 hr of thapsigargin (0.5 μ M) treatment. Each group was compared to untreated negative control in the same time course. Data shown of IRE1 α foci are representative of two independent biological repeats. Each dot represents one field, 20 fields were analyzed, an average of 60 cells were analyzed per condition. The mean was presented. **p<0.01, ***p<0.001, ****p<0.0001. Scale bar, 10 μ m.

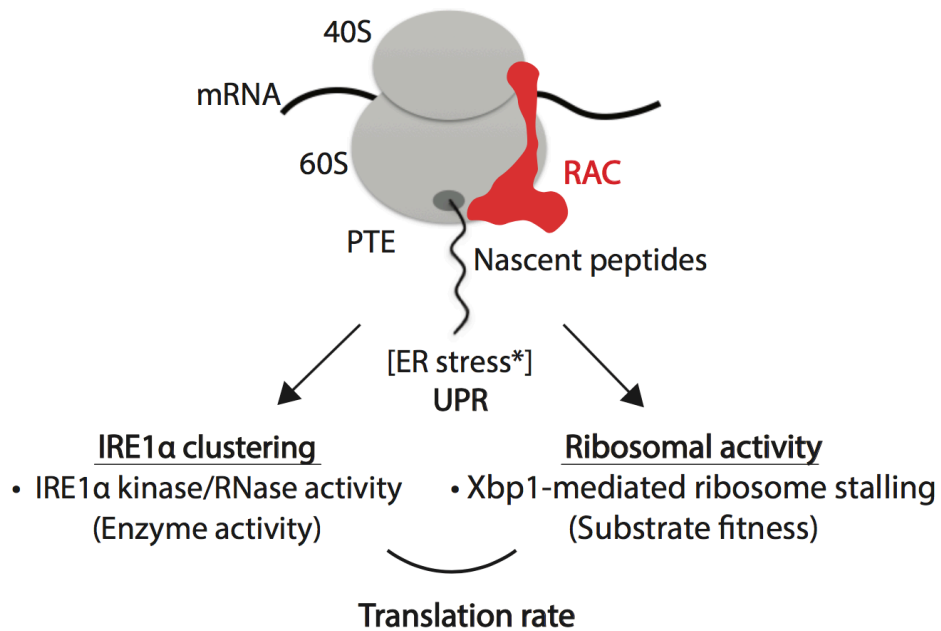


Figure 15. RAC is an ER stress-responsive regulator

Proposed model for the mechanism of RAC in the UPR. RAC is essential for cellular adaptation to the UPR by coupling the IRE1α activity, including its kinase, endonuclease (RNase), and high-order oligomerization activity, of the UPR with ribosomal activity, which reflects by Xbp1-mediated ribosome stalling as IRE1α's substrate fitness, *via* translation.

Discussions

RAC is an ubiquitous, highly-conserved complex directly anchored to the ribosomes near both the polypeptide exit tunnel and the decoding center. Initially, homology to canonical cytosolic Hsp70 chaperones led to the suggestion that RAC was involved in cytosolic cotranslational folding and response to cytosolic heat shock response (HSR). More recently, RAC's involvement in translational activity has been reported (Gribling-Burrer et al., 2019; Lee et al., 2016; Muldoon-Jacobs and Dinman, 2006; Nelson et al., 1992; Rakwalska and Rospert, 2004). In spite of the structures revealing RAC is uniquely positioned to govern protein homeostasis by coordinating co-translational protein folding and translational activity, to our knowledge, such coordination has not been demonstrated. The results presented here demonstrate RAC's role in mediating communication between ER stress, translational activity, and the coordinated splicing of the Xbp1 mRNA. Moreover, the data reveal an unexpected and critical role of mammalian RAC in the UPR related to these activities. RAC acts as a stress-responsive element by coordinating two ribosomal associated activities as required for Xbp1 mRNA splicing through modulation of stalling of Xbp1 translation on the ribosome and IRE1 α clustering as required for splicing.

RAC is composed of two subunits: Hsp70L1 and Mpp11, a DNAJ homologue. Here, both subunits were acutely reduced by transient knockdown of Hsp70L1 with siRNA pools in HeLa and HEK293 cells, as Mpp11 stability depends on the presence of Hsp70L1. The use of this transient model reduced the influence of adaptive responses observed when RAC was reduced over a longer term. Knockout lines produced using

CRISPR/Cas9 against Hsp70L1 using two independent gRNAs, respectively, in 293T cells (Appendix 1) dramatically impaired cell growth. However, the slow growth rate of the knockout RAC cells began to recover after continuous cultured, suggesting that adaptations are occurring over extended culture times. Together, these results suggest that mammalian RAC is an essential gene product and long-term knockout models may not be suitable for mechanistic studies.

Consistent with their homology, mammalian and yeast RAC share some common structural and functional features. Like the yeast RAC, human Hsp70L1 is associated with the ribosome *via* Mpp11 (Appendix 3). RAC deficient human cells exhibited profound growth defects consistent with the yeast system (Gautschi et al., 2001; Hundley et al., 2005; Jaiswal et al., 2011; Otto et al., 2005; Yan et al., 1998). Human RAC deficient cells were sensitized to ER stress by contrast to reduction of RAC sensitized both yeast and human cells to translation stress (Jaiswal et al., 2011; Otto et al., 2005). Unexpectedly, knockdown of RAC did not activate the cytosolic HSR as predicted by the hypothesis that RAC is required for cytosolic cotranslational folding in human cells (Otto et al., 2005). Rather the results indicate that one role RAC plays is a central part of the ER stress response—knockdown blunting activation of this pathway rather than sensitizing cells to stress.

Rather than a general effect on the UPR, transient reduction of RAC specifically inhibited the activation of the IRE1 arm of the UPR in response to several ER stress-promoting agents. The data indicate that RAC is required for IRE1 α oligomerization, but does not have significant effects on dimerization of the kinase. While dimerization is

required for the early autophosphorylation event, Xbp1 splicing is carried out by IRE1 α oligomers (Aragon et al., 2009; Kimata et al., 2007; Li et al., 2010), which form subsequent to hyperphosphorylation. By contrast, RIDD substrates are spliced by IRE1 α dimers (Tam et al., 2014), an activity unaffected by RAC knockdown. The unexpected role of RAC in modulating IRE1 α oligomerization raises the question of how a ribosome-associated chaperone is capable of modulating association of IRE1 α , an ER integral membrane protein whose dimerization is controlled by the luminal chaperone BiP, from the cytosol.

Strikingly, we discovered that knockdown of RAC results in enhancement of ribosome stalling on uXbp1 *in vitro* and *in vivo*, in addition to more general effects on mRNA translation. The data also demonstrated that IRE1 oligomerization requires translation, providing a link between RAC, the ribosome and IRE1 activities. Notably, the effects of RAC on translation were restricted to endogenous mRNAs as we did not detect any differential changes of GFP and Luc activities between wild type and knockdown RAC cell-free systems. One possibility may be because cells have more complex and precise regulation for natural cellular gene, but not toward the non-naturally occurring gene in human. Additionally, ribosome profiling data indicated that ribosomes stalled at codon Asn261 on uXbp1 in knockdown RAC upon ER stress, and was counteracted by knockdown Pelo, suggesting that RAC and Pelo may act on the same pathway but work oppositely. Since Pelo recognizes stalled ribosome complexes by binding to the ribosome A-site triggering the NGD mRNA surveillance system (Becker et al., 2011; Graille et al., 2008; Kobayashi et al., 2010), this suggests that RAC may have a

role in modulating ribosome A-site, which is consistent with the structure characteristics that yeast Mpp11 interacts with the ES12 of H44 (Leidig et al., 2013; Yan et al., 1998; Zhang et al., 2014), where the ribosome A-site originates from. The structural and functional data fortifies a potential role of RAC in mRNA quality control.

In conclusion, RAC has an unexpected and central role as a master ER stress sensor through its control of IRE1 α clustering and uXBP1 translational stalling. The role of RAC in modulating the translation rate of natural substrate mRNAs and its presence on most ribosomes suggest this activity is not restricted to XBP1. The reciprocal effects of RAC and Pelo knockdown suggest RAC may also play a role in NGD and NSD. Thus, the ubiquitously expressed RAC, occupying an evocative position on ribosomes and required for optimal growth, likely fills a central axis in governing protein homeostasis by coordinating both protein and mRNA quality control pathways.

Supplements

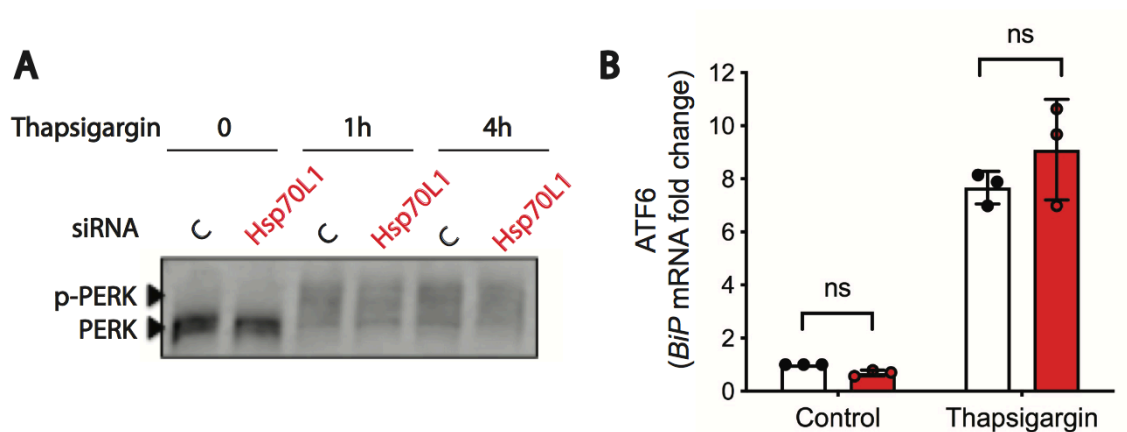


Figure S1. (Related to Figure 9) RAC does not affect the PERK and ATF6 branch of the UPR

Effects of Hsp70L1 knockdown on the molecular details of PERK and ATF6 arms of the UPR were examined in HeLa cells. Cells were challenged with thapsigargin ($0.5 \mu\text{M}$) for 4 hr and subsequent to pretreatment with either vehicle control or Hsp70L1 siRNA for 48 hr (**A**) Representative phos-tag gel analysis of PERK phosphorylation and (**B**) qRT-PCR of BiP mRNA fold change, reflecting the PERK and ATF6 branch, respectively. mRNA expression level was shown as fold change ($2^{-\Delta\Delta\text{CT}}$), which normalized to internal control, HPRT, relative to vehicle si-control. $n=3$. ns, not significant. Error bars, mean \pm SD.

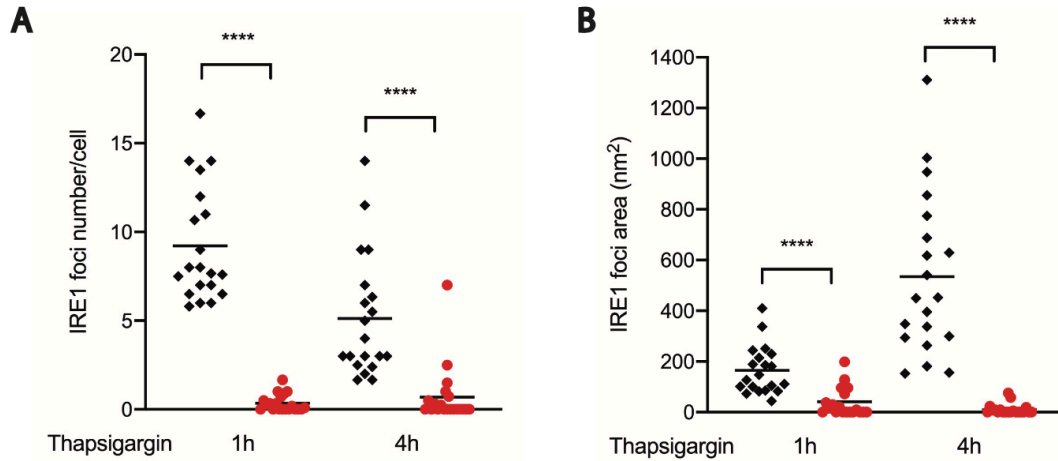


Figure S2-1. (Related to Figure 11) Selective inhibition effect on IRE1 α activity in RAC knockdown

Biological replicates of monitoring IRE1 α activities in RAC knockdown using T-REx293 IRE1-GFP cell line. Cells were pretreated with either vehicle control (black diamond) or Hsp70L1 (red circle) siRNA for 48 hr. Cells were challenged with thapsigargin for 1 and 4 hr after doxycycline (50 ng/ μ l) induction for 24 hr and quantification of **(A)** IRE1 α foci numbers and **(B)** foci area size by ImageJ. An average of 60 cells per condition. The Mean was presented. ****p<0.0001.

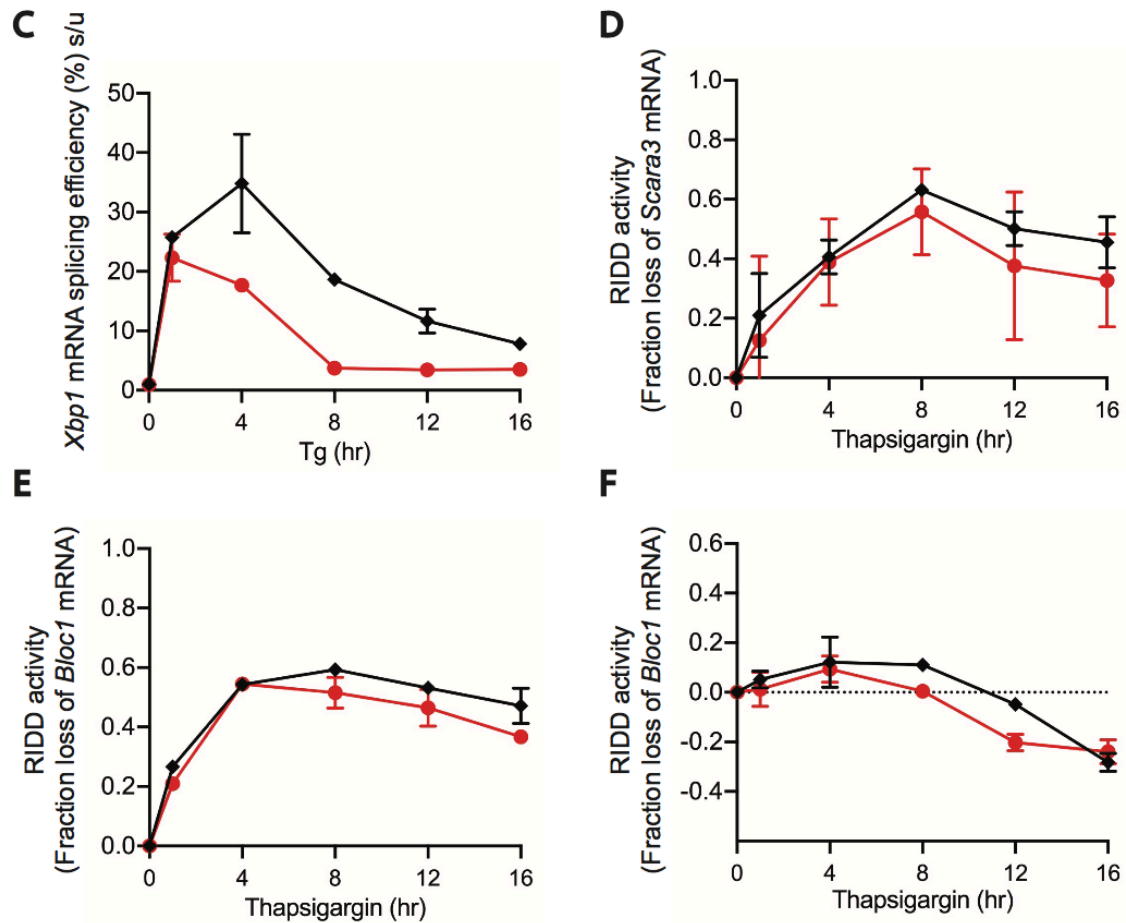


Figure S2-2. (Related to Figure 11) Selective inhibition effect on IRE1 α activity in RAC knockdown (continued)

(C) Xbp1 mRNA splicing efficiency (%) was analyzed for IRE1a oligomer activity, while mRNA fold change of (D) Scara3 and biogenesis of lysosome-related organelles complex 1 (Bloc1) were monitored for IRE1a RIDD activity in (E) HEK293 and (F) HeLa cells.

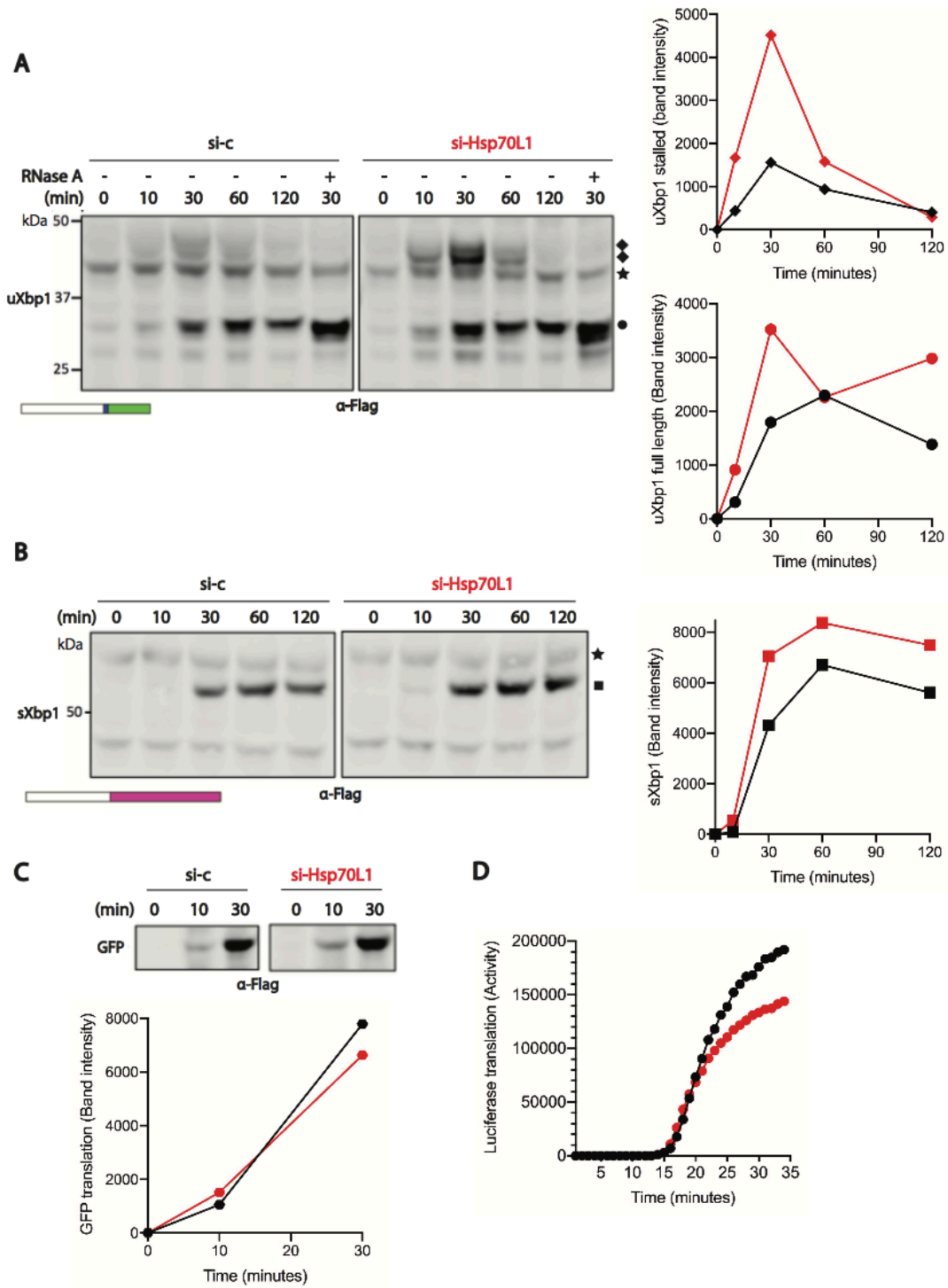


Figure S3-1. (Related to Figure 12) Enhancement of Xbp1 ribosome stalling and cellular translation rate in RAC knockdown by *in vitro* cell-free translation

Figure S3-2. (Related to Figure 12) Enhancement of Xbp1 ribosome stalling and cellular translation rate in RAC knockdown by *in vitro* cell-free translation (continued)

Biological replicates of *in vitro* translation assay. HEK293T cells lysates were collected subsequent to either vehicle control (black) or Hsp70L1 (red) siRNA treatment for 48 hr. (A) uXbp1, (B) sXbp1, (C) GFP, or (D) luciferase mRNA were translated in cell-free lysate analyzed by NuPAGE Bis-Tris gel (left) and quantified using *LI-COR*. uXbp1, sXbp1, and GFP mRNAs were engineered to carry an N-terminal FLAG tag. The stalling intermediate was confirmed by adding RNase A to break the peptidyl-tRNA ester bond. White box, the shared region of both uXbp1 and sXbp1. Blue box, the segment of the spliced intron. Green and magenta box, the distinct domain of uXbp1, sXbp1, respectively. ◆, uXbp1 stalling intermediates. ★, non-specific band. ●, uXbp1 full-length product. ■, sXbp1 full-length product.

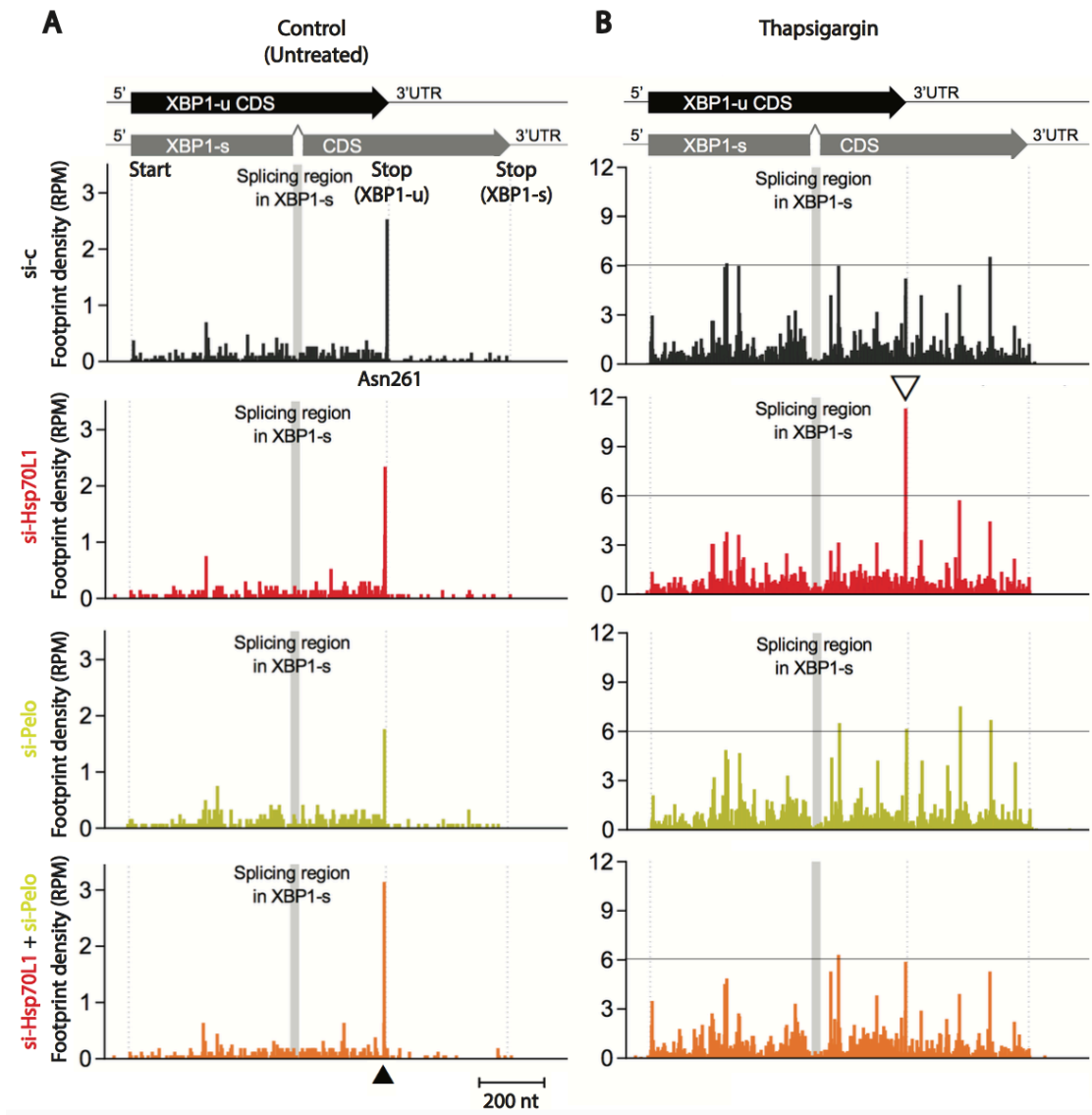


Figure S4-1. (Related to Figure 13) Enhancement of Xbp1 ribosome stalling in RAC knockdown and counteract effect by Pelo knockdown in RAC knockdown under ER stress by ribosome profiling

Figure S4-2. (Related to Figure 13) Enhancement of Xbp1 ribosome stalling in RAC knockdown and counteract effect by Pelo knockdown in RAC knockdown under ER stress by ribosome profiling (continued).

Ribosome footprints of the *Xbp1* transcript from siRNA against vehicle control (black), Hsp70L1 (red), Pelo (chartreuse), or both Hsp70L1 and Pelo (orange) in HEK293 Cells under basal condition and ER stress treatment. Cells were pretreated with designated siRNA for 48 hr and challenge with (A) DMSO or (B) thapsigargin (0.5 μ M) for 4 hr. Ribosome footprint density was shown as reads per million (RPM), with footprint displayed the position of ribosome A-site. First dot line, start site of *Xbp1*. Second dot line, stop codon of *Xbp1-u*. Third dot line, stop codon of *Xbp1-s*. Grey box, the *Xbp1* splicing region. ▲, ribosome stalling at Asn261 of *Xbp1-u*, one codon prior to *Xbp1-u* stop codon. ▽, the enhancement of *Xbp1* ribosome stalling in Hsp70L1 knockdown cells. Scale bar, 200 nt.

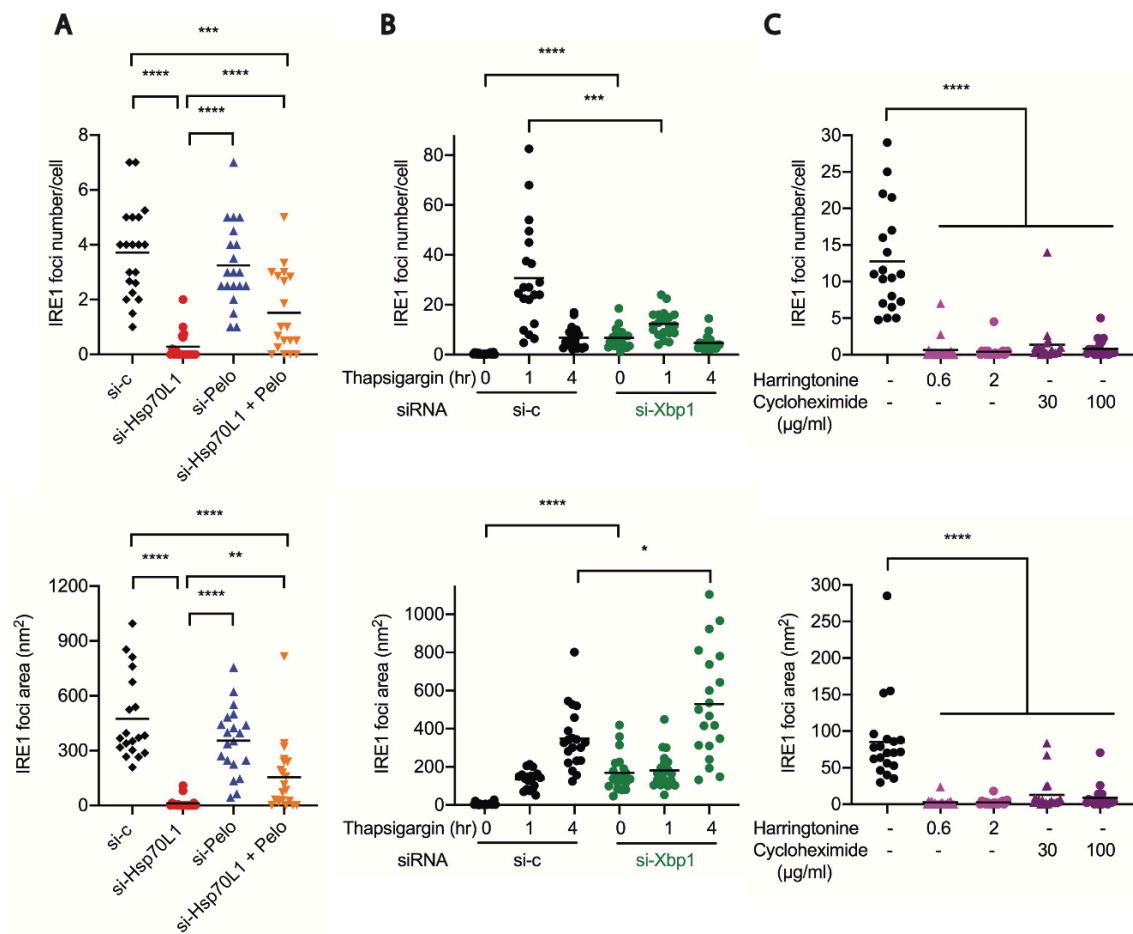


Figure S5. (Related to Figure 14) Counteract effect of IRE1 α activity by Pelo knockdown in RAC knockdown cells

Biological replicates of monitoring IRE1 α foci number (top) and foci area size (bottom) in T-REx293 IRE1-GFP cells after designated treatment by ImageJ. Cells were transfected with siRNA against vehicle control, Hsp70L1, Pelo, both Hsp70L1 and Pelo, or Xbp1 for 48 hr. IRE1 α foci were observed after cells treated with (A) thapsigargin (0.5 μ M) for 4 hr or (B) the indicated time course in knockdown cells. (C) IRE1 α foci were examined after cells pretreated with control, harringtonine (0.6, 2 μ g/ml), or cycloheximide (30, 100 μ g/ml) for 20 min followed by 1 hr of thapsigargin (0.5 μ M) treatment. The mean was presented. * p <0.05, ** p <0.01, *** p <0.001, **** p <0.0001. Scale bar, 10 μ m.

Material and Methods

Cell culture, transfection and RNA interference experiments

HeLa^{Tet-on} (Clontech), HEK293 (American Type Culture Collection, ATCC), HEK293T (ATCC), and T-REx293 IRE1-GFP cells (Li et al., 2010) were maintained at 37 °C, 5% CO₂ in Dulbecco's Modified Eagle's Medium (Sigma) supplemented with 4500 mg/L glucose, L-glutamine, sodium pyruvate, sodium bicarbonate, 10% fetal bovine serum (Sigma), 100 U/ml penicillin, and 100 μg/ml streptomycin (Sigma). T-REx293 IRE1-GFP cells were kindly provided by Dr. Peter Walter (UCSF/HHMI). Transient transfection of plasmid was performed using Lipofectamine 2000 Transfection Reagent (Thermo Fisher Scientific) according to the manufacturer's instructions. Transient gene knockdown was accomplished by transfection of small double-stranded interfering RNAs (siRNA) into cells using Lipofectamine RNAiMAX Transfection Reagent (Thermo Fisher Scientific) according to manufacturer's instructions. The siRNAs were synthesized from Dharmacon and sequence in Table 3. Silencer Negative Control No. 1 siRNA (Ambion) or ON-TARGET plus Non-targeting Control siRNA #1 (Dharmacon) were used as vehicle negative control.

Cell Viability (MTS assay)

HeLa cells were transiently transfected with siRNA against either control or Hsp70L1 for 48 hr. Cells were plated at a density of 5,000 cells per well in triplicates in 96-well. Cells were treated with either DMSO control, Celastrol (0.1, 1, 5, 10, 25 μM) or Thapsigargin (0.05, 0.1, 1, 5, 50 μM) for 24 hr. Cell viability was measured using

CellTiter 96 (Promega), which is an MTS-based assay (3-(4,5-dimethylthiazol-2-yl)-5-(3-carboxymethoxyphenyl)-2-(4-sulfofenyl)-2H-tetrazolium), according to manufacturer's instructions. Briefly, 20 μ l of CellTiter reagent was added into 100 μ l of cell medium at the indicated time point, incubated at 37°C for 1 hr, and monitored absorbance at 490 nm using SpectraMax plus 384 microplate reader (Molecular Devices). Cell viability (%) was normalized to DMSO control of vehicle si-control cells.

RNA isolation, cDNA synthesis and quantitative real time-PCR

Total RNA was isolated from cells using the NucleoSpin RNA kit (Machery-Nagel) according to the manufacturer's instructions. RNA was quantified using NanoDrop 2000c Spectrophotometers. cDNA was synthesized from 2 μ g of total RNA template using the High-Capacity cDNA Reverse Transcription kit (Thermo Fisher Scientific). cDNA synthesis conditions were as follows: 25°C for 10 min, 37°C for 120 min, 85°C for 5 min. qPCR was performed using Power SYBR Green PCR Master Mix (Thermo Fisher Scientific) on the 7900HT Fast Real-Time PCR System with 384 well block module (Applied Biosystems). qPCR conditions were as follows: 50°C for 2 min, 95°C for 10 min, 95°C 15 s, 60°C for 1 min, with 40 cycles of amplification. The primers used for qPCR measurements are shown in Table 4. Fold change mRNA expression levels were determined by the $2^{-\Delta\Delta CT}$ method (Livak and Schmittgen, 2001). The Ct value in each condition was normalized to HPRT internal control and then normalized to siRNA vehicle control sample. Each cDNA was measured in triplicate per sample for each primer pair.

Xbp1 mRNA splicing assay

Xbp1 mRNA splicing was measured either by PCR amplification flanking the intron splicing site or qPCR with spliced and unspliced specific primers. cDNA was used as template to amplify the Xbp1 fragments. For PCR amplification, flanking primers (Table 4) were used to generate a 474 bp amplicon from unspliced Xbp1, a 448bp amplicon from spliced Xbp1. PCR conditions were as follows: 98°C for 30 s, 98°C for 10 s, 60°C for 30 s, 72°C for 30 s, with 30 cycles of amplification followed by 72°C 10 min. The fragments were resolved on 2 % Agarose/1X TBE gel (Lonza, MetaPhor Agarose), visualized by ethidium bromide staining, and detected using a GelDoc-It² imager (UVP). For qPCR, specific primers (Table 4) were used. Xbp1 splicing efficacy (%) was calculated by: [(spliced Xbp1/unspliced Xbp1) normalized to thsigargin 4h si-control] X 100 %.

Protein analysis by immunoblotting

Cells were lysed in radioimmunoprecipitation assay buffer (RIPA) (50 mM Tris-HCl, pH 8.0, 150 mM NaCl, 1 % (v/v) NP-40, 0.5 % (w/v) Sodium deoxycholate, 0.1 % SDS) supplemented with 1X cOmplete EDTA-free protease and phosphatase inhibitor cocktail (Roche). Total cell lysates were cleared by centrifugation at 16,000 g for 10 min at 4°C. Total protein concentrations were determined by BCA protein assay (Thermo Fisher Scientific). 18 µg of total cell lysates were supplement with 5X Laemmli sample buffer (10 % SDS, 250 mM Tris-HCl pH 6.8, 0.1 % (w/v) Bromophenol blue, 50 % Glycerol, 500 mM DTT), heated at 95°C for 10 min, analyzed by 10 % Tris-glycine gel,

transferred onto 0.45 μ m PVDF membranes (Millipore Immobilon-FL), blocked in 5 % (w/v) nonfat dry milk in 1X TBS with 0.1 % Tween-20 for 1 hr in room temperature. Blots were incubated with the indicated primary antibodies at 4°C overnight in 1X TBS with 0.1 % Tween-20, followed by indicated secondary antibodies at room temperature for 1 h in 1X TBS with 0.1 % Tween-20 and visualized by LI-COR Odyssey CLx.

Phos-tag mobility shift assay

For phos-tag assay, samples were collected in RIPA buffer as similar as total cell lysates and heated at 95°C for 5 min. 25 μ g of total cell lysates were analyzed by 6 % Tris-glycine gel supplemented with 25 μ M Phos-tag acrylamide (Wako) and 50 μ M MnCl₂. SDS-PAGE gels were run constantly at 100 V for 3 hr, transferred onto 0.45 μ m PVDF membranes (Millipore Immobilon-FL) at 100 V for 1 hr and visualized by LI-COR Odyssey CLx.

Subcellular Fractionation

Cell fractionation was performed by sequential detergent extraction method (Jagannathan et al., 2011). HeLa cells were plated onto 6-well plate one day prior to cell harvest and were about 70-80% confluent on the harvest day. Cells were washed with 2 ml cold PBS and pretreated with 100 μ g/ml cycloheximide in PBS for 10 min on ice. Cells were permeabilized using 200 μ l Permeabilization buffer (110 mM KOAc, 25 mM K-HEPES, pH 7.2, 2.5 mM Mg(OAc)₂, 1 mM EGTA, 0.03 % Digitonin, 1 mM DTT, 50 μ g/ml cycloheximide, 1x cOmplete EDTA-free protease inhibitor cocktail (Roche), 100

U/ml RNasin ribonuclease inhibitors (Promega) and incubate on ice for 5 min. Plates were tilted to drain the soluble material and collected as the cytosolic fraction. Cells were then washed with 200 μ l Wash buffer (110 mM KOAc, 25 mM K-HEPES, pH 7.2, 2.5 mM Mg(OAc)₂, 1 mM EGTA, 0.004 % Digitonin, 1 mM DTT, 50 μ g/ml cycloheximide, 1x cOmplete EDTA-free protease inhibitor cocktail, 100 U/ml RNasin ribonuclease inhibitors). Next, cells were treated with 200 μ l Lysis buffer (400 mM KOAc, 25 mM K-HEPES, pH 7.2, 15 mM Mg(OAc)₂, 1 % NP-40, 1 mM DTT, 50 μ g/ml cycloheximide, 1x cOmplete EDTA-free protease inhibitor cocktail, 100 U/ml RNasin ribonuclease inhibitors) and incubate on ice for 5 min. Plates were tilted to drain the soluble material and collected as membrane fraction. Both cytosolic and membrane fractions were subjected to centrifugation at 7,500 g for 10 min to remove debris. Samples were supplemented with 5x Laemmli sample buffer and DTT, heated at 95°C for 10 min, analyzed by SDS-PAGE. For analysis of uXBP1 RNA localization, each fraction was subjected to RNA purification by NucleoSpin RNA (Machery-Nagel) followed by cDNA synthesis and analysis by qRT-PCR.

RNA immunoprecipitation

HeLa cells were pretreated with 100 μ g/ml cycloheximide in growth medium at 37°C for 10 min. RNA immunoprecipitation was performed as previously described (Sanz et al., 2009) with modifications. Cells were washed with cold PBS, solubilized in polysome buffer (50 mM Tris-HCl, pH 7.5, 12 mM MgCl₂, 100 mM KCl, 1 % NP-40, 1 mM DTT, 100 μ g/ml cycloheximide, 1X EDTA-free protease inhibitor cocktail and 200

U/ml ribonuclease inhibitor and incubated on ice for 20 min. Samples were subjected to a 10,000g centrifugation step for 10 min at 4°C to isolate post-mitochondrial supernatant. The resulting supernatants were quantified by BCA assay. 2 mg of supernatants were incubated with either rabbit monoclonal anti-Mpp11 antibody or a normal rabbit IgG as negative control rotating at 4°C. After 3 hr, 40 μ l of Protein G Dynabead (Thermo Fisher Scientific) were washed once with polysome buffer and supplement to the supernatants and incubation with rotation at 4°C for 16 hr. The beads were placed in a magnet on ice to separate the bound and unbound fractions. The beads were washed in high salt buffer (50 mM Tris-HCl, pH 7.5, 12 mM MgCl₂, 300 mM KCl, 1 % NP-40, 1 mM DTT, 100 μ g/ml cycloheximide, 1X EDTA-free protease inhibitor cocktail and 200 U/ml ribonuclease inhibitor) four times for 5 min. The bound and unbound materials were divided into two equal portions, either for protein or RNA analysis. For protein analysis, the beads were directly eluted with 5X Laemmli sample buffer and heated at 99 °C for 10 min. For RNA analysis, RNA was harvested from the beads by NucleoSpin RNA kit (Machery-Nagel), subjected to cDNA synthesis, and analyzed by qPCR.

IRE1 α foci imaging

T-REx293 IRE1-GFP cells were seeded at 3x10⁵/6 well and reverse transfection of siRNA against control, Hsp70L1, Pelo, and both Hsp70L1 and Pelo were performed using Lipofectamine™ RNAiMAX (Thermo Fisher Scientific) according to manufacturer's instructions, respectively. Cells were re-plated onto Poly-L-Lysine coated 12 mm coverslips (Corning) at 6x10⁴/24 well. Cells were treated with doxycycline

(Sigma) and were replaced with normal growth medium after 24h, then treated with thapsigargin (0.5 μ M) (Sigma) for 0, 1 or 4 hr. Cells were fixed with 4 % paraformaldehyde for 20 min at room temperature at indicated time points. Nuclei were stained with Hoechst (Thermo Fisher Scientific) for 10 min at room temperature. Coverslips were mounted with ProLong diamond antifade mountant (Thermo Fisher Scientific). Images were captured with LSM 880 laser scanning confocal microscope (Zeiss). Plan Apochromat 100x/1.4 numerical aperture (NA) oil objective was used. Foci were analyzed using ImageJ (Fiji).

Plasmids

To generate the uXbp1 and sXbp1 in vitro transcription plasmids, the uXbp1 and sXbp1 human open reading frame (ORF) were designed containing a N-terminal Flag epitope and 30 nt poly-A sequence after the Xbp1 stop codon, which is synthesized by GenScript, and inserted into pcDNA3.1 (+) downstream of a T7 promoter at HindIII and KpnI sites. The GFP and luciferase plasmids, which both containing a T7 promoter and 30 nt poly-A sequence after stop codon, were previously described (Yang et al., 2019). The GFP plasmid was designed containing three tandem Flag-tag at the N-terminus and the luciferase gene was codon optimized in the luciferase plasmid.

***In vitro* transcription**

uXbp1 and sXbp1 templates were generated by plasmids linearized with BamHI and eGFP and Luc templates were linearized with EcoRI followed by phenol/chloroform extraction and ethanol precipitation. RNA was synthesized by T7 RNA polymerase (NEB), capped by 3'-O-Me-m7G(5')ppp(5')G RNA Cap Structure Analog (NEB) and purified using RNA Cleanup Kit (NEB). The quality of RNA transcripts was monitored by denaturing RNA electrophoresis in 1X TAE agarose gels and quantified by NanoDrop 2000c Spectrophotometers.

***In vitro* translation by mammalian cell-free lysate**

In vitro translation extracts were harvested at 48 hr post-transfection of siRNA against either control or Mpp11 in HEK293T cells. Cells were re-plated in 10-cm dishes 18 hr prior collection. Mammalian cell-free lysate was harvested as previously described (Rakotondrafara and Hentze, 2011) with modifications. Cells were collected by trypsin, washed with cold DPBS, harvested by centrifugation at 1000 g for 5 min at 4°C, resuspended the cell pellet in fresh ice-cold hypotonic buffer (10 mM HEPES-KOH, pH 7.6, 10 mM potassium acetate, 0.5 mM magnesium acetate, 5 mM DTT, proteasome inhibitor cocktail) in a 1:1 volume ratio and incubate on ice for 30 min. Cells were homogenized by a 1 ml syringes with a 27 G $\frac{3}{4}$ needle for 10-20 times until > 95 % cells ruptured monitored by trypan blue staining, and potassium acetate was adjusted to a final concentration of 50 mM. Lysate was collected by centrifugation at 16,000g for 10 min at 4°C, the supernatant was snap frozen in liquid nitrogen, and store at -80°C before use.

Each translation reaction contained 66% in vitro translation lysate, 180 ng of RNA templates and buffer to make the final reaction with 1 mM ATP (NEB), 0.2 mM GFP (Sigma), 8 mM Creatine phosphate (Sigma), 0.13 units/ μ l Creatine phosphokinase (Sigma), 20 mM HEPES-KOH pH 7.6, 2 mM DTT, 0.83 mM Mg (OAc)₂, 0.1 M KOAc, 20 μ M amino acid mixtures (Promega), 500 μ M Spermidine (Sigma), 0.4 units/ μ l RNase inhibitor (Thermo Fisher Scientific). The reactions were incubated in a 30°C water bath for indicated incubation time and stop by adding 4X Native PAGE sample Buffer (Thermo Fisher Scientific). The samples were subsequently analyzed by native electrophoresis. For RNase A treatment, 1 μ l of 10 mg/ml RNase A (Thermo Fisher Scientific) was added to each reaction after indicated translation time and incubated for 15 min at 37°C. For luciferase assay, each reaction contained Luc RNA template, 0.12 μ l of Steady-Glo luciferase assay substrate (Promega) in the mammalian cell free translation buffer system, and real-time monitoring luciferase activity by FLUOstar OPTIMA microplate reader (BMG Labtech) at 30°C.

Native protein electrophoresis

To preserve peptidyl-tRNA ester bonds, in vitro translation products were denatured with 4X Native PAGE sample Buffer (Thermo Fisher Scientific), run on NuPAGE Bis-Tris gels (Invitrogen) with MES-SDS running buffer at 170 V for 2 hr and transferred onto 0.45 μ m PVDF membranes (Millipore Immobilon-FL #IPFL00010) at 35 V for 1 h.

Pulse labeling global nascent proteins with bioorthogonal non-canonical amino-acid tagging

Cell lysates were harvested at 48 hr post-transfection of siRNA against either control or Mpp11 in HeLa cells. Cells were re-seeded in 6-well plate 16 hr prior collection. Cells were washed twice with PBS and incubated in DMEM high glucose without methionine (Gibco) with 10% dialyzed FBS at 37°C for 30 min and replaced with methionine-free medium containing a final concentration of 50 μ M Click-IT L-Azidohomoalanine (AHA) (Thermo Fisher Scientific). After 5 hr, cells were washed twice with PBS, lysed in lysis buffer (1 % SDS in 50 mM Tris-HCl, pH 8.0, 1X protease inhibitor cocktail, 1X phosphatase inhibitor cocktail), incubated on ice for 15 min, vortex for 5 min followed by a 16,000 g centrifugation step for 5 min at 4°C. The supernatants were collected and subjected to azide-alkyne ligation (click chemistry) using Biotin-alkyne (Thermo Fisher Scientific) and Click-iT Protein Reaction Buffer Kit (Thermo Fisher Scientific) according to manufacturer's instructions followed by methanol/chloroform protein precipitation. Samples were loaded onto 10 % SDS-PAGE, transferred onto 0.45 μ m PVDF membranes (Millipore Immobilon-FL), blocked in 5 % (w/v) bovine serum albumin in 1X TBS with 0.1 % Tween-20 for 1 hr in room temperature. Blots were incubated with IRDye 800CW Streptavidin at 4°C overnight in 1X TBS with 0.1 % Tween-20, and visualized by LI-COR Odyssey CLx.

Ribosome profiling

Ribosome profiling was performed as previously described with few adaptations (Ingolia et al. 2012). HEK293 cells were harvested after 48 hr post-transfection of siRNA against vehicle control, Hsp70L1, Pelo, or both Pelo and Hsp70L1 and followed by 4 hr thapsigargin (0.5 μ M) treatment. Cells were washed in ice-cold PBS, lysed in lysis buffer (20 mM Tris-HCl, pH7.4, 150 mM NaCl, 5 mM MgCl₂, 1 mM DTT, 1% (v/v) Triton X-100, and 25 U/ml Turbo DNase I), and incubated on ice for 10 min. Cells were then triturated through a 26-G needle ten times and subjected to centrifugation at 16,000g for 10 min at 4°C. Cell lysates were digested with 100 U RNase I (Ambion) per A260 lysate at room temperature for 45 min with gentle agitation and followed by the addition of 200 U RiboLock RNase Inhibitor (Thermo Scientific). Ribosome protected mRNA fragments were isolated by 1M sucrose cushion in polysome buffer (20 mM Tris-HCl, pH7.4, 150 mM NaCl, 7.5 mM MgCl₂, 0.5 mM DTT, 20 U/ml RiboLock RNase Inhibitor) and centrifuged at 70,000 rpm for 2 h at 4°C by Beckmen TLA-110 rotor. Ribosome pellets containing mRNA footprints were isolated using TRIzol and separated by denaturing 12% polyacrylamide gel containing 8M urea. RNA was visualized by SYBR Gold (Invitrogen), and the size of the fragments ranging from 18 to 34 nt were isolated to generate the ribosome-protected fragment library. 3' oligonucleotide adaptor ligation, reverse transcription, circularization, and secondary rRNA depletion using biotinylated rRNA depletion oligos were performed as previously described (Ingolia et al. 2012). Libraries were barcoded using indexing primers for each sample during PCR amplification.

Statistical Analysis

Statistical analyses were performed by unpaired two-tailed Student's t test using GraphPad Prism 8 software. Statistically significant was considered as P-values less than 0.05. Error bars represent means and standard deviation (SD). The number of independent experiments is designated as n in the figure legends.

Table 1. Antibodies

Reagent	Source	Identifier
Mpp11	Cell Signaling	12844
Hsp70L1	Abcam	ab108612
GAPDH	Cell Signaling	2118S
PERK	Cell Signaling	3192
Calnexin	Cell Signaling	2679
BiP	Cell Signaling	3177
Rpl10	Abnova	PAB17331
SRP54	BD	610940
IRE1 α	Cell Signaling	3294
Hsp70	Cell Signaling	4872
Pelo	Proteintech	10582-1-AP
Flag	Sigma	F1804
IRDye 680RD Secondary Antibodies Goat anti-Mouse IgG	Licor	926-68070
IRDye 680RD Secondary Antibodies Goat anti-Rabbit IgG	Licor	926-68071

Table 2. Key reagents

Reagent	Source	Identifier
Thapsigargin	Sigma	T9033
Celastrol	Sigma	C0869
Cycloheximide	Sigma	C7698
Homoharringtonine	Sigma	SML1091-10MG
Doxycycline	Sigma	D9891
Digitonin	Millipore	300410

Table 3. siRNA sequences

Gene		siRNA target sequence	Source	Identifier
Hsp70L1	1	CAGAAAUACAUCGCGGAAA	Dharmacon	M-021084-01-0005
	2	UAACAUCGGUGGUGCACAU		
	3	GGAAAUGCGCGAGCCAUGA		
	4	GUAUUGGGCUCAGAUGCAA		
Mpp11		GAACCAAGAUCAUUAUGCA	Dharmacon	M-025435-02-0005
		GAAAUCAACUGGUGGAGGU		
		GAACUUGUCGAGAUGGUAA		
		AGGACUGCAUGAAACGAUA		
Pelo		GGACACAAGUACUCCUGA	Dharmacon	M-019068-00-0005
		ACACGGAGCCGGUAUGUGA		
		AGGAAGGCCUCGCCCAUUAU		
		AGUGAAGACCGACAACAAA		
Xbp1		GGUAUUGACUCUUCAGAUU	Dharmacon	M-009552-02-0005
		CGAAAGAAGGCUCGAAUGA		
		CAACUUGGACCCAGUCAUG		
		GCAAGCGGCAGACCCAGAA		
ON-TARGET plus Non-targeting Control siRNAs #1		UGGUUUACAUGUCGACUAA	Horizon	D-001810-01-20

Table 4. Primer sequences

Primer		Sequence	Purpose
XBP1	F	AAACAGAGTAGCAGCTCAGACTGC	XBP1 splicing assay
	R	TCCTTCTGGGTAGACCTCTGGGAG	
Actin	F	CACCTTCTACAATGAGCTGAG	
	R	TAGCACAGCCTGGATAGCAAC	
sXBP1	F	CGCTTGGGGATGGATGCCCTG	qPCR
	R	CCTGCACCTGCTGCGGACT	
uXBP1	F	CAGCACTCAGACTACGTGCA	
	R	ATCCATGGGGAGATGTTCTGG	
HPRT	F	CTGAGGATTTGGAAAGGGTGT	
	R	ATCTCCTTCATCACATCTCGAG	
Hsp70	F	TTCCGTTTCCAGCCCCCAATC	
	R	CGTTGAGCCCCGCGATGACA	
Bip	F	TGTTCAACCAATTATCAGCAAATC	
	R	TTCTGCTGTATCCTCTTACCAGT	
Scara3	F	GGCTGACATTCTCTGGCCTT	
	R	GCTTGGATTCCTTCCAGGCT	
Bloc1	F	TGGTGGAGAACTTCAACCAGG	
	R	GCAGCTGCCCTTTGTAGACAT	

Chapter IV

Conclusion and Future Directions

The ribosome-associated complex (RAC) directly interacts with the nascent chain near the polypeptide exit tunnel on the 60S ribosomal subunit and interacts with the decoding center on the 40S subunit. RAC's unique position spanning both ribosomal subunits put it in a perfect location to coordinate nascent polypeptide status and mRNA translation. Although RAC had been presumed to be an exclusively cytosolic chaperone, knockdown of RAC in mammalian cells did not lead to protein aggregation or induction of HSF, which are hallmarks in cytosolic misfolding stress. Surprisingly, contrary to the predictions of the hypothesis, knockdown of RAC selectively inhibits IRE1 α branch of the UPR, including disturbing IRE1 α phosphorylation, IRE1 α high-order oligomerization, Xbp1 translation arrest, and Xbp1 mRNA splicing upon ER stress. Notably, the inhibition of IRE1 α and Xbp1 activities are counteracted by depletion of Pelo, a ribosome rescue factor recognizing stalled ribosomes, in RAC knockdown cells, implying RAC and Pelo may play opposing roles in tuning Xbp1 mRNA splicing. Collectively, this study reveals a central role of RAC in the UPR modulating IRE1 α oligomerization and mRNA translation.

Mechanism of action of RAC

This study indicated that RAC regulates the IRE1 α activation from the cytosolic side of the ER membrane in conjunction with the known luminal mechanisms of activation. The experiments conducted in this dissertation demonstrated that RAC is enriched on the ER membrane, and Mpp11 re-localizes to cytosol upon ER stress in mammalian cells, while Hsp70L1 still localizes on the ER membrane. The molecular mechanism of how RAC modulates IRE1 α clustering and whether RAC components work together or individually regulate ER stress remains obscure. Understanding the mechanisms of RAC on IRE1 α clustering will facilitate a greater understanding of the UPR pathway and may provide a potential target to modulate UPR activity in diseases. One model presented in chapter III is that RAC modulates IRE1 α clustering by regulating global translation. Another possible model could be RAC facilitates IRE1 α high-order oligomerization by acting as an adapter protein to stabilize the IRE1 oligomer. These models may occur concurrently as well as other indirect interaction models.

Does RAC modulate IRE1 high-order oligomerization by physical interaction?

To further dissect RAC's detailed mechanism in regulating IRE1 α high-order oligomerization, whether RAC and IRE1 α are in close proximity was assessed. Immunoprecipitation with anti-IRE1 α antibody was performed in HeLa cell lysates, and a weak Mpp11 signal was detected by immunoblotting in the absence of ER stress (Appendix 5A), whereas the signal was undetectable in the presence of ER stress. Inversely, immunoprecipitation was performed with anti-Mpp11 antibody to validate the

interaction (Appendix 5B). A signal slightly below the predicted molecular weight of IRE1 α was detected by immunoblotting in the absence and presence of ER stress. Whether the band represents IRE1 α or a non-specific band needs to be addressed. In addition, crosslinking prior to immunoprecipitation to preserve weak and flexible interaction could provide insights into the process. Furthermore, an IRE1 α mutant with deletion of the cytoplasmic domain, where RAC is predicted to interact, could be included as a control for immunoprecipitation.

In contrast, the interaction of RAC and IRE1 α was also examined by immunofluorescence (Appendix 5C). In the absence of ER stress, the IRE1 α -GFP reporter's signal was too weak to draw any conclusion whether Mpp11 and IRE1 α are in close proximity; in the presence of ER stress, Mpp11 does not co-localize with IRE1 α foci. However, whether Hsp70L1 co-localizes to IRE1 α foci remains to be addressed. To enhance the signal for IRE1 α at basal conditions, anti-GFP antibody could be used in immunofluorescence staining. Preliminary data have supported the model that RAC and IRE1 α may be in close proximity at basal conditions; however, experiment conditions need to be optimized to draw a decisive conclusion.

What are the roles of RAC on the ribosome? What are the substrates for RAC?

Although mammalian RAC is a ubiquitous and highly conserved protein discovered 15 years ago (Hundley et al., 2005), the function and physiological substrates of mammalian RAC remain obscure. The study detailed in this dissertation suggests that reduction of RAC enhances Xbp1 ribosome stalling in mammalian cells. Interestingly,

Rospert's group also indicated that cells lack of RAC increase ribosome pausing on reporter containing C-terminus poly-AAG/A sequences in yeast, which may result from the absence of RAC distorting the ribosomal peptidyl transferase center (PTC) and the decoding center (DC) (Gribling-Burrer et al., 2019). Collectively, these results indicate RAC' role on modulating ribosome stalling is conserved from yeast to mammals and may act on a broader set of substrates.

Notably, the effects of RAC on translation discovered in this dissertation were limited to endogenous mRNAs. There is no differential change of GFP and Luc activities between wild type and knockdown RAC cells. It is important to note that the GFP and Luc reporter genes used in this study were codon-optimized, while Xbp1 contains rare codons. RAC's position on ribosomes interacting with the PTC and the DC supports the model that RAC could modulate the translation of rare codons. To test this hypothesis, Luc reporter bearing either optimized codons or rare codons could be tested in wild type and knockdown RAC in cell-free assays.

To monitor whether RAC regulates ribosome stalling of other substrates, further bioinformatics analyses of the ribosome profiling data performed in this study would be revealing. However, it should be noted that based on the ribosome profiling analysis from other studies, Xbp1 stalling is one of the strongest translational arrests observed in basal physiological condition by ribosome profiling in mammalian cells. This suggests that one may not detect other stalling substrates using basal conditions. Since cells trigger mRNA quality control mechanisms to prevent aberrant product production when ribosome stalling occurs, performing ribosome profiling of cells reduction in the mRNA QC

machinery (Pelo, hbs1, ABCE1, Ski complex or Xrn1) may be required to reveal potential ribosome stalling sites. Additionally, whether RAC regulates global translation efficiency can be tested by monitoring both ribosome profiling and RNA-sequencing data. Understanding the mechanism action of RAC on translation may provide detailed information about how the proteostasis network is co-translationally modulated on the ribosome.

To globally dissect the physiological substrates of RAC and disclose where and how RAC engages with the nascent chain, selective ribosome profiling (Becker et al., 2013) could be determined by selectively isolating RAC-associated mRNA-ribosome-nascent chain complexes followed by ribosome profiling. The interplay of RAC with other ribosome-associated factors like SRP has been a long-term puzzle. Since studies also suggested that SRP facilitates membrane targeting of Xbp1, together with the studies in this dissertation that indicate RAC is on Xbp1 translating ribosome, suggests that Xbp1 could be a prospective substrate to study the interplay of RAC and SRP. Site-specific crosslinking assays of serial deletion of Xbp1 with SRP or RAC could also be performed to monitor the interactions of Xbp1 nascent chain with SRP and RAC.

The unknown in the IRE1 branch

Is uXbp1 mRNA crucial for maintaining IRE1 inactive in the absence of ER stress?

This dissertation revealed that knockdown of Xbp1 does not affect IRE1 α clustering ability upon ER stress in mammalian cells. This demonstrates that IRE1 α clustering upon ER stress is independent of Xbp1 mRNA, consistent with the finding in

the yeast system (Aragon et al., 2009). Unexpectedly, IRE1 α clustering is activated in knockdown Xbp1 cells even without stress treatment, suggesting lack of Xbp1 leads to a smoldering basal ER stress. A study has shown that uXbp1 protein is a negative regulator of sXbp1 protein (Yoshida et al., 2006). During the recovery stage of the UPR, uXbp1 forms a complex with sXbp1 protein triggering proteasome degradation, and shuts off the UPR. Although the negative correlation between the protein of uXbp1 and sXbp1 has been established, the relationship between the mRNA of uXbp1 and sXbp1 has yet to be defined. To better understand the relationship between IRE1 and Xbp1 at basal condition, one can re-express either the protein or mRNA of uXbp1 and sXbp1 in a Xbp1 knockdown model and monitor whether the IRE1 activation is restored.

IRE1 foci formation depends on the translation of which messages?

This study revealed that the formation of IRE1 foci required translation. Since this study also indicated that the formation of IRE1 foci does not required its substrate, Xbp1 mRNA, in mammalian systems, as well as Hac1 mRNA in yeast system shown by Peter Walter's group (Aragon et al., 2009), messages other than Xbp1 could be modulating IRE1 foci formation. To identify the messages regulating IRE1 foci formation, pull down of IRE1 followed by analyzing IRE1 associated RNAs could be performed. Interestingly, Walter's group has reported that IRE1 associated to numbers of RNAs using photoactivatable ribonucleoside enhanced crosslinking and immunoprecipitation (PAR-CLIP) followed by RNA-sequencing in the absence or presence of ER stress, induced by tunicamycin for 4 hr, in HEK293 cells (Acosta-Alvear et al., 2018). Notably,

there are some translation related IRE1-bound substrates induced in the presence of ER stress, such as eukaryotic translation initiation factor 4E binding protein 1 (EIF4EBP1), eukaryotic translation elongation factor 2 (EEF2), and YARS (tyrosyl-tRNA synthetase/ligase). These could be the potential targets that modulate the translation dependent IRE1 foci formation. IRE1 foci formation could be monitored in the presence of ER stress in knockdown of these genes, respectively.

Physiological function and disease relevance of RAC

Emerging studies have indicated that Zuo1 transcriptionally activates pleiotropic drug resistance 1 (Pdr1) gene to adapt to nutrient limited conditions by exporting quorum sensing molecules in *S. cerevisiae* (Ducett et al., 2013; Prunuske et al., 2012). Additionally, Mpp11 directly interacts with ubiquitinated histone H2A transcriptionally and induces polycomb-repressed genes that govern cell fate decisions, including self-renewal and differentiation of mouse pluripotent embryonic stem cells (ESC) (Aloia et al., 2013; Aloia et al., 2014; Aloia et al., 2015b; Richly et al., 2010).

The role of RAC in cancer

In mice, Mpp11 was originally named mouse Id associate 1 (MIDA1) due to its ability to directly interact with Id1 helix-loop-helix (HLH) protein (Shoji et al., 1995), which is a master cell growth regulator (Norton, 2000). Reduction of Mpp11 retards cell growth as well as accumulates cells in S phase and blocks cells entering G2-M phase in murine erythroleukemia cells (Inoue et al., 1999, 2000; Shoji et al., 1995). This is

consistent with the notion that Mpp11 is first identified as an M phase phosphoprotein in human cell lines (Matsumoto-Taniura et al., 1996) and decreases cell growth in Mpp11 reduction cells (Jaiswal et al., 2011; Otto et al., 2005).

Accumulating clinical patients data have demonstrated that Mpp11 is overexpressed in head and neck squamous cell carcinoma (HNSCC) (Resto et al., 2000), acute myeloid leukemia (AML) (Demajo et al., 2014; Greiner et al., 2004), chronic myeloid leukemia (CML) (Greiner et al., 2004; Schmitt et al., 2006), and B-cell chronic lymphocytic leukemia (Aloia et al., 2015a; Giannopoulos et al., 2006). A study has indicated that depletion of Mpp11 inhibits cell proliferation and increases apoptosis in human AML cells and decreases leukemogenesis in a xenograft mouse model *via* modulating retinoic acid (RA) pathway by interacting with RA receptor α (RAR α) and controls histone acetylation (Demajo et al., 2014), suggesting that Mpp11 could serve as an oncogene. In contrast, another study has suggested that depletion of Mpp11 impairs activation at the INK4A-ARF locus bypassing oncogene-induced senescence in human and mouse fibroblasts (Braig and Schmitt, 2006; Gorgoulis and Halazonetis, 2010; Ribeiro et al., 2013), indicating that Mpp11 could also act as a tumor suppressor gene. The contradictory role of Mpp11 may imply its distinct functions in benign and malignant cell models, yet the molecular mechanism of Mpp11 in cancer remains obscure.

Moreover, other studies have suggested that Hsp70L1 is a potent T helper cell (Th1) polarizing adjuvant for antitumor immune responses (Fang et al., 2011; Liu et al., 2018; Wan et al., 2004; Wu et al., 2005). Hsp70L1 directly binds to toll like receptor 4

(TLR4) on the surface of dendritic cells (DC), activates mitogen activated protein kinase (MAPK) and nuclear factor kappa-B (NF- κ B), induces secretion of tumor necrosis factor- α (TNF- α), cytokines interleukin 12p70 (IL-12p70), IL-1 β , and chemokine IP-10 and leads to DC maturation and activation (Fang et al., 2011; Husebye et al., 2006; Kagan et al., 2008; Wan et al., 2004). However, the molecular mechanism of Hsp70L1 in cancer is less well understood.

The emerging role of IRE1 in cancer

Growing evidence indicates that prolonged ER stress may play a central role in various diseases, such as inflammation, diabetes, neurodegenerative disorders, including Alzheimer and Parkinson disease, as well as cancer (Limia et al., 2019; Lin et al., 2008; Madden et al., 2019; Navid and Colbert, 2017; Ozcan and Tabas, 2012). To adapt to rapid proliferation needs and the hypoxic and nutrient-deprived tumor microenvironment, cancer cells trigger the activation of the UPR to meet the increased demands of lipid and protein production and quality control. When the ER stress induces severe and irreversible cell damage, the UPR switches from a pro-survival to pro-apoptotic mechanism. However, tumor cells manage to circumvent the apoptotic switch and exploit the UPR in favor of cancer progression (Sheng et al., 2019), metastasis (Li et al., 2015; Tanjore et al., 2011) and chemoresistance (Chen et al., 2017; Feng et al., 2011; Jiang et al., 2009; Logue et al., 2018; Salaroglio et al., 2017).

Constitutive IRE1 RNase activity in metastatic and poorly differentiated tissue samples in colorectal cancer have been reported (Jin et al., 2016; Mhaidat et al., 2015),

breast cancer (Li et al., 2015; Logue et al., 2018), oral squamous cell carcinoma (Hsu et al., 2018; Sun et al., 2018), esophageal squamous cell carcinoma (Xia et al., 2016), hepatocellular carcinoma (Wu et al., 2018), and multiple myeloma (Harnoss et al., 2019). A recent study indicated that IRE1 branch is essential for c-Myc signaling in prostate cancer (Sheng et al., 2019). Additionally, studies indicated that activation of IRE1 branch promotes cancer metastasis and invasion via modulating cytokine production of VEGF-A, IL-1 β , IL-6, IL-8, TGF- β 2 and CXCL3 (Auf et al., 2010; Logue et al., 2018), Xbp1s transcriptional induction of cell cycle gene cyclin D1 (Jin et al., 2016), epithelial-to-mesenchymal transition (EMT) genes, such as snail, twist, vimentin (Li et al., 2015; Wu et al., 2018), extracellular matrix (ECM) remodeling proteins, such as MMP-1, 3, and 9 (Sun et al., 2018; Xia et al., 2016), as well as VEGF-R2 expression (Mhaidat et al., 2015).

However, another study indicated that the expression of dominant-negative IRE1 induces tumor cell migration *via* inhibiting RIDD activity resulting in increasing in its target gene extracellular matrix protein SPARC expression in U87 glioma cells (Dejeans et al., 2012). Additionally, a recent study also indicated that the tumor of Xbp1 high and RIDD low activity has more metastatic ability and a lower survival rate than the tumor of Xbp1 low and RIDD high activity in Glioblastoma multiforme (Lhomond et al., 2018). These studies highlight the diverse roles of IRE1 substrates, Xbp1 and RIDD activity, in cancer metastasis.

Interestingly, treatment of an IRE1 α RNase-specific inhibitor, MKC8866, potently reduced prostate cancer viability in preclinical models as a monotherapy or

combination therapy with current prostate cancer drugs (Sheng et al., 2019). Another study also indicated that an IRE1 α kinase inhibitor, 18, selectively inhibited patient-derived multiple myeloma cell proliferation while sparing normal cells (Harnoss et al., 2019). These findings accentuate the importance of understanding the physiological role and dual functions of IRE1 activity in the tumor and its surrounding microenvironment and also the need to develop therapeutic interventions that enable selectively targeting of the IRE1 RNase downstream Xbp1 and RIDD activity.

The potential role of RAC in cancer therapeutics

Does Mpp11 function as a J protein for Hsp70L1 in cell proliferation?

Studies have indicated that cells lacking Mpp11 results in reduced cell growth in human cell lines as well as interfering with cells entering the G2-M phase in murine erythroleukemia cells. However, whether the cell inhibition effect is due to Mpp11 function as a J protein for its hsp70L1 partner remains undefined in mammalian cells. Understanding the mechanism action of RAC in cell growth in human cell lines may provide detailed mechanistic information to modulate cancer cell progression. To test this hypothesis, one can re-express Mpp11 mutant that abolishes interaction with its Hsp70L1 chaperone, and monitor whether the mutant can compensate for the cell growth inhibition in Mpp11 depletion cell line.

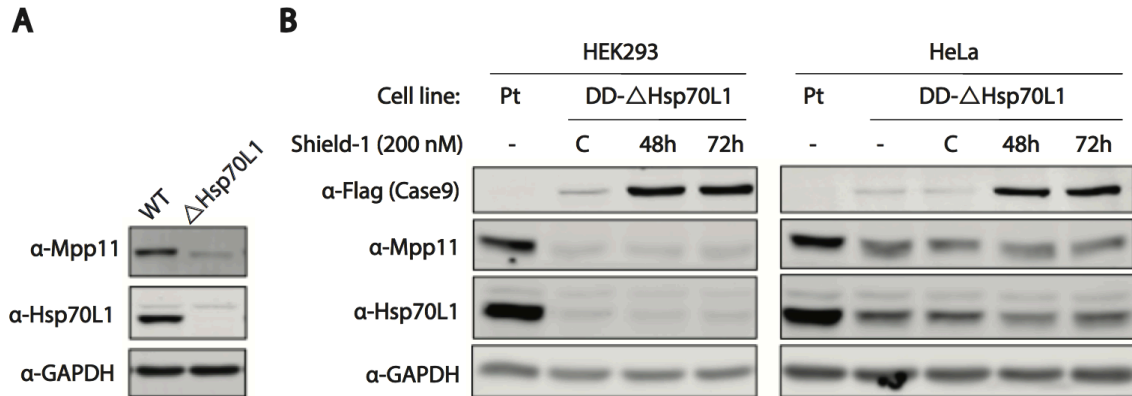
Studies have also indicated that Mpp11 is overexpressed in numbers of cancers, yet whether both RAC components overexpressed in cancer remain undefined. If RAC plays a crucial role in cancer progression, one can design molecules to interfere with the

Mpp11-Hsp70L1 interactions site, or target depletion of RAC. Based on the gene expression analysis by RNA-seq from the TCGA and the GTEx database, Mpp11 and Hsp70L1 are both overexpressed across common cancer types when comparing patient tumor samples to normal tissues, including lymphoid neoplasm diffuse large B-cell lymphoma, pancreatic adenocarcinoma, and thymoma. However, whether the RNA expression level directly correlates to protein levels remains undefined. The concurrence of RAC overexpression in the same patient tissues and the cancer progression of RAC could be further analyzed in detail using available protein and RNA databases.

RAC could serve as a dual pathway drug candidate in cancer

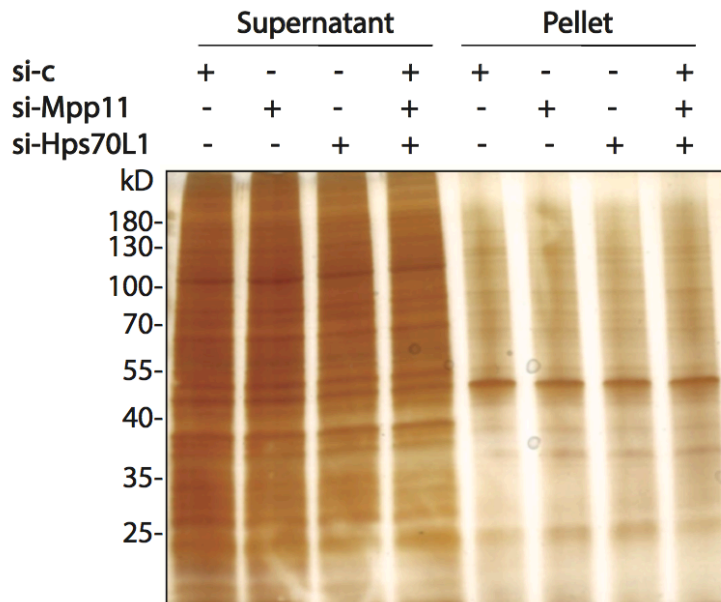
Recent studies have indicated that IRE1 α RNase/kinase inhibitors selectively inhibit cancer cell proliferation and spare normal cells in prostate cancer and multiple myeloma (Harnoss et al., 2019; Sheng et al., 2019). Accumulating evidence also suggests that the constitutive activation of IRE1, especially the activity of Xbp1, results in a more metastatic tumor phenotype and has a lower overall patient survival rate. Additionally, the study in this dissertation revealed a central role of RAC in the IRE1 branch of UPR selectively modulating Xbp1 activity, suggesting that RAC could serve as a potential target to selectively modulate IRE1 activity. Furthermore, RAC is overexpressed in a wide variety of malignant tumors, and studies have indicated a crucial role of RAC in cell proliferation. RAC's central role in cell proliferation and UPR makes it an attractive dual pathway drug candidate in cancer.

Appendix



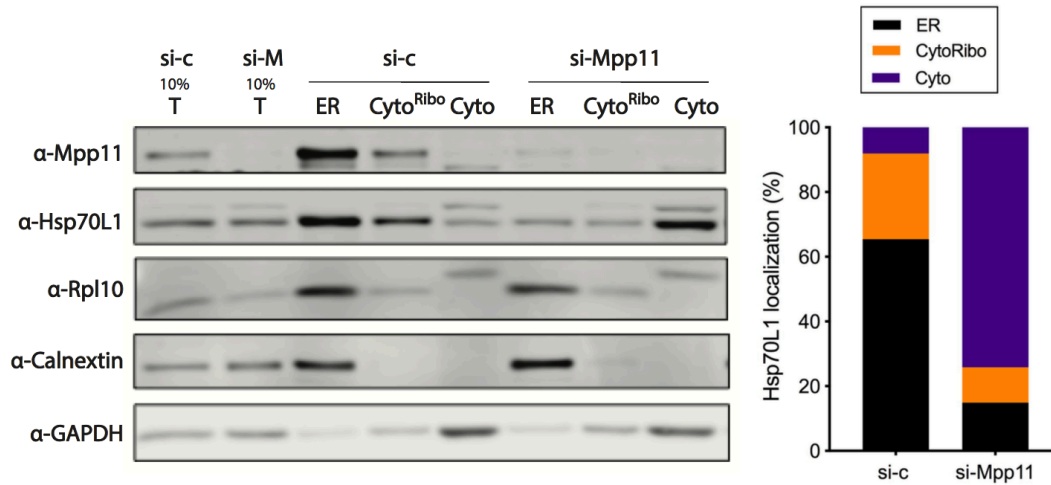
Appendix-1. RAC knockout in mammalian cells

Representative western blot analysis by *LI-COR* of RAC components from whole cell lysates in (A) stable Hsp70L1 knockout system in HEK293 cells by CRISPR/Cas9 and (B) conditional Hsp70L1 knockout system in HEK293 cells or HeLa cells by DD-Cas9, an FKBP12 destabilizing domain fused to Cas9 that induced rapid proteasome degradation of Cas9 in the absence of an FKBP12 ligand (Shield-1, 200nM) (Banaszynski et al., 2006).



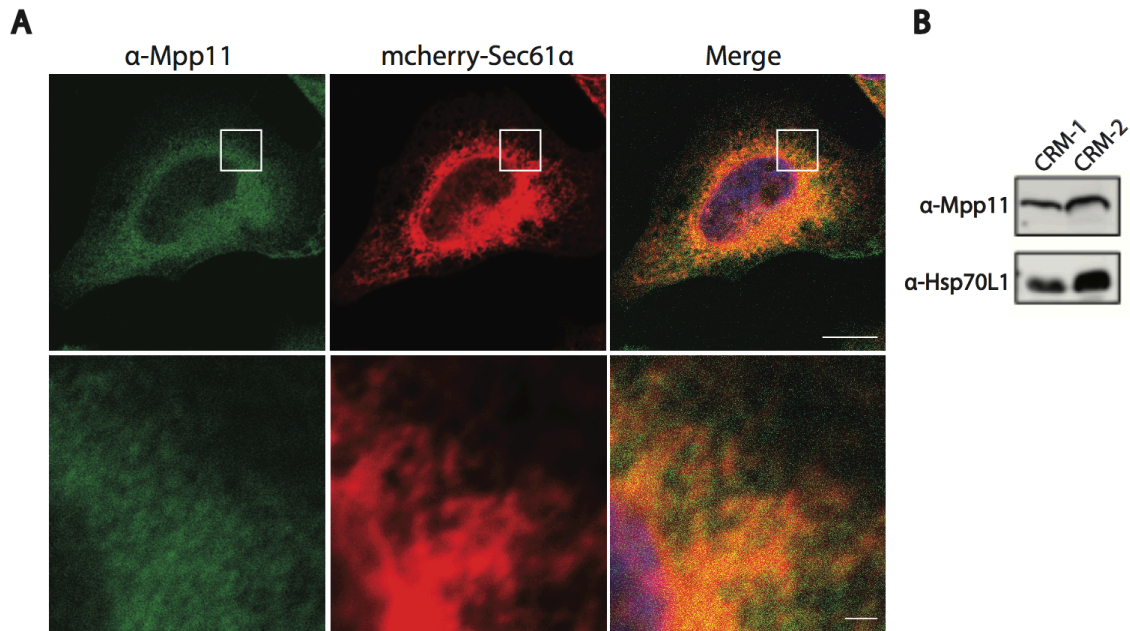
Appendix 2. Knockdown RAC does not lead to protein aggregation

Cells were harvested after 48 hr of siRNA treatment against either vehicle control, Mpp11, Hsp70L1, or both Mpp11 and Hsp70L1 in HeLa cells. Protein aggregates were isolated by sedimentation and analyzed by SDS-PAGE and visualized by silver staining.



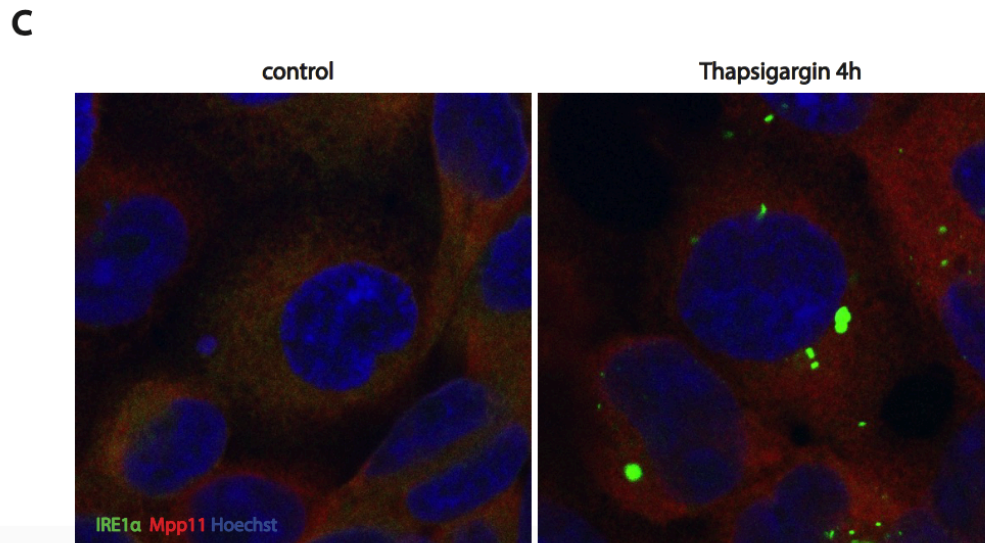
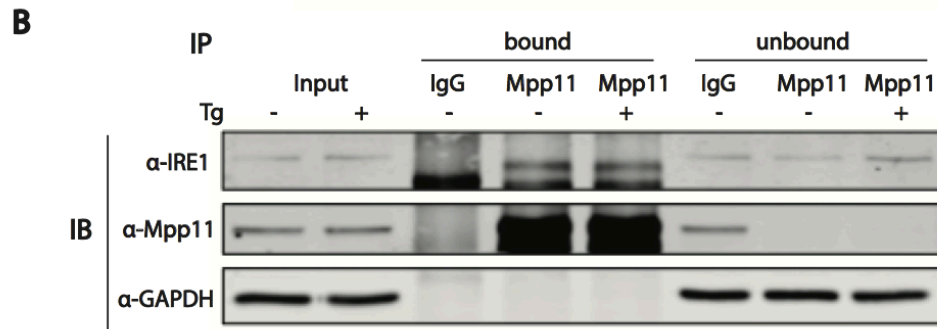
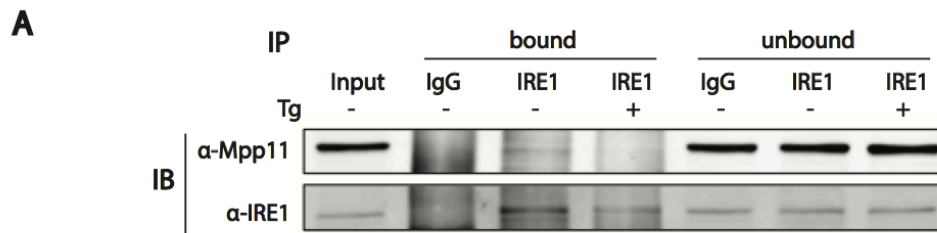
Appendix-3. Hsp70L1 associated to the ribosome *via* Mpp11 in mammalian cells

Subcellular fractionation of HeLa cells pretreated with either vehicle control or Mpp11 siRNA for 48 hr and harvested by sequential detergent extraction method. 10% of total lysate was loaded, cytosol, cytosolic ribosome, and ER membrane-bound fraction were collected and loaded equal amount in each lane. Representative western blot images of subcellular fractionation (left). Rpl10 was used as ribosome marker, BiP as ER lumen marker, Calnexin as ER membrane marker, and GAPDH as cytosol marker. Quantification of subcellular localization of Hsp70L1 (right) by *LI-COR*. The segmented bar chart represents relative Hsp70L1 protein localization (%) in each condition.



Appendix-4. Colocalization of RAC to the ER

Subcellular distribution of RAC in HeLa cells. **(A)** Representative immunostaining images of RAC using anti-Mpp11 antibody and transiently expression of mcherry-Sec61α after 18 hr in HeLa cells (top row). Nuclei were visualized using Hoechst stain. Scale bar, 10 μ m. High magnification images of the region were framed by white squared area (bottom row). Scale bar, 1 μ m. Colocalization analysis was performed using Person's correlation coefficient (PCC) from three images. $PCC (Mpp11/ Sec61\alpha) = 0.43$. **(B)** RAC is enriched on canine pancreas rough microsomes (CRM) from two biological repeats. CRM from previously described (Karamyshev et al., 2014).



Appendix-5. RAC may be in close proximity to IRE1α

Immunoprecipitation was performed in HeLa cells immunoprecipitated with antibody against IgG control of IRE1α (A) or Mpp11 (B). Representative western blot of bound and unbound fraction of IP. 1% total lysate as input. GAPDH as loading control. (C) Immunostaining images of RAC using anti-Mpp11 antibody in T-REx293 IRE1-GFP cells after DMSO control or thapsigargin treatment for 4 hr. Nuclei were visualized using Hoechst stain.

Appendix-Materials and methods

Generation of knockout cell lines by CRISPR/Cas9

For Hsp70L1 knockout cell lines, guide RNA (5'-GAACTCCGATGGCCGCC ATG-3') was cloned into lentiCRISPR v2 (Addgene #52961) as described previously (Shalem et al., 2014). EGFP guide RNA (5'-GGGCGAGGAGCTGTTCACCG-3') was used as non-targeting negative control (a gift from Dr. Joshua T. Mendell's lab at UTSW). To generate lentivirus, 6×10^5 of 293T cells were plated into 6-well followed by total 1 μg plasmids transfection of LentiCRISPR, psPAX2 (Addgene #12260), and pMD2 (Addgene #12259) (at 5:3:2 ratio) *via* FuGENE HD as previously described (Golden et al., 2017). Post-transfection 48 hr, virus-containing medium was collected and filtered through a 0.45 μm SFCA membrane. Filtered virus-containing medium was diluted with fresh medium at 1:1 ratio and infected to HCT116 cells for 8 hr with polybrene at a final concentration of 8 $\mu\text{g}/\text{mL}$. Post-infection 48 hr, cells were plated into puromycin (1 $\mu\text{g}/\text{mL}$) selection medium for 48 hr. Clonal knockout cell lines were generated by serial dilution in 96-well plates. Knockout conditions were analyzed by western blot using Hsp70L1 antibody (Abcam #ab108612). For conditional knockout cell lines, guide RNA was cloned into modified lentiCRISPR v2 fusing with a human mutant FKBP12 destabilizing domain to Cas9 (DD-Cas9) (Senturk et al., 2017), which the destabilizing domain induced rapid proteasome degradation in the abstracted of an FKBP12 ligand (Shield-1) (Banaszynski et al., 2006). In the presence of Shield-1 (200 nM), the plasmid shields from degradation and conditionally expresses the gene-editing construct.

Subcellular localization of RAC by immunofluorescence

HeLa cells were plated at 5×10^4 cells/6 well 1-day prior transfection. Cells were transfected with either siRNA control or MPP11 using Lipofectamine RNAiMAX (Thermo Fisher Scientific #13778-150) according to the manufacturer's instructions the following day. Cells were replated at 3×10^4 onto 12 mm coverslips (Fisher Scientific #12-545-80). Cells were transfected with mcherry-Sec61 β using Lipofectamine™ 2000 (Thermo Fisher Scientific #11668019) according to the manufacturer's instructions the next day. After 18h transfection, cells were fixed with 4% paraformaldehyde for 20 min at room temperature, permeabilized with 0.05% Triton-X100 for 10 min at room temperature, blocked in 10% normal goat serum (Thermo Fisher Scientific #50-062) for 30 min at room temperature, and incubated with Mpp11 antibody (gift from Dr. Rospert) using 1:500 dilution in blocking buffer overnight at 4 °C. Anti-rabbit IgG secondary antibody Alexa Fluor 488 (Thermo Fisher Scientific #A11034) were used as 1:500 dilution in blocking buffer for 1h at 4 °C. Nuclei were stained with Hoechst (Thermo Fisher Scientific #33342). Coverslips were mounted with ProLong diamond antifade mountant (Thermo Fisher Scientific #P36965). Images were captured with LSM 880 laser scanning confocal microscope (Zeiss). Plan Apochromat 100x/1.4 Oil DIC M27 objective was used.

Analysis of protein aggregates

Post-transfection 48hr of siRNA, cells were harvested in lysis buffer (20 mM sodium phosphate, pH 6.8, 1 mM EDTA, 0.1% Tween, 10 mM DTT) (Koplin et al., 2010) supplemented with 1X cOmplete protease inhibitor and incubated on ice for 20 min. Protein aggregates were isolated by centrifuging at 16,000 g for 20 min at 4°C, and supernatants were collected. Protein aggregated were washed in buffer (2 % NP-40, 20 mM sodium phosphate, pH 6.8, 1X cOmplete protease inhibitor), sonicated, and centrifuged at 16,000 g for 20 min at 4°C. Protein aggregates were boiled in 5X Laemmli sample buffer, separated by SDS-PAGE (Biorad, Any kD Mini-PROTEAN TGX Gel #456-9033), and analyzed by silver staining (Pierce #24612).

Bibliography

- Acosta-Alvear, D., Karagoz, G.E., Frohlich, F., Li, H., Walther, T.C., and Walter, P. (2018). The unfolded protein response and endoplasmic reticulum protein targeting machineries converge on the stress sensor IRE1. *Elife* 7.
- Adams, C.J., Kopp, M.C., Larburu, N., Nowak, P.R., and Ali, M.M.U. (2019). Structure and Molecular Mechanism of ER Stress Signaling by the Unfolded Protein Response Signal Activator IRE1. *Front Mol Biosci* 6, 11.
- Albanese, V., Reissmann, S., and Frydman, J. (2010). A ribosome-anchored chaperone network that facilitates eukaryotic ribosome biogenesis. *J Cell Biol* 189, 69-81.
- Aloia, L., Demajo, S., and Di Croce, L. (2015a). ZRF1: a novel epigenetic regulator of stem cell identity and cancer. *Cell Cycle* 14, 510-515.
- Aloia, L., Di Stefano, B., and Di Croce, L. (2013). Polycomb complexes in stem cells and embryonic development. *Development* 140, 2525-2534.
- Aloia, L., Di Stefano, B., Sessa, A., Morey, L., Santanach, A., Gutierrez, A., Cozzuto, L., Benitah, S.A., Graf, T., Broccoli, V., *et al.* (2014). Zrf1 is required to establish and maintain neural progenitor identity. *Genes Dev* 28, 182-197.
- Aloia, L., Gutierrez, A., Caballero, J.M., and Di Croce, L. (2015b). Direct interaction between Id1 and Zrf1 controls neural differentiation of embryonic stem cells. *EMBO Rep* 16, 63-70.

Amin-Wetzel, N., Saunders, R.A., Kamphuis, M.J., Rato, C., Preissler, S., Harding, H.P., and Ron, D. (2017). A J-Protein Co-chaperone Recruits BiP to Monomerize IRE1 and Repress the Unfolded Protein Response. *Cell* 171, 1625-1637 e1613.

Anckar, J., and Sistonen, L. (2011). Regulation of HSF1 function in the heat stress response: implications in aging and disease. *Annu Rev Biochem* 80, 1089-1115.

Aragon, T., van Anken, E., Pincus, D., Serafimova, I.M., Korennykh, A.V., Rubio, C.A., and Walter, P. (2009). Messenger RNA targeting to endoplasmic reticulum stress signalling sites. *Nature* 457, 736-740.

Ariosa, A., Lee, J.H., Wang, S., Saraogi, I., and Shan, S.O. (2015). Regulation by a chaperone improves substrate selectivity during cotranslational protein targeting. *Proc Natl Acad Sci U S A* 112, E3169-3178.

Arribere, J.A., and Fire, A.Z. (2018). Nonsense mRNA suppression via nonstop decay. *Elife* 7.

Atkinson, G.C., Baldauf, S.L., and Hauryliuk, V. (2008). Evolution of nonstop, no-go and nonsense-mediated mRNA decay and their termination factor-derived components. *BMC Evol Biol* 8, 290.

Auf, G., Jabouille, A., Guerit, S., Pineau, R., Delugin, M., Bouche-careilh, M., Magnin, N., Favereaux, A., Maitre, M., Gaiser, T., *et al.* (2010). Inositol-requiring enzyme 1alpha is a key regulator of angiogenesis and invasion in malignant glioma. *Proc Natl Acad Sci U S A* 107, 15553-15558.

Back, S.H., Schroder, M., Lee, K., Zhang, K., and Kaufman, R.J. (2005). ER stress signaling by regulated splicing: IRE1/HAC1/XBP1. *Methods* 35, 395-416.

Balchin, D., Hayer-Hartl, M., and Hartl, F.U. (2016). In vivo aspects of protein folding and quality control. *Science* 353, aac4354.

Banaszynski, L.A., Chen, L.C., Maynard-Smith, L.A., Ooi, A.G., and Wandless, T.J. (2006). A rapid, reversible, and tunable method to regulate protein function in living cells using synthetic small molecules. *Cell* 126, 995-1004.

Batey, R.T., Rambo, R.P., Lucast, L., Rha, B., and Doudna, J.A. (2000). Crystal structure of the ribonucleoprotein core of the signal recognition particle. *Science* 287, 1232-1239.

Beatrix, B., Sakai, H., and Wiedmann, M. (2000). The alpha and beta subunit of the nascent polypeptide-associated complex have distinct functions. *J Biol Chem* 275, 37838-37845.

Becker, A.H., Oh, E., Weissman, J.S., Kramer, G., and Bukau, B. (2013). Selective ribosome profiling as a tool for studying the interaction of chaperones and targeting factors with nascent polypeptide chains and ribosomes. *Nat Protoc* 8, 2212-2239.

Becker, T., Armache, J.P., Jarasch, A., Anger, A.M., Villa, E., Sieber, H., Motaal, B.A., Mielke, T., Berninghausen, O., and Beckmann, R. (2011). Structure of the no-go mRNA decay complex Dom34-Hbs1 bound to a stalled 80S ribosome. *Nat Struct Mol Biol* 18, 715-720.

Becker, T., Franckenberg, S., Wickles, S., Shoemaker, C.J., Anger, A.M., Armache, J.P., Sieber, H., Ungewickell, C., Berninghausen, O., Daberkow, I., *et al.* (2012). Structural basis of highly conserved ribosome recycling in eukaryotes and archaea. *Nature* 482, 501-506.

Beckmann, R., Spahn, C.M., Eswar, N., Helmers, J., Penczek, P.A., Sali, A., Frank, J., and Blobel, G. (2001). Architecture of the protein-conducting channel associated with the translating 80S ribosome. *Cell* *107*, 361-372.

Bernstein, H.D., Poritz, M.A., Strub, K., Hoben, P.J., Brenner, S., and Walter, P. (1989). Model for signal sequence recognition from amino-acid sequence of 54K subunit of signal recognition particle. *Nature* *340*, 482-486.

Bertolotti, A., Wang, X., Novoa, I., Jungreis, R., Schlessinger, K., Cho, J.H., West, A.B., and Ron, D. (2001). Increased sensitivity to dextran sodium sulfate colitis in IRE1beta-deficient mice. *J Clin Invest* *107*, 585-593.

Bertolotti, A., Zhang, Y., Hendershot, L.M., Harding, H.P., and Ron, D. (2000). Dynamic interaction of BiP and ER stress transducers in the unfolded-protein response. *Nat Cell Biol* *2*, 326-332.

Bloss, T.A., Witze, E.S., and Rothman, J.H. (2003). Suppression of CED-3-independent apoptosis by mitochondrial betaNAC in *Caenorhabditis elegans*. *Nature* *424*, 1066-1071.

Bornemann, T., Holtkamp, W., and Wintermeyer, W. (2014). Interplay between trigger factor and other protein biogenesis factors on the ribosome. *Nat Commun* *5*, 4180.

Boyer, L.A., Langer, M.R., Crowley, K.A., Tan, S., Denu, J.M., and Peterson, C.L. (2002). Essential role for the SANT domain in the functioning of multiple chromatin remodeling enzymes. *Mol Cell* *10*, 935-942.

Boyer, L.A., Latek, R.R., and Peterson, C.L. (2004). The SANT domain: a unique histone-tail-binding module? *Nat Rev Mol Cell Biol* *5*, 158-163.

Braig, M., and Schmitt, C.A. (2006). Oncogene-induced senescence: putting the brakes on tumor development. *Cancer Res* 66, 2881-2884.

Brandman, O., and Hegde, R.S. (2016). Ribosome-associated protein quality control. *Nat Struct Mol Biol* 23, 7-15.

Brodsky, J.L. (2012). Cleaning up: ER-associated degradation to the rescue. *Cell* 151, 1163-1167.

Buchberger, A., Bukau, B., and Sommer, T. (2010). Protein quality control in the cytosol and the endoplasmic reticulum: brothers in arms. *Mol Cell* 40, 238-252.

Bukau, B., Weissman, J., and Horwich, A. (2006). Molecular chaperones and protein quality control. *Cell* 125, 443-451.

Buskiewicz, I., Deuerling, E., Gu, S.Q., Jockel, J., Rodnina, M.V., Bukau, B., and Wintermeyer, W. (2004). Trigger factor binds to ribosome-signal-recognition particle (SRP) complexes and is excluded by binding of the SRP receptor. *Proc Natl Acad Sci U S A* 101, 7902-7906.

Buskirk, A.R., and Green, R. (2017). Ribosome pausing, arrest and rescue in bacteria and eukaryotes. *Philos Trans R Soc Lond B Biol Sci* 372.

Calfon, M., Zeng, H., Urano, F., Till, J.H., Hubbard, S.R., Harding, H.P., Clark, S.G., and Ron, D. (2002). IRE1 couples endoplasmic reticulum load to secretory capacity by processing the XBP-1 mRNA. *Nature* 415, 92-96.

Caliskan, N., Peske, F., and Rodnina, M.V. (2015). Changed in translation: mRNA recoding by -1 programmed ribosomal frameshifting. *Trends Biochem Sci* 40, 265-274.

- Chang, T.K., Lawrence, D.A., Lu, M., Tan, J., Harnoss, J.M., Marsters, S.A., Liu, P., Sandoval, W., Martin, S.E., and Ashkenazi, A. (2018). Coordination between Two Branches of the Unfolded Protein Response Determines Apoptotic Cell Fate. *Mol Cell* *71*, 629-636 e625.
- Chen, B., Retzlaff, M., Roos, T., and Frydman, J. (2011). Cellular strategies of protein quality control. *Cold Spring Harb Perspect Biol* *3*, a004374.
- Chen, D., Rauh, M., Buchfelder, M., Eyupoglu, I.Y., and Savaskan, N. (2017). The oxido-metabolic driver ATF4 enhances temozolamide chemo-resistance in human gliomas. *Oncotarget* *8*, 51164-51176.
- Chen, L., Muhrad, D., Hauryliuk, V., Cheng, Z., Lim, M.K., Shyp, V., Parker, R., and Song, H. (2010). Structure of the Dom34-Hbs1 complex and implications for no-go decay. *Nat Struct Mol Biol* *17*, 1233-1240.
- Chiba, Y., Ishikawa, M., Kijima, F., Tyson, R.H., Kim, J., Yamamoto, A., Nambara, E., Leustek, T., Wallsgrove, R.M., and Naito, S. (1999). Evidence for autoregulation of cystathionine gamma-synthase mRNA stability in Arabidopsis. *Science* *286*, 1371-1374.
- Chiba, Y., Sakurai, R., Yoshino, M., Ominato, K., Ishikawa, M., Onouchi, H., and Naito, S. (2003). S-adenosyl-L-methionine is an effector in the posttranscriptional autoregulation of the cystathionine gamma-synthase gene in Arabidopsis. *Proc Natl Acad Sci U S A* *100*, 10225-10230.
- Chiti, F., and Dobson, C.M. (2006). Protein misfolding, functional amyloid, and human disease. *Annu Rev Biochem* *75*, 333-366.

Connolly, T., and Gilmore, R. (1989). The signal recognition particle receptor mediates the GTP-dependent displacement of SRP from the signal sequence of the nascent polypeptide. *Cell* 57, 599-610.

Conz, C., Otto, H., Peisker, K., Gautschi, M., Wolfle, T., Mayer, M.P., and Rospert, S. (2007). Functional characterization of the atypical Hsp70 subunit of yeast ribosome-associated complex. *J Biol Chem* 282, 33977-33984.

Cox, J.S., Shamu, C.E., and Walter, P. (1993). Transcriptional induction of genes encoding endoplasmic reticulum resident proteins requires a transmembrane protein kinase. *Cell* 73, 1197-1206.

Cox, J.S., and Walter, P. (1996). A novel mechanism for regulating activity of a transcription factor that controls the unfolded protein response. *Cell* 87, 391-404.

Credle, J.J., Finer-Moore, J.S., Papa, F.R., Stroud, R.M., and Walter, P. (2005). On the mechanism of sensing unfolded protein in the endoplasmic reticulum. *Proc Natl Acad Sci U S A* 102, 18773-18784.

D'Orazio, K.N., Wu, C.C., Sinha, N., Loll-Kripplleber, R., Brown, G.W., and Green, R. (2019). The endonuclease Cue2 cleaves mRNAs at stalled ribosomes during No Go Decay. *Elife* 8.

Dejeans, N., Pluquet, O., Lhomond, S., Grise, F., Bouchecareilh, M., Juin, A., Meynard-Cadars, M., Bidaud-Meynard, A., Gentil, C., Moreau, V., *et al.* (2012). Autocrine control of glioma cells adhesion and migration through IRE1alpha-mediated cleavage of SPARC mRNA. *J Cell Sci* 125, 4278-4287.

del Alamo, M., Hogan, D.J., Pechmann, S., Albanese, V., Brown, P.O., and Frydman, J. (2011). Defining the specificity of cotranslationally acting chaperones by systematic analysis of mRNAs associated with ribosome-nascent chain complexes. *PLoS Biol* 9, e1001100.

Delibegovic, M., Zimmer, D., Kauffman, C., Rak, K., Hong, E.G., Cho, Y.R., Kim, J.K., Kahn, B.B., Neel, B.G., and Bence, K.K. (2009). Liver-specific deletion of protein-tyrosine phosphatase 1B (PTP1B) improves metabolic syndrome and attenuates diet-induced endoplasmic reticulum stress. *Diabetes* 58, 590-599.

Demajo, S., Uribesalgo, I., Gutierrez, A., Ballare, C., Capdevila, S., Roth, M., Zuber, J., Martin-Caballero, J., and Di Croce, L. (2014). ZRF1 controls the retinoic acid pathway and regulates leukemogenic potential in acute myeloid leukemia. *Oncogene* 33, 5501-5510.

Deng, J.M., and Behringer, R.R. (1995). An insertional mutation in the BTF3 transcription factor gene leads to an early postimplantation lethality in mice. *Transgenic Res* 4, 264-269.

Deuerling, E., Gamedinger, M., and Kreft, S.G. (2019). Chaperone Interactions at the Ribosome. *Cold Spring Harb Perspect Biol* 11.

Deuerling, E., Patzelt, H., Vorderwulbecke, S., Rauch, T., Kramer, G., Schaffitzel, E., Mogk, A., Schulze-Specking, A., Langen, H., and Bukau, B. (2003). Trigger Factor and DnaK possess overlapping substrate pools and binding specificities. *Mol Microbiol* 47, 1317-1328.

Deuerling, E., Schulze-Specking, A., Tomoyasu, T., Mogk, A., and Bukau, B. (1999). Trigger factor and DnaK cooperate in folding of newly synthesized proteins. *Nature* *400*, 693-696.

Doma, M.K., and Parker, R. (2006). Endonucleolytic cleavage of eukaryotic mRNAs with stalls in translation elongation. *Nature* *440*, 561-564.

Doring, K., Ahmed, N., Riemer, T., Suresh, H.G., Vainshtein, Y., Habich, M., Riemer, J., Mayer, M.P., O'Brien, E.P., Kramer, G., *et al.* (2017). Profiling Ssb-Nascent Chain Interactions Reveals Principles of Hsp70-Assisted Folding. *Cell* *170*, 298-311 e220.

Dorner, A.J., Wasley, L.C., and Kaufman, R.J. (1992). Overexpression of GRP78 mitigates stress induction of glucose regulated proteins and blocks secretion of selective proteins in Chinese hamster ovary cells. *EMBO J* *11*, 1563-1571.

Doudna, J.A., and Batey, R.T. (2004). Structural insights into the signal recognition particle. *Annu Rev Biochem* *73*, 539-557.

Dubnikov, T., Ben-Gedalya, T., and Cohen, E. (2017). Protein Quality Control in Health and Disease. *Cold Spring Harb Perspect Biol* *9*.

Ducett, J.K., Peterson, F.C., Hoover, L.A., Prunuske, A.J., Volkman, B.F., and Craig, E.A. (2013). Unfolding of the C-terminal domain of the J-protein Zuo1 releases autoinhibition and activates Pdr1-dependent transcription. *J Mol Biol* *425*, 19-31.

Duttler, S., Pechmann, S., and Frydman, J. (2013). Principles of cotranslational ubiquitination and quality control at the ribosome. *Mol Cell* *50*, 379-393.

Fang, H., Wu, Y., Huang, X., Wang, W., Ang, B., Cao, X., and Wan, T. (2011). Toll-like receptor 4 (TLR4) is essential for Hsp70-like protein 1 (HSP70L1) to activate dendritic cells and induce Th1 response. *J Biol Chem* 286, 30393-30400.

Feng, R., Zhai, W.L., Yang, H.Y., Jin, H., and Zhang, Q.X. (2011). Induction of ER stress protects gastric cancer cells against apoptosis induced by cisplatin and doxorubicin through activation of p38 MAPK. *Biochem Biophys Res Commun* 406, 299-304.

Ferbitz, L., Maier, T., Patzelt, H., Bukau, B., Deuerling, E., and Ban, N. (2004). Trigger factor in complex with the ribosome forms a molecular cradle for nascent proteins. *Nature* 431, 590-596.

Fiaux, J., Horst, J., Scior, A., Preissler, S., Koplin, A., Bukau, B., and Deuerling, E. (2010). Structural analysis of the ribosome-associated complex (RAC) reveals an unusual Hsp70/Hsp40 interaction. *J Biol Chem* 285, 3227-3234.

Forte, G.M., Pool, M.R., and Stirling, C.J. (2011). N-terminal acetylation inhibits protein targeting to the endoplasmic reticulum. *PLoS Biol* 9, e1001073.

Freymann, D.M., Keenan, R.J., Stroud, R.M., and Walter, P. (1997). Structure of the conserved GTPase domain of the signal recognition particle. *Nature* 385, 361-364.

Frischmeyer, P.A., van Hoof, A., O'Donnell, K., Guerrerio, A.L., Parker, R., and Dietz, H.C. (2002). An mRNA surveillance mechanism that eliminates transcripts lacking termination codons. *Science* 295, 2258-2261.

Frydman, J. (2001). Folding of newly translated proteins in vivo: the role of molecular chaperones. *Annu Rev Biochem* 70, 603-647.

Frydman, J., Nimmesgern, E., Ohtsuka, K., and Hartl, F.U. (1994). Folding of nascent polypeptide chains in a high molecular mass assembly with molecular chaperones. *Nature* 370, 111-117.

Funfschilling, U., and Rospert, S. (1999). Nascent polypeptide-associated complex stimulates protein import into yeast mitochondria. *Mol Biol Cell* 10, 3289-3299.

Gamerding, M., Hanebuth, M.A., Frickey, T., and Deuerling, E. (2015). The principle of antagonism ensures protein targeting specificity at the endoplasmic reticulum. *Science* 348, 201-207.

Gandhi, R., Manzoor, M., and Hudak, K.A. (2008). Depurination of Brome mosaic virus RNA3 in vivo results in translation-dependent accelerated degradation of the viral RNA. *J Biol Chem* 283, 32218-32228.

Gardner, B.M., and Walter, P. (2011). Unfolded proteins are Ire1-activating ligands that directly induce the unfolded protein response. *Science* 333, 1891-1894.

Gautschi, M., Lilie, H., Funfschilling, U., Mun, A., Ross, S., Lithgow, T., Rucknagel, P., and Rospert, S. (2001). RAC, a stable ribosome-associated complex in yeast formed by the DnaK-DnaJ homologs Ssz1p and zuotin. *Proc Natl Acad Sci U S A* 98, 3762-3767.

Gautschi, M., Mun, A., Ross, S., and Rospert, S. (2002). A functional chaperone triad on the yeast ribosome. *Proc Natl Acad Sci U S A* 99, 4209-4214.

George, R., Beddoe, T., Landl, K., and Lithgow, T. (1998). The yeast nascent polypeptide-associated complex initiates protein targeting to mitochondria in vivo. *Proc Natl Acad Sci U S A* 95, 2296-2301.

George, R., Walsh, P., Beddoe, T., and Lithgow, T. (2002). The nascent polypeptide-associated complex (NAC) promotes interaction of ribosomes with the mitochondrial surface in vivo. *FEBS Lett* 516, 213-216.

Giannopoulos, K., Li, L., Bojarska-Junak, A., Rolinski, J., Dmoszynska, A., Hus, I., Greiner, J., Renner, C., Dohner, H., and Schmitt, M. (2006). Expression of RHAMM/CD168 and other tumor-associated antigens in patients with B-cell chronic lymphocytic leukemia. *Int J Oncol* 29, 95-103.

Gigliione, C., Fieulaine, S., and Meinnel, T. (2009). Cotranslational processing mechanisms: towards a dynamic 3D model. *Trends Biochem Sci* 34, 417-426.

Gilmore, R., Walter, P., and Blobel, G. (1982). Protein translocation across the endoplasmic reticulum. II. Isolation and characterization of the signal recognition particle receptor. *J Cell Biol* 95, 470-477.

Golden, R.J., Chen, B., Li, T., Braun, J., Manjunath, H., Chen, X., Wu, J., Schmid, V., Chang, T.C., Kopp, F., *et al.* (2017). An Argonaute phosphorylation cycle promotes microRNA-mediated silencing. *Nature* 542, 197-202.

Gomez-Lorenzo, M.G., Spahn, C.M., Agrawal, R.K., Grassucci, R.A., Penczek, P., Chakraborty, K., Ballesta, J.P., Lavandera, J.L., Garcia-Bustos, J.F., and Frank, J. (2000). Three-dimensional cryo-electron microscopy localization of EF2 in the *Saccharomyces cerevisiae* 80S ribosome at 17.5 Å resolution. *EMBO J* 19, 2710-2718.

Gomez-Pastor, R., Burchfiel, E.T., and Thiele, D.J. (2018). Regulation of heat shock transcription factors and their roles in physiology and disease. *Nat Rev Mol Cell Biol* 19, 4-19.

- Gonzalez, T.N., Sidrauski, C., Dorfler, S., and Walter, P. (1999). Mechanism of non-spliceosomal mRNA splicing in the unfolded protein response pathway. *EMBO J* 18, 3119-3132.
- Gorgoulis, V.G., and Halazonetis, T.D. (2010). Oncogene-induced senescence: the bright and dark side of the response. *Curr Opin Cell Biol* 22, 816-827.
- Graille, M., Chaillet, M., and van Tilbeurgh, H. (2008). Structure of yeast Dom34: a protein related to translation termination factor Erf1 and involved in No-Go decay. *J Biol Chem* 283, 7145-7154.
- Greiner, J., Ringhoffer, M., Taniguchi, M., Li, L., Schmitt, A., Shiku, H., Dohner, H., and Schmitt, M. (2004). mRNA expression of leukemia-associated antigens in patients with acute myeloid leukemia for the development of specific immunotherapies. *Int J Cancer* 108, 704-711.
- Gribbling-Burrer, A.S., Chiabudini, M., Zhang, Y., Qiu, Z., Scazzari, M., Wolfle, T., Wohlwend, D., and Rospert, S. (2019). A dual role of the ribosome-bound chaperones RAC/Ssb in maintaining the fidelity of translation termination. *Nucleic Acids Res* 47, 7018-7034.
- Gu, F., Nguyen, D.T., Stuible, M., Dube, N., Tremblay, M.L., and Chevet, E. (2004). Protein-tyrosine phosphatase 1B potentiates IRE1 signaling during endoplasmic reticulum stress. *J Biol Chem* 279, 49689-49693.
- Gu, S.Q., Peske, F., Wieden, H.J., Rodnina, M.V., and Wintermeyer, W. (2003). The signal recognition particle binds to protein L23 at the peptide exit of the Escherichia coli ribosome. *RNA* 9, 566-573.

Gupta, S., Deepti, A., Deegan, S., Lisbona, F., Hetz, C., and Samali, A. (2010). HSP72 protects cells from ER stress-induced apoptosis via enhancement of IRE1alpha-XBP1 signaling through a physical interaction. *PLoS Biol* 8, e1000410.

Guydosh, N.R., and Green, R. (2014). Dom34 rescues ribosomes in 3' untranslated regions. *Cell* 156, 950-962.

Guydosh, N.R., Kimmig, P., Walter, P., and Green, R. (2017). Regulated Ire1-dependent mRNA decay requires no-go mRNA degradation to maintain endoplasmic reticulum homeostasis in *S. pombe*. *Elife* 6.

Halic, M., Becker, T., Pool, M.R., Spahn, C.M., Grassucci, R.A., Frank, J., and Beckmann, R. (2004). Structure of the signal recognition particle interacting with the elongation-arrested ribosome. *Nature* 427, 808-814.

Halic, M., Blau, M., Becker, T., Mielke, T., Pool, M.R., Wild, K., Sinning, I., and Beckmann, R. (2006). Following the signal sequence from ribosomal tunnel exit to signal recognition particle. *Nature* 444, 507-511.

Han, D., Lerner, A.G., Vande Walle, L., Upton, J.P., Xu, W., Hagen, A., Backes, B.J., Oakes, S.A., and Papa, F.R. (2009). IRE1alpha kinase activation modes control alternate endoribonuclease outputs to determine divergent cell fates. *Cell* 138, 562-575.

Harigaya, Y., and Parker, R. (2010). No-go decay: a quality control mechanism for RNA in translation. *Wiley Interdiscip Rev RNA* 1, 132-141.

Harnoss, J.M., Le Thomas, A., Shemorry, A., Marsters, S.A., Lawrence, D.A., Lu, M., Chen, Y.A., Qing, J., Totpal, K., Kan, D., *et al.* (2019). Disruption of IRE1alpha through

its kinase domain attenuates multiple myeloma. *Proc Natl Acad Sci U S A* *116*, 16420-16429.

Hartl, F.U., Bracher, A., and Hayer-Hartl, M. (2011). Molecular chaperones in protein folding and proteostasis. *Nature* *475*, 324-332.

Hartl, F.U., and Hayer-Hartl, M. (2009). Converging concepts of protein folding in vitro and in vivo. *Nat Struct Mol Biol* *16*, 574-581.

Hetz, C. (2012). The unfolded protein response: controlling cell fate decisions under ER stress and beyond. *Nat Rev Mol Cell Biol* *13*, 89-102.

Hetz, C., Bernasconi, P., Fisher, J., Lee, A.H., Bassik, M.C., Antonsson, B., Brandt, G.S., Iwakoshi, N.N., Schinzel, A., Glimcher, L.H., *et al.* (2006). Proapoptotic BAX and BAK modulate the unfolded protein response by a direct interaction with IRE1 α . *Science* *312*, 572-576.

Hipp, M.S., Park, S.H., and Hartl, F.U. (2014). Proteostasis impairment in protein-misfolding and -aggregation diseases. *Trends Cell Biol* *24*, 506-514.

Hoffmann, A., Becker, A.H., Zachmann-Brand, B., Deuerling, E., Bukau, B., and Kramer, G. (2012). Concerted action of the ribosome and the associated chaperone trigger factor confines nascent polypeptide folding. *Mol Cell* *48*, 63-74.

Hoffmann, A., Merz, F., Rutkowska, A., Zachmann-Brand, B., Deuerling, E., and Bukau, B. (2006). Trigger factor forms a protective shield for nascent polypeptides at the ribosome. *J Biol Chem* *281*, 6539-6545.

Hollien, J., and Weissman, J.S. (2006). Decay of endoplasmic reticulum-localized mRNAs during the unfolded protein response. *Science* *313*, 104-107.

Hotokezaka, Y., van Leyen, K., Lo, E.H., Beatrix, B., Katayama, I., Jin, G., and Nakamura, T. (2009). alphaNAC depletion as an initiator of ER stress-induced apoptosis in hypoxia. *Cell Death Differ* 16, 1505-1514.

Hsu, H.T., Hsing, M.T., Yeh, C.M., Chen, C.J., Yang, J.S., and Yeh, K.T. (2018). Decreased cytoplasmic X-box binding protein-1 expression is associated with poor prognosis and overall survival in patients with oral squamous cell carcinoma. *Clin Chim Acta* 479, 66-71.

Huang, P., Gautschi, M., Walter, W., Rospert, S., and Craig, E.A. (2005). The Hsp70 Ssz1 modulates the function of the ribosome-associated J-protein Zuo1. *Nat Struct Mol Biol* 12, 497-504.

Hundley, H., Eisenman, H., Walter, W., Evans, T., Hotokezaka, Y., Wiedmann, M., and Craig, E. (2002). The in vivo function of the ribosome-associated Hsp70, Ssz1, does not require its putative peptide-binding domain. *Proc Natl Acad Sci U S A* 99, 4203-4208.

Hundley, H.A., Walter, W., Bairstow, S., and Craig, E.A. (2005). Human Mpp11 J protein: ribosome-tethered molecular chaperones are ubiquitous. *Science* 308, 1032-1034.

Husebye, H., Halaas, O., Stenmark, H., Tunheim, G., Sandanger, O., Bogen, B., Brech, A., Latz, E., and Espevik, T. (2006). Endocytic pathways regulate Toll-like receptor 4 signaling and link innate and adaptive immunity. *EMBO J* 25, 683-692.

Hwang, C.S., Shemorry, A., and Varshavsky, A. (2010). N-terminal acetylation of cellular proteins creates specific degradation signals. *Science* 327, 973-977.

Ikeuchi, K., Izawa, T., and Inada, T. (2018). Recent Progress on the Molecular Mechanism of Quality Controls Induced by Ribosome Stalling. *Front Genet* 9, 743.

Inada, T. (2017). The Ribosome as a Platform for mRNA and Nascent Polypeptide Quality Control. *Trends Biochem Sci* 42, 5-15.

Ingolia, N.T., Lareau, L.F., and Weissman, J.S. (2011). Ribosome profiling of mouse embryonic stem cells reveals the complexity and dynamics of mammalian proteomes. *Cell* 147, 789-802.

Inoue, T., Shoji, W., and Obinata, M. (1999). MIDA1, an Id-associating protein, has two distinct DNA binding activities that are converted by the association with Id1: a novel function of Id protein. *Biochem Biophys Res Commun* 266, 147-151.

Inoue, T., Shoji, W., and Obinata, M. (2000). MIDA1 is a sequence specific DNA binding protein with novel DNA binding properties. *Genes Cells* 5, 699-709.

Ito-Harashima, S., Kuroha, K., Tatematsu, T., and Inada, T. (2007). Translation of the poly(A) tail plays crucial roles in nonstop mRNA surveillance via translation repression and protein destabilization by proteasome in yeast. *Genes Dev* 21, 519-524.

Jagannathan, S., Nwosu, C., and Nicchitta, C.V. (2011). Analyzing mRNA localization to the endoplasmic reticulum via cell fractionation. *Methods Mol Biol* 714, 301-321.

Jaiswal, H., Conz, C., Otto, H., Wolfle, T., Fitzke, E., Mayer, M.P., and Rospert, S. (2011). The chaperone network connected to human ribosome-associated complex. *Mol Cell Biol* 31, 1160-1173.

Jha, S., and Komar, A.A. (2011). Birth, life and death of nascent polypeptide chains. *Biotechnol J* 6, 623-640.

- Jiang, C.C., Yang, F., Thorne, R.F., Zhu, B.K., Hersey, P., and Zhang, X.D. (2009). Human melanoma cells under endoplasmic reticulum stress acquire resistance to microtubule-targeting drugs through XBP-1-mediated activation of Akt. *Neoplasia* *11*, 436-447.
- Jin, C., Jin, Z., Chen, N.Z., Lu, M., Liu, C.B., Hu, W.L., and Zheng, C.G. (2016). Activation of IRE1alpha-XBP1 pathway induces cell proliferation and invasion in colorectal carcinoma. *Biochem Biophys Res Commun* *470*, 75-81.
- Joazeiro, C.A.P. (2017). Ribosomal Stalling During Translation: Providing Substrates for Ribosome-Associated Protein Quality Control. *Annu Rev Cell Dev Biol* *33*, 343-368.
- Joazeiro, C.A.P. (2019). Mechanisms and functions of ribosome-associated protein quality control. *Nat Rev Mol Cell Biol* *20*, 368-383.
- Johnson, A.E., and van Waes, M.A. (1999). The translocon: a dynamic gateway at the ER membrane. *Annu Rev Cell Dev Biol* *15*, 799-842.
- Jurkin, J., Henkel, T., Nielsen, A.F., Minnich, M., Popow, J., Kaufmann, T., Heindl, K., Hoffmann, T., Busslinger, M., and Martinez, J. (2014). The mammalian tRNA ligase complex mediates splicing of XBP1 mRNA and controls antibody secretion in plasma cells. *EMBO J* *33*, 2922-2936.
- Kagan, J.C., Su, T., Horng, T., Chow, A., Akira, S., and Medzhitov, R. (2008). TRAM couples endocytosis of Toll-like receptor 4 to the induction of interferon-beta. *Nat Immunol* *9*, 361-368.

Kaiser, C.M., Chang, H.C., Agashe, V.R., Lakshmipathy, S.K., Etchells, S.A., Hayer-Hartl, M., Hartl, F.U., and Barral, J.M. (2006). Real-time observation of trigger factor function on translating ribosomes. *Nature* *444*, 455-460.

Kampinga, H.H., and Craig, E.A. (2010). The HSP70 chaperone machinery: J proteins as drivers of functional specificity. *Nat Rev Mol Cell Biol* *11*, 579-592.

Kanda, S., Yanagitani, K., Yokota, Y., Esaki, Y., and Kohno, K. (2016). Autonomous translational pausing is required for XBP1u mRNA recruitment to the ER via the SRP pathway. *Proc Natl Acad Sci U S A* *113*, E5886-E5895.

Kaneko, M., Niinuma, Y., and Nomura, Y. (2003). Activation signal of nuclear factor-kappa B in response to endoplasmic reticulum stress is transduced via IRE1 and tumor necrosis factor receptor-associated factor 2. *Biol Pharm Bull* *26*, 931-935.

Karagoz, G.E., Acosta-Alvear, D., Nguyen, H.T., Lee, C.P., Chu, F., and Walter, P. (2017). An unfolded protein-induced conformational switch activates mammalian IRE1. *Elife* *6*.

Karamyshev, A.L., and Karamysheva, Z.N. (2018). Lost in Translation: Ribosome-Associated mRNA and Protein Quality Controls. *Front Genet* *9*, 431.

Karamyshev, A.L., Patrick, A.E., Karamysheva, Z.N., Griesemer, D.S., Hudson, H., Tjon-Kon-Sang, S., Nilsson, I., Otto, H., Liu, Q., Rospert, S., *et al.* (2014). Inefficient SRP interaction with a nascent chain triggers a mRNA quality control pathway. *Cell* *156*, 146-157.

Keenan, R.J., Freymann, D.M., Stroud, R.M., and Walter, P. (2001). The signal recognition particle. *Annu Rev Biochem* *70*, 755-775.

Kimata, Y., Ishiwata-Kimata, Y., Ito, T., Hirata, A., Suzuki, T., Oikawa, D., Takeuchi, M., and Kohno, K. (2007). Two regulatory steps of ER-stress sensor Ire1 involving its cluster formation and interaction with unfolded proteins. *J Cell Biol* *179*, 75-86.

Kimata, Y., Oikawa, D., Shimizu, Y., Ishiwata-Kimata, Y., and Kohno, K. (2004). A role for BiP as an adjustor for the endoplasmic reticulum stress-sensing protein Ire1. *J Cell Biol* *167*, 445-456.

Kimmig, P., Diaz, M., Zheng, J., Williams, C.C., Lang, A., Aragon, T., Li, H., and Walter, P. (2012). The unfolded protein response in fission yeast modulates stability of select mRNAs to maintain protein homeostasis. *Elife* *1*, e00048.

Klauer, A.A., and van Hoof, A. (2012). Degradation of mRNAs that lack a stop codon: a decade of nonstop progress. *Wiley Interdiscip Rev RNA* *3*, 649-660.

Kobayashi, K., Kikuno, I., Kuroha, K., Saito, K., Ito, K., Ishitani, R., Inada, T., and Nureki, O. (2010). Structural basis for mRNA surveillance by archaeal Pelota and GTP-bound EF1alpha complex. *Proc Natl Acad Sci U S A* *107*, 17575-17579.

Koch, H.G., Moser, M., and Muller, M. (2003). Signal recognition particle-dependent protein targeting, universal to all kingdoms of life. *Rev Physiol Biochem Pharmacol* *146*, 55-94.

Kohno, K., Normington, K., Sambrook, J., Gething, M.J., and Mori, K. (1993). The promoter region of the yeast KAR2 (BiP) gene contains a regulatory domain that responds to the presence of unfolded proteins in the endoplasmic reticulum. *Mol Cell Biol* *13*, 877-890.

Koplin, A., Preissler, S., Ilina, Y., Koch, M., Scior, A., Erhardt, M., and Deuerling, E. (2010). A dual function for chaperones SSB-RAC and the NAC nascent polypeptide-associated complex on ribosomes. *J Cell Biol* *189*, 57-68.

Korennykh, A.V., Egea, P.F., Korostelev, A.A., Finer-Moore, J., Zhang, C., Shokat, K.M., Stroud, R.M., and Walter, P. (2009). The unfolded protein response signals through high-order assembly of Ire1. *Nature* *457*, 687-693.

Kosmaczewski, S.G., Edwards, T.J., Han, S.M., Eckwahl, M.J., Meyer, B.I., Peach, S., Hesselberth, J.R., Wolin, S.L., and Hammarlund, M. (2014). The RtcB RNA ligase is an essential component of the metazoan unfolded protein response. *EMBO Rep* *15*, 1278-1285.

Kramer, G., Boehringer, D., Ban, N., and Bukau, B. (2009). The ribosome as a platform for co-translational processing, folding and targeting of newly synthesized proteins. *Nat Struct Mol Biol* *16*, 589-597.

Kramer, G., Rauch, T., Rist, W., Vorderwulbecke, S., Patzelt, H., Schulze-Specking, A., Ban, N., Deuerling, E., and Bukau, B. (2002). L23 protein functions as a chaperone docking site on the ribosome. *Nature* *419*, 171-174.

Kurita, K., Honda, K., Suzuma, S., Takamatsu, H., Nakamura, K., and Yamane, K. (1996). Identification of a region of *Bacillus subtilis* Ffh, a homologue of mammalian SRP54 protein, that is essential for binding to small cytoplasmic RNA. *J Biol Chem* *271*, 13140-13146.

Kuroha, K., Akamatsu, M., Dimitrova, L., Ito, T., Kato, Y., Shirahige, K., and Inada, T. (2010). Receptor for activated C kinase 1 stimulates nascent polypeptide-dependent translation arrest. *EMBO Rep* 11, 956-961.

Lakshmipathy, S.K., Tomic, S., Kaiser, C.M., Chang, H.C., Genevoux, P., Georgopoulos, C., Barral, J.M., Johnson, A.E., Hartl, F.U., and Etchells, S.A. (2007). Identification of nascent chain interaction sites on trigger factor. *J Biol Chem* 282, 12186-12193.

Lee, K., Sharma, R., Shrestha, O.K., Bingman, C.A., and Craig, E.A. (2016). Dual interaction of the Hsp70 J-protein cochaperone Zuo1 with the 40S and 60S ribosomal subunits. *Nat Struct Mol Biol* 23, 1003-1010.

Lee, K.P., Dey, M., Neculai, D., Cao, C., Dever, T.E., and Sicheri, F. (2008). Structure of the dual enzyme Ire1 reveals the basis for catalysis and regulation in nonconventional RNA splicing. *Cell* 132, 89-100.

Leidig, C., Bange, G., Kopp, J., Amlacher, S., Aravind, A., Wickles, S., Witte, G., Hurt, E., Beckmann, R., and Sinning, I. (2013). Structural characterization of a eukaryotic chaperone--the ribosome-associated complex. *Nat Struct Mol Biol* 20, 23-28.

Lhomond, S., Avril, T., Dejeans, N., Voutetakis, K., Doultzinos, D., McMahon, M., Pineau, R., Obacz, J., Papadodima, O., Jouan, F., *et al.* (2018). Dual IRE1 RNase functions dictate glioblastoma development. *EMBO Mol Med* 10.

Li, H., Chen, X., Gao, Y., Wu, J., Zeng, F., and Song, F. (2015). XBP1 induces snail expression to promote epithelial- to-mesenchymal transition and invasion of breast cancer cells. *Cell Signal* 27, 82-89.

- Li, H., Korennykh, A.V., Behrman, S.L., and Walter, P. (2010). Mammalian endoplasmic reticulum stress sensor IRE1 signals by dynamic clustering. *Proc Natl Acad Sci U S A* *107*, 16113-16118.
- Limia, C.M., Sauzay, C., Urra, H., Hetz, C., Chevet, E., and Avril, T. (2019). Emerging Roles of the Endoplasmic Reticulum Associated Unfolded Protein Response in Cancer Cell Migration and Invasion. *Cancers (Basel)* *11*.
- Lin, J.H., Walter, P., and Yen, T.S. (2008). Endoplasmic reticulum stress in disease pathogenesis. *Annu Rev Pathol* *3*, 399-425.
- Lisbona, F., Rojas-Rivera, D., Thielen, P., Zamorano, S., Todd, D., Martinon, F., Glavic, A., Kress, C., Lin, J.H., Walter, P., *et al.* (2009). BAX inhibitor-1 is a negative regulator of the ER stress sensor IRE1alpha. *Mol Cell* *33*, 679-691.
- Liu, C.Y., Schroder, M., and Kaufman, R.J. (2000). Ligand-independent dimerization activates the stress response kinases IRE1 and PERK in the lumen of the endoplasmic reticulum. *J Biol Chem* *275*, 24881-24885.
- Liu, S., Yi, L., Ling, M., Jiang, J., Song, L., Liu, J., and Cao, X. (2018). HSP70L1-mediated intracellular priming of dendritic cell vaccination induces more potent CTL response against cancer. *Cell Mol Immunol* *15*, 135-145.
- Livak, K.J., and Schmittgen, T.D. (2001). Analysis of relative gene expression data using real-time quantitative PCR and the 2^{(-Delta Delta C(T))} Method. *Methods* *25*, 402-408.
- Logue, S.E., McGrath, E.P., Cleary, P., Greene, S., Mnich, K., Almanza, A., Chevet, E., Dwyer, R.M., Oommen, A., Legembre, P., *et al.* (2018). Inhibition of IRE1 RNase

activity modulates the tumor cell secretome and enhances response to chemotherapy. *Nat Commun* 9, 3267.

Lu, J., and Deutsch, C. (2008). Electrostatics in the ribosomal tunnel modulate chain elongation rates. *J Mol Biol* 384, 73-86.

Lu, Y., Liang, F.X., and Wang, X. (2014). A synthetic biology approach identifies the mammalian UPR RNA ligase RtcB. *Mol Cell* 55, 758-770.

Madden, E., Logue, S.E., Healy, S.J., Manie, S., and Samali, A. (2019). The role of the unfolded protein response in cancer progression: From oncogenesis to chemoresistance. *Biol Cell* 111, 1-17.

Marcu, M.G., Doyle, M., Bertolotti, A., Ron, D., Hendershot, L., and Neckers, L. (2002). Heat shock protein 90 modulates the unfolded protein response by stabilizing IRE1alpha. *Mol Cell Biol* 22, 8506-8513.

Markesich, D.C., Gajewski, K.M., Nazimiec, M.E., and Beckingham, K. (2000). bicaudal encodes the Drosophila beta NAC homolog, a component of the ribosomal translational machinery*. *Development* 127, 559-572.

Martin, E.M., Jackson, M.P., Gamerding, M., Gense, K., Karamonos, T.K., Humes, J.R., Deuerling, E., Ashcroft, A.E., and Radford, S.E. (2018). Conformational flexibility within the nascent polypeptide-associated complex enables its interactions with structurally diverse client proteins. *J Biol Chem* 293, 8554-8568.

Matlack, K.E., Mothes, W., and Rapoport, T.A. (1998). Protein translocation: tunnel vision. *Cell* 92, 381-390.

Matsumoto-Taniura, N., Pirollet, F., Monroe, R., Gerace, L., and Westendorf, J.M. (1996). Identification of novel M phase phosphoproteins by expression cloning. *Mol Biol Cell* 7, 1455-1469.

Maurel, M., Chevet, E., Tavernier, J., and Gerlo, S. (2014). Getting RIDD of RNA: IRE1 in cell fate regulation. *Trends Biochem Sci* 39, 245-254.

Mayer, M.P., and Bukau, B. (2005). Hsp70 chaperones: cellular functions and molecular mechanism. *Cell Mol Life Sci* 62, 670-684.

Mhaidat, N.M., Alzoubi, K.H., and Abushbak, A. (2015). X-box binding protein 1 (XBP-1) enhances colorectal cancer cell invasion. *J Chemother* 27, 167-173.

Mishiba, K., Nagashima, Y., Suzuki, E., Hayashi, N., Ogata, Y., Shimada, Y., and Koizumi, N. (2013). Defects in IRE1 enhance cell death and fail to degrade mRNAs encoding secretory pathway proteins in the Arabidopsis unfolded protein response. *Proc Natl Acad Sci U S A* 110, 5713-5718.

Mori, K. (2009). Signalling pathways in the unfolded protein response: development from yeast to mammals. *J Biochem* 146, 743-750.

Mori, K., Ma, W., Gething, M.J., and Sambrook, J. (1993). A transmembrane protein with a cdc2+/CDC28-related kinase activity is required for signaling from the ER to the nucleus. *Cell* 74, 743-756.

Morris, J.A., Dorner, A.J., Edwards, C.A., Hendershot, L.M., and Kaufman, R.J. (1997). Immunoglobulin binding protein (BiP) function is required to protect cells from endoplasmic reticulum stress but is not required for the secretion of selective proteins. *J Biol Chem* 272, 4327-4334.

Moser, C., Mol, O., Goody, R.S., and Sinning, I. (1997). The signal recognition particle receptor of *Escherichia coli* (FtsY) has a nucleotide exchange factor built into the GTPase domain. *Proc Natl Acad Sci U S A* *94*, 11339-11344.

Muldoon-Jacobs, K.L., and Dinman, J.D. (2006). Specific effects of ribosome-tethered molecular chaperones on programmed -1 ribosomal frameshifting. *Eukaryot Cell* *5*, 762-770.

Navid, F., and Colbert, R.A. (2017). Causes and consequences of endoplasmic reticulum stress in rheumatic disease. *Nat Rev Rheumatol* *13*, 25-40.

Nelson, R.J., Ziegelhoffer, T., Nicolet, C., Werner-Washburne, M., and Craig, E.A. (1992). The translation machinery and 70 kd heat shock protein cooperate in protein synthesis. *Cell* *71*, 97-105.

Nishitoh, H., Matsuzawa, A., Tobiume, K., Saegusa, K., Takeda, K., Inoue, K., Hori, S., Kakizuka, A., and Ichijo, H. (2002). ASK1 is essential for endoplasmic reticulum stress-induced neuronal cell death triggered by expanded polyglutamine repeats. *Genes Dev* *16*, 1345-1355.

Norton, J.D. (2000). ID helix-loop-helix proteins in cell growth, differentiation and tumorigenesis. *J Cell Sci* *113* (Pt 22), 3897-3905.

Nyathi, Y., and Pool, M.R. (2015). Analysis of the interplay of protein biogenesis factors at the ribosome exit site reveals new role for NAC. *J Cell Biol* *210*, 287-301.

Ogle, J.M., Carter, A.P., and Ramakrishnan, V. (2003). Insights into the decoding mechanism from recent ribosome structures. *Trends Biochem Sci* *28*, 259-266.

Oh, E., Becker, A.H., Sandikci, A., Huber, D., Chaba, R., Gloge, F., Nichols, R.J., Typas, A., Gross, C.A., Kramer, G., *et al.* (2011). Selective ribosome profiling reveals the cotranslational chaperone action of trigger factor in vivo. *Cell* *147*, 1295-1308.

Oikawa, D., Kimata, Y., Kohno, K., and Iwawaki, T. (2009). Activation of mammalian IRE1alpha upon ER stress depends on dissociation of BiP rather than on direct interaction with unfolded proteins. *Exp Cell Res* *315*, 2496-2504.

Oikawa, D., Tokuda, M., Hosoda, A., and Iwawaki, T. (2010). Identification of a consensus element recognized and cleaved by IRE1 alpha. *Nucleic Acids Res* *38*, 6265-6273.

Okamura, K., Kimata, Y., Higashio, H., Tsuru, A., and Kohno, K. (2000). Dissociation of Kar2p/BiP from an ER sensory molecule, Ire1p, triggers the unfolded protein response in yeast. *Biochem Biophys Res Commun* *279*, 445-450.

Otto, H., Conz, C., Maier, P., Wolfle, T., Suzuki, C.K., Jenö, P., Rucknagel, P., Stahl, J., and Rospert, S. (2005). The chaperones MPP11 and Hsp70L1 form the mammalian ribosome-associated complex. *Proc Natl Acad Sci U S A* *102*, 10064-10069.

Ozcan, L., and Tabas, I. (2012). Role of endoplasmic reticulum stress in metabolic disease and other disorders. *Annu Rev Med* *63*, 317-328.

Passos, D.O., Doma, M.K., Shoemaker, C.J., Muhlrads, D., Green, R., Weissman, J., Hollien, J., and Parker, R. (2009). Analysis of Dom34 and its function in no-go decay. *Mol Biol Cell* *20*, 3025-3032.

Pech, M., Spreter, T., Beckmann, R., and Beatrix, B. (2010). Dual binding mode of the nascent polypeptide-associated complex reveals a novel universal adapter site on the ribosome. *J Biol Chem* 285, 19679-19687.

Pechmann, S., Willmund, F., and Frydman, J. (2013). The ribosome as a hub for protein quality control. *Mol Cell* 49, 411-421.

Peisker, K., Braun, D., Wolfle, T., Hentschel, J., Funfschilling, U., Fischer, G., Sickmann, A., and Rospert, S. (2008). Ribosome-associated complex binds to ribosomes in close proximity of Rpl31 at the exit of the polypeptide tunnel in yeast. *Mol Biol Cell* 19, 5279-5288.

Pellegrino, M.W., Nargund, A.M., and Haynes, C.M. (2013). Signaling the mitochondrial unfolded protein response. *Biochim Biophys Acta* 1833, 410-416.

Pfund, C., Huang, P., Lopez-Hoyo, N., and Craig, E.A. (2001). Divergent functional properties of the ribosome-associated molecular chaperone Ssb compared with other Hsp70s. *Mol Biol Cell* 12, 3773-3782.

Pfund, C., Lopez-Hoyo, N., Ziegelhoffer, T., Schilke, B.A., Lopez-Buesa, P., Walter, W.A., Wiedmann, M., and Craig, E.A. (1998). The molecular chaperone Ssb from *Saccharomyces cerevisiae* is a component of the ribosome-nascent chain complex. *EMBO J* 17, 3981-3989.

Pinarbasi, E.S., Karamyshev, A.L., Tikhonova, E.B., Wu, I.H., Hudson, H., and Thomas, P.J. (2018). Pathogenic Signal Sequence Mutations in Progranulin Disrupt SRP Interactions Required for mRNA Stability. *Cell Rep* 23, 2844-2851.

Pincus, D., Chevalier, M.W., Aragon, T., van Anken, E., Vidal, S.E., El-Samad, H., and Walter, P. (2010). BiP binding to the ER-stress sensor Ire1 tunes the homeostatic behavior of the unfolded protein response. *PLoS Biol* 8, e1000415.

Pisarev, A.V., Skabkin, M.A., Pisareva, V.P., Skabkina, O.V., Rakotondrafara, A.M., Hentze, M.W., Hellen, C.U., and Pestova, T.V. (2010). The role of ABCE1 in eukaryotic posttermination ribosomal recycling. *Mol Cell* 37, 196-210.

Pisareva, V.P., Skabkin, M.A., Hellen, C.U., Pestova, T.V., and Pisarev, A.V. (2011). Dissociation by Pelota, Hbs1 and ABCE1 of mammalian vacant 80S ribosomes and stalled elongation complexes. *EMBO J* 30, 1804-1817.

Plumb, R., Zhang, Z.R., Appathurai, S., and Mariappan, M. (2015). A functional link between the co-translational protein translocation pathway and the UPR. *Elife* 4.

Pohlschroder, M., Prinz, W.A., Hartmann, E., and Beckwith, J. (1997). Protein translocation in the three domains of life: variations on a theme. *Cell* 91, 563-566.

Polevoda, B., Brown, S., Cardillo, T.S., Rigby, S., and Sherman, F. (2008). Yeast N(alpha)-terminal acetyltransferases are associated with ribosomes. *J Cell Biochem* 103, 492-508.

Pool, M.R. (2005). Signal recognition particles in chloroplasts, bacteria, yeast and mammals (review). *Mol Membr Biol* 22, 3-15.

Pool, M.R., Stumm, J., Fulga, T.A., Sinning, I., and Dobberstein, B. (2002). Distinct modes of signal recognition particle interaction with the ribosome. *Science* 297, 1345-1348.

- Popp, M.W., and Maquat, L.E. (2014). Defective secretory-protein mRNAs take the RAPP. *Trends Biochem Sci* 39, 154-156.
- Preissler, S., and Deuerling, E. (2012). Ribosome-associated chaperones as key players in proteostasis. *Trends Biochem Sci* 37, 274-283.
- Prunuske, A.J., Waltner, J.K., Kuhn, P., Gu, B., and Craig, E.A. (2012). Role for the molecular chaperones Zuo1 and Ssz1 in quorum sensing via activation of the transcription factor Pdr1. *Proc Natl Acad Sci U S A* 109, 472-477.
- Raine, A., Ivanova, N., Wikberg, J.E., and Ehrenberg, M. (2004). Simultaneous binding of trigger factor and signal recognition particle to the E. coli ribosome. *Biochimie* 86, 495-500.
- Rakotondrafara, A.M., and Hentze, M.W. (2011). An efficient factor-depleted mammalian in vitro translation system. *Nat Protoc* 6, 563-571.
- Rakwalska, M., and Rospert, S. (2004). The ribosome-bound chaperones RAC and Ssb1/2p are required for accurate translation in *Saccharomyces cerevisiae*. *Mol Cell Biol* 24, 9186-9197.
- Reimann, B., Bradsher, J., Franke, J., Hartmann, E., Wiedmann, M., Prehn, S., and Wiedmann, B. (1999). Initial characterization of the nascent polypeptide-associated complex in yeast. *Yeast* 15, 397-407.
- Resto, V.A., Caballero, O.L., Buta, M.R., Westra, W.H., Wu, L., Westendorf, J.M., Jen, J., Hieter, P., and Sidransky, D. (2000). A putative oncogenic role for MPP11 in head and neck squamous cell cancer. *Cancer Res* 60, 5529-5535.

Ribeiro, J.D., Morey, L., Mas, A., Gutierrez, A., Luis, N.M., Mejetta, S., Richly, H., Benitah, S.A., Keyes, W.M., and Di Croce, L. (2013). ZRF1 controls oncogene-induced senescence through the INK4-ARF locus. *Oncogene* 32, 2161-2168.

Richly, H., Rocha-Viegas, L., Ribeiro, J.D., Demajo, S., Gundem, G., Lopez-Bigas, N., Nakagawa, T., Rospert, S., Ito, T., and Di Croce, L. (2010). Transcriptional activation of polycomb-repressed genes by ZRF1. *Nature* 468, 1124-1128.

Romisch, K., Webb, J., Lingelbach, K., Gausepohl, H., and Dobberstein, B. (1990). The 54-kD protein of signal recognition particle contains a methionine-rich RNA binding domain. *J Cell Biol* 111, 1793-1802.

Rosenzweig, R., Nillegoda, N.B., Mayer, M.P., and Bukau, B. (2019). The Hsp70 chaperone network. *Nat Rev Mol Cell Biol* 20, 665-680.

Ruegsegger, U., Leber, J.H., and Walter, P. (2001). Block of HAC1 mRNA translation by long-range base pairing is released by cytoplasmic splicing upon induction of the unfolded protein response. *Cell* 107, 103-114.

Salaroglio, I.C., Panada, E., Moiso, E., Buondonno, I., Provero, P., Rubinstein, M., Kopecka, J., and Riganti, C. (2017). PERK induces resistance to cell death elicited by endoplasmic reticulum stress and chemotherapy. *Mol Cancer* 16, 91.

Sanz, E., Yang, L., Su, T., Morris, D.R., McKnight, G.S., and Amieux, P.S. (2009). Cell-type-specific isolation of ribosome-associated mRNA from complex tissues. *Proc Natl Acad Sci U S A* 106, 13939-13944.

Schmitt, M., Li, L., Giannopoulos, K., Chen, J., Brunner, C., Barth, T., Schmitt, A., Wiesneth, M., Dohner, K., Dohner, H., *et al.* (2006). Chronic myeloid leukemia cells

express tumor-associated antigens eliciting specific CD8⁺ T-cell responses and are lacking costimulatory molecules. *Exp Hematol* 34, 1709-1719.

Schroder, M., and Kaufman, R.J. (2005). The mammalian unfolded protein response. *Annu Rev Biochem* 74, 739-789.

Schuller, A.P., and Green, R. (2018). Roadblocks and resolutions in eukaryotic translation. *Nat Rev Mol Cell Biol* 19, 526-541.

Senturk, S., Shirole, N.H., Nowak, D.G., Corbo, V., Pal, D., Vaughan, A., Tuveson, D.A., Trotman, L.C., Kinney, J.B., and Sordella, R. (2017). Rapid and tunable method to temporally control gene editing based on conditional Cas9 stabilization. *Nat Commun* 8, 14370.

Shalem, O., Sanjana, N.E., Hartenian, E., Shi, X., Scott, D.A., Mikkelsen, T., Heckl, D., Ebert, B.L., Root, D.E., Doench, J.G., *et al.* (2014). Genome-scale CRISPR-Cas9 knockout screening in human cells. *Science* 343, 84-87.

Shamu, C.E., and Walter, P. (1996). Oligomerization and phosphorylation of the Ire1p kinase during intracellular signaling from the endoplasmic reticulum to the nucleus. *EMBO J* 15, 3028-3039.

Shanmuganathan, V., Schiller, N., Magoulopoulou, A., Cheng, J., Braunger, K., Cymer, F., Berninghausen, O., Beatrix, B., Kohno, K., von Heijne, G., *et al.* (2019). Structural and mutational analysis of the ribosome-arresting human XBP1u. *Elife* 8.

Shen, J., Chen, X., Hendershot, L., and Prywes, R. (2002). ER stress regulation of ATF6 localization by dissociation of BiP/GRP78 binding and unmasking of Golgi localization signals. *Dev Cell* 3, 99-111.

Sheng, X., Nenseth, H.Z., Qu, S., Kuzu, O.F., Frahnnow, T., Simon, L., Greene, S., Zeng, Q., Fazli, L., Rennie, P.S., *et al.* (2019). IRE1alpha-XBP1s pathway promotes prostate cancer by activating c-MYC signaling. *Nat Commun* *10*, 323.

Shoemaker, C.J., Eyler, D.E., and Green, R. (2010). Dom34:Hbs1 promotes subunit dissociation and peptidyl-tRNA drop-off to initiate no-go decay. *Science* *330*, 369-372.

Shoemaker, C.J., and Green, R. (2011). Kinetic analysis reveals the ordered coupling of translation termination and ribosome recycling in yeast. *Proc Natl Acad Sci U S A* *108*, E1392-1398.

Shoemaker, C.J., and Green, R. (2012). Translation drives mRNA quality control. *Nat Struct Mol Biol* *19*, 594-601.

Shoji, W., Inoue, T., Yamamoto, T., and Obinata, M. (1995). MIDA1, a protein associated with Id, regulates cell growth. *J Biol Chem* *270*, 24818-24825.

Shrestha, O.K., Sharma, R., Tomiczek, B., Lee, W., Tonelli, M., Cornilescu, G., Stolarska, M., Nierzwicki, L., Czub, J., Markley, J.L., *et al.* (2019). Structure and evolution of the 4-helix bundle domain of Zuotin, a J-domain protein co-chaperone of Hsp70. *PLoS One* *14*, e0217098.

Sidrauski, C., Cox, J.S., and Walter, P. (1996). tRNA ligase is required for regulated mRNA splicing in the unfolded protein response. *Cell* *87*, 405-413.

Sidrauski, C., and Walter, P. (1997). The transmembrane kinase Ire1p is a site-specific endonuclease that initiates mRNA splicing in the unfolded protein response. *Cell* *90*, 1031-1039.

Siegel, V., and Walter, P. (1986). Removal of the Alu structural domain from signal recognition particle leaves its protein translocation activity intact. *Nature* 320, 81-84.

Siegel, V., and Walter, P. (1988). Each of the activities of signal recognition particle (SRP) is contained within a distinct domain: analysis of biochemical mutants of SRP. *Cell* 52, 39-49.

Simms, C.L., Thomas, E.N., and Zaher, H.S. (2017). Ribosome-based quality control of mRNA and nascent peptides. *Wiley Interdiscip Rev RNA* 8.

Spahn, C.M., Gomez-Lorenzo, M.G., Grassucci, R.A., Jorgensen, R., Andersen, G.R., Beckmann, R., Penczek, P.A., Ballesta, J.P., and Frank, J. (2004). Domain movements of elongation factor eEF2 and the eukaryotic 80S ribosome facilitate tRNA translocation. *EMBO J* 23, 1008-1019.

Spreter, T., Pech, M., and Beatrix, B. (2005). The crystal structure of archaeal nascent polypeptide-associated complex (NAC) reveals a unique fold and the presence of a ubiquitin-associated domain. *J Biol Chem* 280, 15849-15854.

Sun, Y., Jiang, F., Pan, Y., Chen, X., Chen, J., Wang, Y., Zheng, X., and Zhang, J. (2018). XBP1 promotes tumor invasion and is associated with poor prognosis in oral squamous cell carcinoma. *Oncol Rep* 40, 988-998.

Szadeczky-Kardoss, I., Gal, L., Auber, A., Taller, J., and Silhavy, D. (2018). The No-go decay system degrades plant mRNAs that contain a long A-stretch in the coding region. *Plant Sci* 275, 19-27.

Tam, A.B., Koong, A.C., and Niwa, M. (2014). Ire1 has distinct catalytic mechanisms for XBP1/HAC1 splicing and RIDD. *Cell Rep* 9, 850-858.

Tanjore, H., Cheng, D.S., Degryse, A.L., Zoz, D.F., Abdolrasulnia, R., Lawson, W.E., and Blackwell, T.S. (2011). Alveolar epithelial cells undergo epithelial-to-mesenchymal transition in response to endoplasmic reticulum stress. *J Biol Chem* 286, 30972-30980.

Teter, S.A., Houry, W.A., Ang, D., Tradler, T., Rockabrand, D., Fischer, G., Blum, P., Georgopoulos, C., and Hartl, F.U. (1999). Polypeptide flux through bacterial Hsp70: DnaK cooperates with trigger factor in chaperoning nascent chains. *Cell* 97, 755-765.

Tirasophon, W., Welihinda, A.A., and Kaufman, R.J. (1998). A stress response pathway from the endoplasmic reticulum to the nucleus requires a novel bifunctional protein kinase/endoribonuclease (Ire1p) in mammalian cells. *Genes Dev* 12, 1812-1824.

Tollner, T.L., Venners, S.A., Hollox, E.J., Yudin, A.I., Liu, X., Tang, G., Xing, H., Kays, R.J., Lau, T., Overstreet, J.W., *et al.* (2011). A common mutation in the defensin DEFB126 causes impaired sperm function and subfertility. *Sci Transl Med* 3, 92ra65.

Tomic, S., Johnson, A.E., Hartl, F.U., and Etchells, S.A. (2006). Exploring the capacity of trigger factor to function as a shield for ribosome bound polypeptide chains. *FEBS Lett* 580, 72-76.

Travers, K.J., Patil, C.K., Wodicka, L., Lockhart, D.J., Weissman, J.S., and Walter, P. (2000). Functional and genomic analyses reveal an essential coordination between the unfolded protein response and ER-associated degradation. *Cell* 101, 249-258.

Tsuboi, T., Kuroha, K., Kudo, K., Makino, S., Inoue, E., Kashima, I., and Inada, T. (2012). Dom34:hbs1 plays a general role in quality-control systems by dissociation of a stalled ribosome at the 3' end of aberrant mRNA. *Mol Cell* 46, 518-529.

Tsuru, A., Fujimoto, N., Takahashi, S., Saito, M., Nakamura, D., Iwano, M., Iwawaki, T., Kadokura, H., Ron, D., and Kohno, K. (2013). Negative feedback by IRE1beta optimizes mucin production in goblet cells. *Proc Natl Acad Sci U S A* 110, 2864-2869.

Ullers, R.S., Houben, E.N., Raine, A., ten Hagen-Jongman, C.M., Ehrenberg, M., Brunner, J., Oudega, B., Harms, N., and Luirink, J. (2003). Interplay of signal recognition particle and trigger factor at L23 near the nascent chain exit site on the Escherichia coli ribosome. *J Cell Biol* 161, 679-684.

Urano, F., Wang, X., Bertolotti, A., Zhang, Y., Chung, P., Harding, H.P., and Ron, D. (2000). Coupling of stress in the ER to activation of JNK protein kinases by transmembrane protein kinase IRE1. *Science* 287, 664-666.

Valastyan, J.S., and Lindquist, S. (2014a). Mechanisms of protein-folding diseases at a glance. *Disease Models & Mechanisms* 7, 9-14.

Valastyan, J.S., and Lindquist, S. (2014b). Mechanisms of protein-folding diseases at a glance. *Dis Model Mech* 7, 9-14.

van Hoof, A., Frischmeyer, P.A., Dietz, H.C., and Parker, R. (2002). Exosome-mediated recognition and degradation of mRNAs lacking a termination codon. *Science* 295, 2262-2264.

Varshavsky, A. (2011). The N-end rule pathway and regulation by proteolysis. *Protein Sci* 20, 1298-1345.

Walter, P., and Blobel, G. (1980). Purification of a membrane-associated protein complex required for protein translocation across the endoplasmic reticulum. *Proc Natl Acad Sci U S A* 77, 7112-7116.

Walter, P., and Blobel, G. (1981). Translocation of proteins across the endoplasmic reticulum. II. Signal recognition protein (SRP) mediates the selective binding to microsomal membranes of in-vitro-assembled polysomes synthesizing secretory protein. *J Cell Biol* 91, 551-556.

Walter, P., and Blobel, G. (1982). Signal recognition particle contains a 7S RNA essential for protein translocation across the endoplasmic reticulum. *Nature* 299, 691-698.

Walter, P., and Ron, D. (2011). The unfolded protein response: from stress pathway to homeostatic regulation. *Science* 334, 1081-1086.

Wan, T., Zhou, X., Chen, G., An, H., Chen, T., Zhang, W., Liu, S., Jiang, Y., Yang, F., Wu, Y., *et al.* (2004). Novel heat shock protein Hsp70L1 activates dendritic cells and acts as a Th1 polarizing adjuvant. *Blood* 103, 1747-1754.

Wang, F., Durfee, L.A., and Huibregtse, J.M. (2013). A cotranslational ubiquitination pathway for quality control of misfolded proteins. *Mol Cell* 50, 368-378.

Wang, L., Zhang, W., Wang, L., Zhang, X.C., Li, X., and Rao, Z. (2010). Crystal structures of NAC domains of human nascent polypeptide-associated complex (NAC) and its alphaNAC subunit. *Protein Cell* 1, 406-416.

Wang, M., and Kaufman, R.J. (2016). Protein misfolding in the endoplasmic reticulum as a conduit to human disease. *Nature* 529, 326-335.

Wegrzyn, R.D., Hofmann, D., Merz, F., Nikolay, R., Rauch, T., Graf, C., and Deuerling, E. (2006). A conserved motif is prerequisite for the interaction of NAC with ribosomal protein L23 and nascent chains. *J Biol Chem* 281, 2847-2857.

Westerheide, S.D., Bosman, J.D., Mbadugha, B.N., Kawahara, T.L., Matsumoto, G., Kim, S., Gu, W., Devlin, J.P., Silverman, R.B., and Morimoto, R.I. (2004). Celastrols as inducers of the heat shock response and cytoprotection. *J Biol Chem* 279, 56053-56060.

Weyer, F.A., Gumiero, A., Gese, G.V., Lapouge, K., and Sinning, I. (2017). Structural insights into a unique Hsp70-Hsp40 interaction in the eukaryotic ribosome-associated complex. *Nat Struct Mol Biol* 24, 144-151.

Wilhelm, M.L., Reinbolt, J., Gangloff, J., Dirheimer, G., and Wilhelm, F.X. (1994). Transfer RNA binding protein in the nucleus of *Saccharomyces cerevisiae*. *FEBS Lett* 349, 260-264.

Willmund, F., del Alamo, M., Pechmann, S., Chen, T., Albanese, V., Dammer, E.B., Peng, J., and Frydman, J. (2013). The cotranslational function of ribosome-associated Hsp70 in eukaryotic protein homeostasis. *Cell* 152, 196-209.

Wilson, D.N., and Beckmann, R. (2011). The ribosomal tunnel as a functional environment for nascent polypeptide folding and translational stalling. *Curr Opin Struct Biol* 21, 274-282.

Wilson, D.N., Blaha, G., Connell, S.R., Ivanov, P.V., Jenke, H., Stelzl, U., Teraoka, Y., and Nierhaus, K.H. (2002). Protein synthesis at atomic resolution: mechanistics of translation in the light of highly resolved structures for the ribosome. *Curr Protein Pept Sci* 3, 1-53.

Wu, S., Du, R., Gao, C., Kang, J., Wen, J., and Sun, T. (2018). The role of XBP1s in the metastasis and prognosis of hepatocellular carcinoma. *Biochem Biophys Res Commun* 500, 530-537.

Wu, Y., Wan, T., Zhou, X., Wang, B., Yang, F., Li, N., Chen, G., Dai, S., Liu, S., Zhang, M., *et al.* (2005). Hsp70-like protein 1 fusion protein enhances induction of carcinoembryonic antigen-specific CD8⁺ CTL response by dendritic cell vaccine. *Cancer Res* 65, 4947-4954.

Xia, T., Tong, S., Fan, K., Zhai, W., Fang, B., Wang, S.H., and Wang, J.J. (2016). XBP1 induces MMP-9 expression to promote proliferation and invasion in human esophageal squamous cell carcinoma. *Am J Cancer Res* 6, 2031-2040.

Yan, W., Schilke, B., Pfund, C., Walter, W., Kim, S., and Craig, E.A. (1998). Zuo1, a ribosome-associated DnaJ molecular chaperone. *EMBO J* 17, 4809-4817.

Yanagitani, K., Imagawa, Y., Iwawaki, T., Hosoda, A., Saito, M., Kimata, Y., and Kohno, K. (2009). Cotranslational targeting of XBP1 protein to the membrane promotes cytoplasmic splicing of its own mRNA. *Mol Cell* 34, 191-200.

Yanagitani, K., Kimata, Y., Kadokura, H., and Kohno, K. (2011). Translational pausing ensures membrane targeting and cytoplasmic splicing of XBP1 mRNA. *Science* 331, 586-589.

Yang, Q., Yu, C.H., Zhao, F., Dang, Y., Wu, C., Xie, P., Sachs, M.S., and Liu, Y. (2019). eRF1 mediates codon usage effects on mRNA translation efficiency through premature termination at rare codons. *Nucleic Acids Res* 47, 9243-9258.

Yi, C.H., Pan, H., Seebacher, J., Jang, I.H., Hyberts, S.G., Heffron, G.J., Vander Heiden, M.G., Yang, R., Li, F., Locasale, J.W., *et al.* (2011). Metabolic regulation of protein N-alpha-acetylation by Bcl-xL promotes cell survival. *Cell* 146, 607-620.

Yoshida, H., Matsui, T., Yamamoto, A., Okada, T., and Mori, K. (2001). XBP1 mRNA is induced by ATF6 and spliced by IRE1 in response to ER stress to produce a highly active transcription factor. *Cell* 107, 881-891.

Yoshida, H., Oku, M., Suzuki, M., and Mori, K. (2006). pXBP1(U) encoded in XBP1 pre-mRNA negatively regulates unfolded protein response activator pXBP1(S) in mammalian ER stress response. *J Cell Biol* 172, 565-575.

Yudin, A.I., Generao, S.E., Tollner, T.L., Treece, C.A., Overstreet, J.W., and Cherr, G.N. (2005). Beta-defensin 126 on the cell surface protects sperm from immunorecognition and binding of anti-sperm antibodies. *Biol Reprod* 73, 1243-1252.

Zaher, H.S., and Green, R. (2009). Fidelity at the molecular level: lessons from protein synthesis. *Cell* 136, 746-762.

Zhang, S., Lockshin, C., Herbert, A., Winter, E., and Rich, A. (1992). Zuotin, a putative Z-DNA binding protein in *Saccharomyces cerevisiae*. *EMBO J* 11, 3787-3796.

Zhang, Y., Berndt, U., Golz, H., Tais, A., Oellerer, S., Wolfle, T., Fitzke, E., and Rospert, S. (2012). NAC functions as a modulator of SRP during the early steps of protein targeting to the endoplasmic reticulum. *Mol Biol Cell* 23, 3027-3040.

Zhang, Y., Ma, C., Yuan, Y., Zhu, J., Li, N., Chen, C., Wu, S., Yu, L., Lei, J., and Gao, N. (2014). Structural basis for interaction of a cotranslational chaperone with the eukaryotic ribosome. *Nat Struct Mol Biol* 21, 1042-1046.

Zhang, Y., Sinning, I., and Rospert, S. (2017). Two chaperones locked in an embrace: structure and function of the ribosome-associated complex RAC. *Nat Struct Mol Biol* 24, 611-619.

Zhang, Y., Valentin Gese, G., Conz, C., Lapouge, K., Kopp, J., Wolfle, T., Rospert, S., and Sinning, I. (2020). The ribosome-associated complex RAC serves in a relay that directs nascent chains to Ssb. *Nat Commun* *11*, 1504.

Zhou, J., Liu, C.Y., Back, S.H., Clark, R.L., Peisach, D., Xu, Z., and Kaufman, R.J. (2006). The crystal structure of human IRE1 luminal domain reveals a conserved dimerization interface required for activation of the unfolded protein response. *Proc Natl Acad Sci U S A* *103*, 14343-14348.

Zopf, D., Bernstein, H.D., Johnson, A.E., and Walter, P. (1990). The methionine-rich domain of the 54 kd protein subunit of the signal recognition particle contains an RNA binding site and can be crosslinked to a signal sequence. *EMBO J* *9*, 4511-4517.

Zopf, D., Bernstein, H.D., and Walter, P. (1993). GTPase domain of the 54-kD subunit of the mammalian signal recognition particle is required for protein translocation but not for signal sequence binding. *J Cell Biol* *120*, 1113-1121.